12-2021

Modeling driver distraction mechanism and its safety impact in automated vehicle environment.

Song Wang
University of Louisville

MODELING DRIVER DISTRACTION MECHANISM AND ITS SAFETY IMPACT IN AUTOMATED VEHICLE ENVIRONMENT

By

Song Wang
B.S., Chongqing Jiaotong University, China, 2013
M.Sc., Chongqing Jiaotong University, China, 2016

A Dissertation
Submitted to the Faculty of the
J. B. Speed School of Engineering of the University of Louisville
in Partial Fulfilment of the Requirements
for the Degree of

Doctor of Philosophy in Civil Engineering

Department of Civil and Environmental Engineering Department
University of Louisville
Louisville, Kentucky

December 2021

MODELING DRIVER DISTRACTION MECHANISM AND ITS SAFETY IMPACT IN AUTOMATED VEHICLE ENVIRONMENT

By

Song Wang
B.S., Chongqing Jiaotong University, China, 2013
M.Sc., Chongqing Jiaotong University, China, 2016

A Dissertation Approved on

November 30, 2021

By the following Dissertation Committee:

_____
Dr. Zhixia Li, Dissertation Director

_____
Dr. Zhihui Sun

_____
Dr. J.P. Mohsen

_____
Dr. Ahmed Desoky

DEDICATION

This dissertation is dedicated to my parents

Mr. Xu Wang

and

Mrs. Ping Li

who have been giving me their unconditional love and full support.

ACKNOWLEDGEMENTS

First and foremost, I would like to express my sincere gratitude to my advisor, Dr. Zhixia Li, for his continuous guidance and support of my Ph.D. study and research. Dr. Li's insights and comments helped me with establishing the overall direction of my dissertation. More importantly, Dr. Li taught me what research is and how research can benefit the general public in a great magnitude. I sincerely believe I will always benefit from the past five years' work with Dr. Li throughout my professional career. Five years ago, when I came to the University of Louisville for the first time, I was unsure how my future would be like. Five years later, I clearly understand where my career path will lead me and what kind of scientific researcher I should be. I am truly grateful for that.

I want to thank my dissertation committee members for their support and encouragement throughout my study at the University of Louisville. My thankfulness goes to Dr. J.P. Mohsen. I met Dr. Mohsen in Chongqing six years ago, and I appreciated that I could have a chance to discuss the potential opportunity of starting my Ph.D. journey in the United States. I also would like to thank Dr. Zhihui Sun for accepting being my dissertation committee. Dr. Sun offered me support and encouragement when I felt depressed with my research. I am very grateful to have Dr. Ahmed Desoky as my dissertation committee member. He offered me so much guidance and helped when I learned statistical modeling with continuous support and constructive comments on my research. In addition, I was also grateful that I could have the opportunity to work with

some of the excellent professors at the University of Louisville. Thank Dr. Yi Wang from the Department of Communication and Dr. Qi Zheng from the Department of Bioinformatics and Biostatistics for sharing their knowledge of their specialized field.

Many thanks go to the Kentucky Transportation Cabinet (KYTC) for their funding support through my research. Specifically, I would like to express my appreciation to Ms. Shane McKenzie, Mr. Jarrod Stanley, Mr. Jason Siwula, Mr. David Durman, Mr. Brad Franklin, and Mr. Brian Schroeder. All of my research data came from the research projects funded by KYTC.

I also would like to thank my fellow graduate researchers, Mr. Abdulmaged Algomaiah, Mr. Muting Ma, Mr. Taoran Li, and Mr. Yingfan Gu from the Center for Transportation Innovation, University of Louisville, for their help during data collection, sharing research ideas, and most importantly, being such good friends. Also, I would like to thank Mr. Shang Jiang from the University of Canterbury for the guidance in terms of deep learning-based modeling techniques.

A big shout-out also goes to the Orangetheory Fitness Studio at the Highland, Louisville. I feel extremely grateful for joining this tremendous studio and working out after a busy day of work so that I can stay positive for conquering any obstacles during the pursuit of my Ph.D. title. I have always been inspired by all coaches and staffs at the Highland studio and learnt that I can always go “all out” for any tasks in my life.

Last but not least, this dissertation is dedicated to my parents, Mr. Xu Wang, and Mrs. Ping Li. They offered me their unconditional love and support throughout my study in a different country.

ABSTRACT

MODELING DRIVER DISTRACTION MECHANISM AND ITS SAFETY IMPACT IN AUTOMATED VEHICLE ENVIRONMENT

Song Wang

November 30, 2021

Automated Vehicle (AV) technology expects to enhance driving safety by eliminating human errors. However, driver distraction still exists under automated driving. The Society of Automotive Engineers (SAE) has defined six levels of driving automation from Level 0~5. Until achieving Level 5, human drivers are still needed. Therefore, the Human-Vehicle Interaction (HVI) necessarily diverts a driver's attention away from driving.

Existing research mainly focused on quantifying distraction in human-operated vehicles rather than in the AV environment. It causes a lack of knowledge on how AV distraction can be detected, quantified, and understood. Moreover, existing research in exploring AV distraction has mainly pre-defined distraction as a binary outcome and investigated the patterns that contribute to distraction from multiple perspectives. However, the magnitude of AV distraction is not accurately quantified. Moreover, past studies in quantifying distraction have mainly used wearable sensors' data. In reality, it is not realistic for drivers to wear these sensors whenever they drive. Hence, a research motivation is to develop a surrogate model that can replace the wearable device-based data to predict

AV distraction. From the safety perspective, there lacks a comprehensive understanding of how AV distraction impacts safety. Furthermore, a solution is needed for safely offsetting the impact of distracted driving.

In this context, this research aims to (1) improve the existing methods in quantifying Human-Vehicle Interaction-induced (HVI-induced) driver distraction under automated driving; (2) develop a surrogate driver distraction prediction model without using wearable sensor data; (3) quantitatively reveal the dynamic nature of safety benefits and collision hazards of HVI-induced visual and cognitive distractions under automated driving by mathematically formulating the interrelationships among contributing factors; and (4) propose a conceptual prototype of an AI-driven, Ultra-advanced Collision Avoidance System (AUCAS-L3) targeting HVI-induced driver distraction under automated driving without eye-tracking and video-recording.

Fixation and pupil dilation data from the eye tracking device are used to model driver distraction, focusing on visual and cognitive distraction, respectively. In order to validate the proposed methods for measuring and modeling driver distraction, a data collection was conducted by inviting drivers to try out automated driving under Level 3 automation on a simulator. Each driver went through a jaywalker scenario twice, receiving a takeover request under two types of HVI, namely “visual only” and “visual and audible”. Each driver was required to wear an eye-tracker so that the fixation and pupil dilation data could be collected when driving, along with driving performance data being recorded by the simulator. In addition, drivers’ demographical information was collected by a pre-experiment survey.

As a result, the magnitude of visual and cognitive distraction was quantified, exploring the dynamic changes over time. Drivers are more concentrated and maintain a higher level of takeover readiness under the "visual and audible" warning, compared to "visual only" warning. The change of visual distraction was mathematically formulated as a function of time. In addition, the change of visual distraction magnitude over time is explained from the driving psychology perspective. Moreover, the visual distraction was also measured by direction in this research, and hotspots of visual distraction were identified with regard to driving safety. When discussing the cognitive distraction magnitude, the driver's age was identified as a contributing factor. HVI warning type contributes to the significant difference in cognitive distraction acceleration rate. After drivers reach the maximum visual distraction, cognitive distraction tends to increase continuously. Also, this research contributes to quantitatively revealing how visual and cognitive distraction impacts the collision hazards, respectively.

Moreover, this research contributes to the literature by developing deep learning-based models in predicting a driver's visual and cognitive distraction intensity, focusing on demographics, HVI warning types, and driving performance. As a solution to safety issues caused by driver distraction, the AUCAS-L3 has been proposed. The AUCAS-L3 is validated with high accuracies in predicting (a) whether a driver is distracted and does not perform takeover actions and (b) whether crashes happen or not if taken over. After predicting the presence of driver distraction or a crash, AUCAS-L3 automatically applies the brake pedal for drivers as effective and efficient protection to driver distraction under automated driving. And finally, a conceptual prototype in predicting AV distraction and

traffic conflict was proposed, which can predict the collision hazards in advance of 1.10 seconds on average.

TABLE OF CONTENTS

LIST OF TABLES

LIST OF FIGURES

CHAPTER 1: INTRODUCTION

1.1 Background

While Automated Vehicle (AV) technology has emerged to provide warnings, assistance, or guidance to ensure safe driving, driver distraction is still a critical component under automated driving in terms of driving safety. A notable reason is that the Society of Automotive Engineers (SAE) has defined six levels of automation from Level 0 (zero automation) to Level 5 (full automation) (SAE International, 2016). As long as Level 5 automation has not been achieved, human drivers are still needed in the automated driving environment. For example, human drivers are responsible for monitoring the driving environment and taking over the vehicle, if necessary, under Level 1 or 2 automation. Although human drivers do not need to monitor the driving environment under Level 3 automation, they are still required for taking over the vehicle if the Level 3 Automated Driving System (ADS) requests. Therefore, human drivers need to be alerted if in a vehicle operating under Level 3 automation. Under this context, the Human-Vehicle Interaction (HVI) necessarily diverts a driver's attention away from safe driving. Moreover, existing research has suggested that the delayed response to HVI under AV disengagement causes safety issues (S. Wang & Li, 2019a, 2019b). To summarize, it is imperative to understand, quantify, and predict driver distraction under automated driving so that strategies can be proposed in alleviating the impact of driver distraction on safety.

Driver distraction has been widely studied, along with modeling visual and cognitive distraction as well as their influences on driving safety (Choudhary & Velaga, 2017a; Hansen et al., 2017; P. Li et al., 2021; Y. Liang & Lee, 2014; Oviedo-Trespalacios et al., 2016; Y. Zhang et al., 2021a). Existing research mainly focuses on measuring non-AV-related driver distraction. Specifically, these driver distraction methods are typically achieved through Detection Response Task (DRT) (Bruyas & Dumont, 2013; Conti-Kufner, 2017; Engström et al., 2013; Innes et al., 2019; Thomas A Ranney et al., 2014; Stojmenova & Sodnik, 2018a), including some of the most recent studies (Biondi et al., 2020; G. Li et al., 2021; Trommler et al., 2021b). Distraction was quantified by the response times and the hit rates as participants are required to respond to a sensory stimulus every 3-5 seconds (Standardization, 2016). Longer reaction times or lower hit rates indicate a higher level of driver distraction. Moreover, similar techniques have been employed in measuring driver distraction, such as the box task method (Morgenstern et al., 2020; Trommler et al., 2021a) and the occlusion technique (Foley, 2008). Although these studies measured the magnitude of driver distraction by conducting various experiments, there are limitations with the existing research in modeling driver distraction from experimental design.

First, many existing studies quantified driver distraction while a human driver is operating the vehicle rather than in the automated driving environment (Morgenstern et al., 2020; Stojmenova & Sodnik, 2018a; Trommler et al., 2021a). Hence, there is a lack of knowledge on how we can understand and quantify driver distraction under automated driving. For example, these studies measured the distraction based on driving a conventional vehicle rather than an automated vehicle, which requires drivers to do tasks

that are unrelated to driving. Hence, the experimental design is not realistic, naturalistic, and suitable for directly applying to the driver distraction research under automated driving. Therefore, there is a research need to set up an experimental environment specifically designed for automated driving and address the distraction issues during the AV disengagement.

From the engineering's point of view, an ultimate solution to address the driver distraction issues is to develop a system that can detect the existence of driver distraction and minimize the impact of driver distraction. Therefore, researchers contribute to filling this gap by employing Artificial Intelligence (AI) techniques to detect driver distraction. These methods are either machine learning-based (Aksjonov et al., 2019; McDonald et al., 2020; Swathi et al., 2021; Z. Zhang et al., 2020) or deep learning-based methods (G. Li et al., 2021; Mase et al., 2020; Y. Zhang et al., 2021b; Zhao et al., 2020). Distraction under automated driving has been using these modeling techniques to model as well. The major advantage of these methods in modeling driver distraction is that drivers do not need to perform a certain non-driving related task (i.e., press the button on the steering wheel when a stimulus at present), which can be easily applied to simulation or real-world driving environment. Along with Controller Area Network-Bus (CAN-Bus) information data (i.e., speed, steering wheel angle, gas pedal position, brake pedal force), these studies have utilized one or more types of the following sensors to monitor the driver states in real-time such as visual sensors (i.e., eye tracking system, in-vehicle cameras), audio sensors (i.e., microphone), wearable sensors (i.e., electroencephalogram, heart rate monitor, galvanic skin response). Moreover, these studies predefine the circumstances that are considered as driver distraction as the ground truth data. With treating the driver distraction as a

categorical variable, these studies have employed the collected data from the aforementioned types of sensors as model inputs and developed prediction models using the predefined driver distraction as the model output. As a result, these studies have achieved high prediction accuracy in terms of detecting driver distraction. Although these studies contribute to the literature by developing models to predict driver distraction accurately and potential safety applications can be further developed based on these studies, these studies have used the Boolean binary classification of driver distraction, which is either distracted or not distracted. Furthermore, despite the fact that the driver distraction duration can be measured through eye-tracking or camera sensors, there lacks a discussion regarding the magnitude of driver distraction.

Figure 1.1 conceptually illustrates the differences between measure-based and estimation-based methods. As illustrated in Figure 1.1, measure-based research in modeling driver distraction primarily focuses on measuring the driver distraction using surrogate measures such as reaction time. Therefore, driver distraction is expected to be measured at certain timestamps depending upon the experiment design. In this case, the magnitude of driver distraction is measured as a discrete value without considering the impact from the time horizon. Figure 1.1(b) illustrates the estimation-based studies in detecting driver distraction, which primarily focuses on the occurrences of driver distraction rather than the magnitude. Moreover, there lacks an exploration of driver distraction duration, although it can be measured through visual sensors such as eye-tracking systems and in-vehicle cameras.

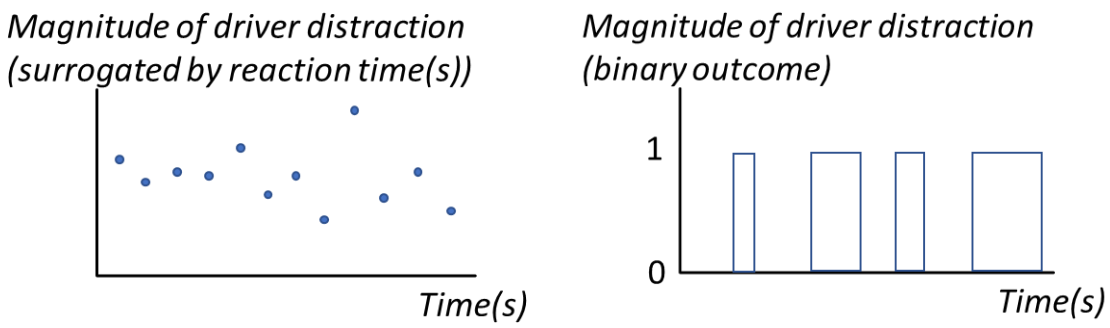

(a) **(b)**

Figure 1. 1 Conceptual Summary of Existing Research in Modeling Driver Distraction with (a) Measure-based and (b) Estimation-based Techniques.

Existing research in quantifying driver distraction has mainly employed data from wearable sensors, including eye-tracking devices (He et al., 2021; Y. Liang & Lee, 2014), heart rate monitors (Brands et al., 2019; Makhtar & Sulaiman, 2020), and Electromyography (EEG) device (Y. Zhang et al., 2021a). In reality, human drivers are unlikely to wear these wearable sensors whenever they drive. Therefore, this research is also motivated to develop a surrogate method to replace the wearable device-based data to predict AV distraction.

Once the distraction under automated driving can be quantified and predicted, it is time to investigate how driver distraction under automated driving impacts driving safety. Existing research also discussed the safety impacts brought by driver distraction. The collision hazards or safety effects caused by driver distractions are measured by the number of crashes, number of near-crashes, minimum time-to-collision (TTC), and braking reaction time. For example, Gao & Davis (2017) investigated the impact of driver distraction on the driver's brake reaction time in freeway rear-end events in a car-following situation. It was concluded that driver distraction was associated with reaction time. Distraction duration (the distracted status when a leader braked) and secondary tasks were

related to reaction time. Yannis et al. (2016) investigated the impact of texting on young drivers' behavior and safety when driving on a simulator. Texting leads to increased crash probability and shorter TTC.

By comparing to visual distraction, the changes in driving performance associated with cognitive distractions have been shown to be qualitatively different (Angell et al., 2006; Engström et al., 2005). One of the major differences is the lane-keeping performance. Strayer et al. (2015) indicated that visual distraction had been shown to increase lane position variability, whereas cognitive distraction has been shown to decrease the variability of lane position. Another major difference is stems from eye movement. Many studies have also found that the driver's visual scanning behavior is more likely to narrow towards the center of the road if he or she is cognitively distracted (Engström et al., 2017; Kountouriotis et al., 2016; Kountouriotis & Merat, 2016; Y. Liang & Lee, 2010).

While existing studies have evaluated collision hazards caused by distracted driving in either macroscopic or microscopic manner, the function of collision hazards caused by distracted driving with the aforementioned contributing factors is not well-established. In other words, the dynamic nature of how and why driver distraction results in collision hazards have not been theoretically modeled. Understanding the driver distraction mechanism will be facilitated if the collision hazards caused by distracted driving can be mathematically described. Vehicle manufacturers can benefit from it the protocol in designing their own distracted driving warning system.

Moreover, driving safety expects to be more enhanced with vehicle-to-infrastructure (V2I) wireless communication enabled by CAV technologies. The CAV technology allows data exchange between vehicles and infrastructures so that drivers are

notified with safety warnings via in-vehicle heads-up or heads-down displays. Although the CAV technology expects to enhance driving safety, human drivers are still responsible for responding to the issued safety warnings. For example, when CAV alerts drivers with a driving safety-related warning, the driver expects to receive the safety benefits provided by the CAV if he or she acts in response to the warning. If the warning is displayed for an extended period that exceeds the time driver's need for processing the meaning of the warning message, the driver's attention will voluntarily be diverted away from the road from time to time. Hence, there is a tradeoff in the display duration that drivers can receive maximum safety benefits provided by CAV technology and minimum collision hazards caused by diverted attention away from the road. In addition, similar tradeoffs in terms of display location (i.e., in-vehicle heads up display, in-vehicle heads-down display, center stack, infotainment), transparency percentage of the displayed safety warning (limited to in-vehicle heads-up display), etc. Existing studies have not identified the optimized thresholds regarding the aforementioned parameters in designing the HVI under the CAV environment.

On the other hand, many of the driving tasks currently performed by human drivers are becoming automated. For example, Level 2 and Level 3 driving automation enables technology readiness to provide human drivers with hands-free and feet-free driving under certain circumstances. However, these levels of driving automation require human drivers to take over driving due to a technology issue caused by the perception, planning, and control of automated vehicles (S. Wang & Li, 2019a). Human drivers expect to take over driving immediately to avoid any potential crashes or near-crashes in these cases. The aforementioned tradeoff issues still exist in vehicles operating under automated driving,

especially under Level 2 or Level 3 automation. Any design flaws regarding the take-over request such as display location, display duration, and transparency of the displayed safety warning (limited to in-vehicle heads-up display) will result in a longer perception-reaction time in response to the take-over request. Suppose the human driver is in a low Situation Awareness (SA) level or distracted by any non-driving related tasks. In that case, it might take an extended time to take over the driving and cause potential collision hazards**.** Existing studies have not identified the optimized thresholds regarding variables of take-over request in automated driving systems, either.

In order to further improve the design of HVI under AV technology by bringing more safety benefits and less distraction to the driver, it is necessary to understand how Advanced Driver-Assistance System (ADAS) or Automated Driving System (ADS) work, especially to mathematically describe the safety benefits and hazards of ADAS and automated driving systems from the mechanisms' perspective. For example, a key parameter in designing ADAS is the duration of issuing safety warnings. The traditional approach of identifying the duration of issuing a safety warning in achieving the maximum safety benefits is to test multiple sets of durations of issuing safety warnings through a driving test, which is time-consuming and inaccurate. Once the mechanisms of both safety benefits and distraction of ADAS are mathematically formulated, the optimum values of the parameters in designing ADAS (i.e., duration of issuing safety warnings) in maximizing safety benefits can be obtained without conducting driving experiments, which is more accurate and convenient.

Although the emerging AV technology acts as a game-changer in improving driving safety performance by eliminating collision hazards caused by human errors, driver

distraction is still a primary concern of driving safety (Cunningham & Regan, 2018; He & Donmez, 2019; S. C. Lee et al., 2021; Q. Li et al., 2021). A major reason is that human drivers are more or less responsible for performing certain driving tasks depending upon the level of automation unless the vehicle is operating under full automation (SAE International, 2018), which might take a few decades. Therefore, driver distraction will still exist under the CAV environment for a long period of time. Existing research has been investigating driver distraction under automated driving. Evidence from current practice has been focusing on non-driving related tasks on either takeover performance or driving safety under automated driving (Choi et al., 2020; Du et al., 2019; S. C. Lee et al., 2020; Wörle et al., 2020; Y. Wu et al., 2020). Although these studies extensively explored the potential hazards under specific non-driving related tasks through both qualitative and quantitative analysis, there lacks an investigation on how to anticipate the collision hazards due to driver distraction and take actions in advance to improve driving safety.

On the other hand, existing studies have been proposing and developing takeover warning systems under specific automated driving systems that can increase drivers' situation awareness so that the takeover action can be performed in a timely manner (He et al., 2021; S. Ma et al., 2021; W. Zhang et al., 2021). Despite the fact that these systems effectively alert drivers in response to an upcoming takeover, the decision to take over the driving is still up to the driver. Any miscommunication between the driver and the system has the potential to result in collision hazards.

The motivations for exploring the driver distraction under automated driving and proposing takeover warning systems come from the terms and definitions of automated driving levels guidelines proposed by the Society of Automotive Engineers (SAE). Per

SAE (SAE International, 2018), the Level 3 Automated Driving System (ADS) requires human drivers to drive when the system requests. However, when the automated driving features are engaged, SAE suggests that human drivers are just seated in the driver's seat and not responsible for monitoring the driving environment. The definition from the SAE leads to a two-part unsafe driving situation:

(1) Human drivers might not be ready to take over the driving as quickly as possible due to potential driver distraction caused by non-driving related tasks. Existing research has suggested that non-driving related tasks significantly impact takeover time (Dogan et al., 2019; Q.-F. Lin et al., 2021; Q. Lin et al., 2020; Naujoks et al., 2019; Wandtner et al., 2018). Unlike manual driving, drivers are less likely to be fully engaged when automated driving is in session. For example, their hands might not be on the steering wheel, and their foot might not be on top of the pedal, attempting to take over the driving under automated driving.

(2) Even if taken over, it is still possible to result in crashes or collision hazards if the driver spends an excessive period of time on taking over or the deceleration rate is not large enough. Existing research has confirmed that longer takeover time significantly impacts the takeover quality in the format of either lateral control or longitudinal control (Du et al., 2020; S. C. Lee et al., 2021).

Moreover, it has been proven that the aforementioned unsafe situations can happen in the real world. In March 2018, a jaywalker was hit by a self-driving Uber in Tempe, Arizona (Wakabayashi, 2018). The National Transportation Safety Board (NTSB) investigated the fatal crash onsite. It published the final report, revealing that the "safety driver" in the self-driving Uber did not take over the driving as requested, who was visually

distracted with non-driving related tasks while colliding with the jaywalker (National Transportation Safety Board, 2018). To summarize, the human driver still plays an important role in determining the safety of automated driving, especially when the automation level has not achieved Level 5 (full) automation. In particular, as the base level of ADS, Level 3 (conditional) automation has the potential to maintain the impact of driver distraction at a high level on takeover quality and, in turn, driving safety under automated driving. As collision avoidance systems (i.e., forward collision avoidance system) have already entered the vehicle market, these systems are conflict-actuated, in which the collision avoidance system works only there are collision hazards about to happen. Therefore, to address the aforementioned issues, what if a collision avoidance system can be added on Level 3 ADS, with predicting the occurrence of a crash in advance so that the current collision avoidance system can be better improved?

Under this context, developing an AI-driven, Ultra-advanced Collision Avoidance System (AUCAS-L3) under Level 3 ADS is highly needed, in which this research attempts to fill this gap. The AUCAS-L3 attempts to prevent collision hazards from happening by addressing the aforementioned issues regarding the absence of taking over when Level 3 ADS requests and the occurrences of traffic conflicts due to excessive long period of takeover time or low deceleration rate. By employing deep learning techniques, the AUCAS-L3 has the capability of automatically applying the brake pedal if (1) predicted the absence of takeover actions due to driver distraction before running into any complex or sudden driving situations where a takeover action is needed; and (2) predicted the probability of having a crash or traffic conflict prior to the occurrence of the crash or the conflict severity that could be measured. Therefore, this research contributes to the

literature by developing an “add-on” automated braking system under Level 3 ADS that can anticipate the safety hazards due to driver distraction and take actions in advance to prevent them from happening. Moreover, the “add-on” automated braking system requires non-human drivers’ involvement to address the controversy regarding AUCAS-L3 regarding human drivers’ responsibility.

1.2 Research gap identification

In summary, the problems that lie in the current practice of driver distraction-related research can be identified as follow:

- Existing research in measuring driver distraction has mainly conducted in human-operating vehicles with requiring human drivers to perform additional tasks, which is unnaturalistic and not suitable for applying the experimental design and results directly to the modeling of driver distraction under automated driving.
- Existing research in measuring driver distraction under AV environment has mainly pre-defined driver distraction as a binary variable (distracted vs. not distracted), which is not quantified accurately and there lacks a comprehensive understanding of driver distraction under automated driving from other dimensions.
- There lacks a surrogate method that predicts driver distraction under automated driving without using data collected by wearable devices (i.e., eye-tracker, heart rate monitor, EEG device).
- There lacks a further investigation on how driver distraction, including visual and cognitive distraction, influences collision hazards through a quantitative manner.

- There is a research need in conceptualizing, proposing, and developing a prototype as an ultimate solution in offsetting distraction's impact on safety by predicting the occurrences of collision hazards due to driver distraction under automated driving.

1.3 Research objectives

In order to address the aforementioned research gaps in Section 1.2, the following objectives are established for this research:

Objective 1: Improve the existing methods in quantifying Human-Vehicle Interaction-induced (HVI-induced) driver distraction under automated driving.

- **Objective 1.1:** Improve the existing methods in quantifying HVI-induced visual distraction under automated driving by adding direction and duration dimensions, with focusing on eye movement data and including temporal and spatial measures.
- **Objective 1.2:** Improve the existing methods in quantifying HVI-induced cognitive distraction under automated driving by incorporating pupil dilation performance.

Objective 2: Develop a surrogate driver distraction prediction model without wearable sensors' data.

Objective 3: Quantitatively reveal the dynamic nature of safety benefits and collision hazards of HVI-induced visual and cognitive distractions under automated driving by mathematically formulating the interrelationships among contributing factors.

Objective 4: Propose a conceptual prototype of an AI-driven, Ultra-advanced collision avoidance system targeting HVI-induced driver distraction under automated driving with eye-tracking free and video-recording free.

1.4 Outline of research methodology

Figure 1.2 illustrates the heuristic framework of the research methodology.

Firstly, an eye-tracker is applied as the major device to collect driver's fixation and pupil dilation information, which is used to model visual and cognitive distraction, respectively. By conducting a driving simulator study in a vehicle operating under Level 3 automation, the aforementioned gaze behavior data can be collected if study subjects (human drivers) wear the eye-tracker while performing the driving simulator study.

Second, the fixation and pupil dilation data reductions are then performed by identifying the fixation information (fixation location, duration) and pupil dilation information (baseline pupil diameter, changes of pupil diameter in percentage) during the process of HVI. Both the fixation and pupil dilation data reduction are completed until the driver engages in the driving. Per definition, driver distraction is a shift in attention away from safe driving towards a competing task. Specifically, visual distraction is defined as drivers' eyes off the road, while cognitive distraction is defined as drivers' minds off the road. Existing research has proved that the driver's eye movement features can be a good indication of both visual and cognitive distraction (Hurtado & Chiasson, 2016; Kret & Sjak-Shie, 2019; Sullivan et al., 2017; Topolšek et al., 2016). Therefore, the fixation data is used to model the driver's visual distraction, while the pupil dilation data is used to model the driver's cognitive distraction. Specifically, the fixation data provides the readiness for modeling visual distraction from three perspectives: magnitude, direction, and time. Visual distraction magnitude is reflected by the fixation distance to the zero point of the visual distraction magnitude when driving. The visual distraction direction information can be obtained by converting the fixation location data from the Cartesian coordinate system to the polar coordinate system. The fixation's duration reflects visual distraction time.

On the other hand, cognitive distraction is one-dimensional data and is reflected by the driver's pupil dilation. As every individual's pupil diameter is different, the pupil dilation is in a percentage format that measures the increase of pupil diameter as the indicator of cognitive distraction. A higher increase of pupil diameter in percentage suggests a higher cognitive distraction magnitude. The visual and cognitive distraction intensity is computed by integrating visual and cognitive distraction magnitude on time. Meanwhile, the changes of driver distraction in real-time are modeled through various statistical modeling and deep learning approaches.

Third, the dynamic nature of how driver distraction influences driving safety is revealed quantitatively. Structural Equation Modeling (SEM) analyses are performed with focusing on both visual and cognitive distraction intensity. The potential factors that are investigated include takeover time, takeover warning types, age, and gender. The identified significant factors are regarded as mediating factors that explain why driver distraction impacts the probability of having a crash or near-crash.

Fourth, the optimized takeover time and driver's age are obtained through a classification tree model. Through the modeling results, specific groups of drivers with age, gender identification are summarized in recommending the use of HVI types in terms of warning modalities.

Finally, a conceptual prototype of the "add-on" application is proposed in this research with addressing the collision hazards due to driver distraction under automated driving. The prototype has two "built-in" prediction functions that can predict whether the driver will take over the driving if requests and whether a traffic conflict will happen if taken over with employing the Artificial Neural Network (ANN) techniques. Once

predicted, the prototype can apply the brake pedal for drivers to avoid any traffic conflicts. The proposed prototype can be the ultimate solution to the collision hazards brought by driver distraction under the CAV environment.

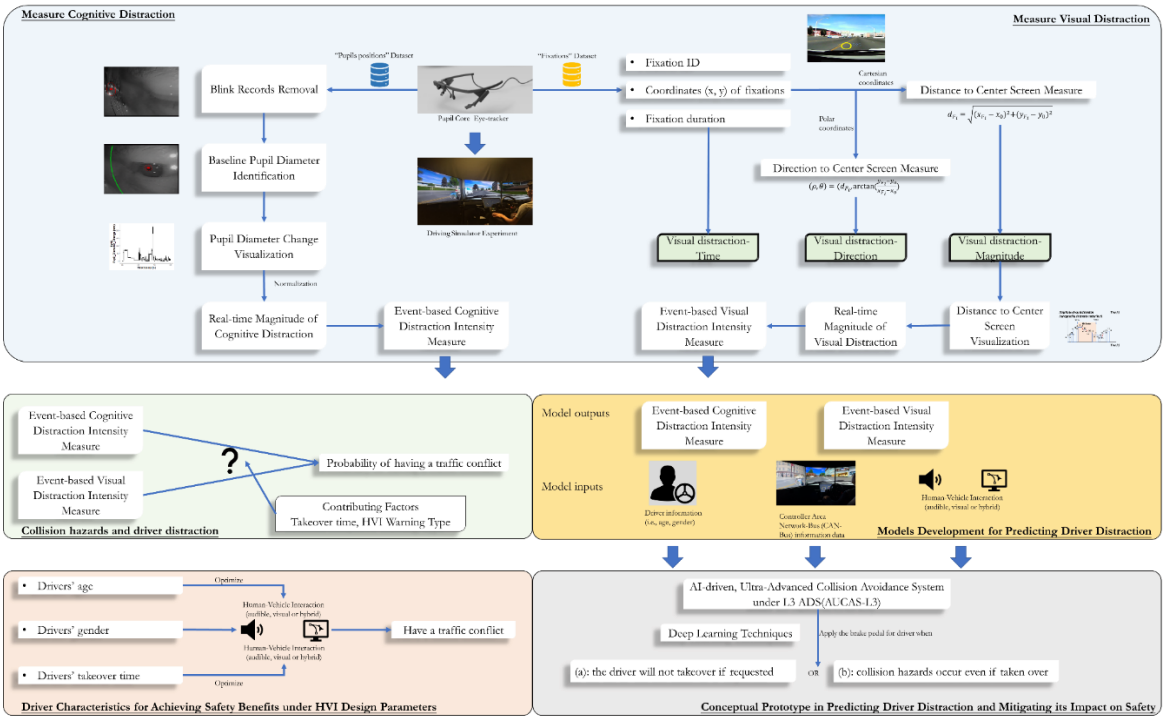

Figure 1. 2 Outline of Research Methodology

1.5 Organization of the dissertation

The dissertation is organized in the following sequence:

Chapter 2 presents an extensive literature review on the current practice of driver distraction research, including both measure-based and estimation-based driver distraction studies. Chapters 3 and 4 discuss the visual and cognitive distraction modeling results and their impact on driving safety, respectively. Chapter 5 presents the framework for developing the optimization function to achieve the maximal safety benefits and discusses the focus groups that recommend or do not recommend for specific modality of HVI.

Chapter 6 proposes the conceptual prototype of AI-driven, Ultra-advanced collision avoidance system with targeting HVI-induced driver distraction under automated driving and discusses its readiness in practice. Chapter 7 wraps the dissertation by drawing conclusions of this research, reinstating research limitations, and proposing future research directions.

CHAPTER 2: LITERATURE REVIEW

2.1 Driver distraction definitions

Driver distraction has become an important issue of road safety throughout the entire world. The definition of driver distraction has been discussed from multiple perspectives to understand it comprehensively. Driver distraction is defined as activities diverting a driver's attention, according to the National Highway Traffic Safety Administration (NHTSA), which includes anything that takes the driver's attention away from safe driving (i.e., talking over phone or texting, talking to people inside the vehicle, eating and driving). Treat (1980) summarized driver distraction as whenever "a driver is delayed in recognizing the information needed to safely accomplish the driving task due to the compelling of some event, activity, object, or person within or outside the vehicle that shifting driver's attention away from the driving task". Tijerina (2000) classifies driver distraction into two categories, namely "selective withdrawal of attention and biomechanical interference". The former one is based on eyelid closure or eyes away from the road scene. The latter refers to the body shifting out of the "neutral seated position". T A Ranney et al. (2001) have included cognitive distraction in the discussion of driver distraction, in which drivers are "lost in thought" and their attention is diverted away from the driving task to their thoughts without being distracted by external sources. Beirness et al. (2002) discovered that it is necessary to distinguish driver inattention from distraction. Green (2004) indicates that the driver's attention is pulled away instead of being redirected voluntarily when distracted driving.

J. D. Lee et al. (2008) discussed various issues regarding the precision in terms of defining “driver distraction”. They suggested a definition of driver distraction from four perspectives:

1) Driver distraction is delayed by the driver in the process of recognizing necessary information to maintain the vehicle safely from both the lateral and longitudinal controls.
2) Driver distraction is caused due to any activity, event, object, or person inside or outside the vehicle.
3) Driver distraction compels or tends to induce the driver’s attention away from driving tasks.
4) Driver distraction compromises the driver’s auditory, biomechanical, cognitive, or visual facilities or combinations.

Hedlund et al. (2006) defined driver distraction as a “diversion of attention from driving”, reducing the driver’s situation awareness, decision-making ability, and vehicle performance, as well as increasing the probability of having near-crashes, or crashes. J. D. Lee et al. (2008) revealed the definition of driver distraction as “the diversion of attention away from activities critical for safe driving toward a competing activity”.

In summary, researchers have been refining the definition of driver distraction over the last 40 years. It can be concluded that when driving is distracted, a diversion of the driver’s attention will occur to a more competing activity or object located either inside or outside the vehicle, which extends the driver’s Perception-Intellection-Emotion-Volition (PIEV) process in safely maintaining the vehicle control from the perspectives of the lateral

and longitudinal control. Driver distraction can be classified as a visual distraction and cognitive distraction.

2.2 Driver distraction studies

2.2.1 Quantification of driver distraction

Existing research measuring driver distraction has mainly adopted the following three methods to measure driver distraction: (a) Detection Response Task (DRT), a method for assessing the "attentional effects of cognitive load in a driving environment", which requires a driver to respond to a stimulus showing up with a certain frequency (Kashevnik et al., 2021); (b) box task method, a method is designed to quantify the cognitive load under various non-driving-related tasks (Trommler et al., 2021b); and (c) occlusion technique, a method in estimating the visual workload of a driver with wearing a special helmet (Kujala et al., 2021). Table 2.1 summarizes the current practice in modeling driver distraction using measure-based techniques.

Table 2. 1 Summary of Existing Research in Modeling Driver Distraction with Measure-based Techniques

Authors	Measure-based techniques	Experimental setup	Findings
Trommler et al. (2021)	DRT + box task method	• Asked participants to react to the presented signal by pressing a button at the steering wheel. • Used the box task to simulate a car-following scenario and asked participants to adjust the size of the box by moving the steering wheel.	• DRT + box task method is an easy-to-use method for measuring visual and cognitive distraction of drivers.
Morgenstern et al. (2020)	Box task method	• Drivers were asked to perform one of the following tasks: box task + DRT, the lane-change test, driving through a simple course on the simulator.	• The box task method reveals comparable results to the lane-change test. • Reaction time was significantly higher if the driver was texting and entering the

			destination than the benchmark driving
N. Li & Boyle (2020)	DRT	• Participants were asked to perform driving tasks with two difficulty levels in three modalities (audio-only, visual-only, hybrid).	• Visual-only mode significantly increases participants' cognitive load with a longer response time compared to audio-only.
Biondi et al. (2020)	DRT	• Participants were asked to complete one of the four experimental tasks with increasing levels of cognitive demand.	• A larger pupil diameter was observed when the n-back task was performed with the DRT in session. • The significant increase in cognitive load that accompanies DRT performance was also reflected in "higher self-reported workload".
Guo et al. (2020)	DRT	• Instructed participants to respond to the vibrated tracker by clicking the button against the steering wheel when a tactile stimulus was presented.	• Response rate is considered a solid indicator for the cognitive workload. • Response time does not appear to effectively detect cognitive workload.
Innes et al. (2019)	DRT	• Participants performed multiple object tracking tasks while performing a DRT simultaneously.	• The DRT is sensitive to workload changes.
Stojmenova & Sodnik (2018b)	DRT	• Participants performed driving sessions with driving, responding to DRT stimuli, and conducting a cognitive task.	• Auditory DRT version is more sensitive to the cognitive load's effect.
Conti-Kufner (2017)	DRT	• The sensitivity of head-mounted, remote, and tactile DRT was evaluated.	• Head-mounted DRT has the minimal "obtrusive and affected concurrent task performance of other tasks the least".
Bruyas & Dumont (2013)	DRT	• Participants tried three DRT versions with head-mounted, tactile, and remote DRT. • Two driving scenarios were applied: driving on the motorway following the speed limit and driving through a series of curves.	• DRT response time increases if the driving demand or the difficulty of the cognitive auditory task increases.
Foley (2008)	Occlusion technique	• Drivers were required to wear the occlusion goggles when performing driving tasks.	• The occlusion technique is an effective method in determining the demand of the driving situation.

2.2.2 Patterns contributing to driver distraction

Technology readiness has offered the potential of collecting data from multiple sources so that driver distraction can be accurately estimated. The estimation-based driver distraction studies collected data from the perspectives of driving performance, eye movements, and physiological data. Specifically, the driving performance was collected by focusing on the lateral control, such as steering wheel turning angle (Z. Li et al., 2018; Y. Liang & Lee, 2014; Yekhshatyan & Lee, 2013; Y. Zhang et al., 2021a), and longitudinal control, including deceleration rate (Haque & Washington, 2015; Z. Li et al., 2018; Przybyla et al., 2015), vehicle speed (Aksjonov et al., 2019; Choudhary & Velaga, 2020; Iio et al., 2021; Iranmanesh et al., 2018; Z. Li et al., 2018; Y. Zhang et al., 2021a). Eye movement data has been proved as a good indication of both visual and cognitive distraction. Drivers' distraction level can be estimated with their gaze behaviors in terms of fixations (Christian & Krause, 2017; Q. Li et al., 2021; Y. Liang & Lee, 2014; Yekhshatyan & Lee, 2013) and pupil dilation (Pfleging et al., 2016; F. Zhou et al., 2021). Recently, physiological data has been favored by researchers to detect driver distraction, including information on heart rate (Kuo et al., 2015), skin conductance (Y. Zhang et al., 2021a), and the electroencephalogram (EEG) (G. Li et al., 2021; Wali et al., 2021).

With the availability of multi-modal data sources, existing research has been employing machine learning or deep learning techniques to train, test, and validate the estimated results of driver distraction. Y. Liang & Lee (2014) developed a "layered algorithm" integrating the "Dynamic Bayesian Network" and supervised clustering to detect cognitive distraction by using eye movement data and vehicle performance measures. Y. Zhang et al. (2021a) introduced a deep "unsupervised multi-modal fusion network" to

detect driver distraction due to non-driving-related tasks (i.e., texting, eating, phone conversation). Z. Li et al. (2018) improved the driver distraction detection accuracy with a nonlinear autoregressive exogenous driving model focusing on naturalist driving data.

Furthermore, these studies predefine the circumstances that are considered as driver distraction as the ground truth data. For example, Zhang et al. (2021) have created a decision rule to determine whether testing data should be classified as "distraction" or "normal driving" by calculating reconstruction error as a score. Li et al. (2018) have inspected the in-vehicle video data to determine whether the driver is attentive or distracted (i.e., texting, dialing). Liang and Lee (2014) have defined distraction as the driver performed a non-driving related task or not. Masood et al. (2020) have identified nine types of distracted driving situations (i.e., texting, calling, operating the radio) through in-vehicle camera sensors.

2.3 Measurements of driver distraction

2.3.1 Longitudinal control of the vehicle

The indicators of driver distraction in terms of longitudinal control of the vehicle are speed-related variables, steering wheel turning angles, and brake reaction time.

Burns et al. (2002) demonstrated that driving performance would be impaired with phone conversations. The study recruited twenty drivers to drive through multiple test routes on a driving simulator. As a result, drivers tend to slow down if they talk via phones. According to speed-related performance measures such as standard deviation of speed, drivers had a significantly poorer control in terms of speed if using the hand-held phone. Jenness et al. (2002) measured driving performance with twenty-six participants driving on a simulator while eating, operating a CD player, reading directions, or placing calls by

using a voice-activated dialing system. The results suggest that reading while operating the CD player has the largest safety impact. Engström et al. (2005) investigated the effects of visual and cognitive load with the in-vehicle information system. They concluded that visual demand led to speed reduction and increased lane-keeping variation, while cognitive load increased gaze concentration toward the center of the road. Lansdown et al. (2004) investigated the impact of various in-vehicle information systems on the driver via a driving simulator study. Results reveal that interacting with secondary tasks resulted in significant speed reductions. Distractions from two separate tasks that happen simultaneously lead to a significantly greater mental workload on the driver compared to the distraction from one secondary task.

Kountouriotis & Merat (2016) validated the finding that under "non-visual distractions" (i.e., talking on the phone, engaging verbal tasks that do not require a visual input), reduced lateral variability in steering and gaze patterns are fewer variables where participants concentrate their gaze towards the center of the road and their control in terms of the steering wheel. They concluded that driver distraction affects gaze, speed, and steering control.

Gao & Davis (2017) investigated the impact of driver distraction on the driver's reaction time in freeway rear-end events under a car-following situation. Driver distraction was associated with reaction time. Distraction duration and the type of secondary tasks were related to reaction time. Strayer et al. (2014) measured cognitive distraction while driving via three experiments. The experiment involved participants performing different mental tasks (i.e., listening to the radio, conversing with a passenger) while seated at a computer monitor to establish the cognitive workload of each task. Then, they were asked

to drive on a simulator with a lead vehicle. Performance measures such as brake reaction time and following distance were measured. In the last experiment, participants were required to drive an instrumented vehicle in a residential area while performing the tasks in the first experiment. Eye movement data were recorded this time. They concluded that the introduction of a voice-based system might increase driver distraction.

In summary, driver distraction indicators from the vehicle's longitudinal control are mainly discussed through vehicle speed. However, simply measuring driver distraction through speed is incomprehensive because the impact of driver distraction on vehicle control is expected to be longitudinal and lateral.

2.3.2 Lateral control of the vehicle

Reed & Green (1999) compared the driving performance of six male and female drivers in driving on a freeway while occasionally dialing simulated phone calls. They found that the addition of the phone task increased the mean lateral speed in the vehicle by approximately 43%, while in the simulator, the mean lateral speed increased by 158% with adding the phone task. Burns et al. (2002) assessed driving performance by twenty-one drivers through the Lane Change Test (LCT), a simple and low-cost standardized test scenario designed to measure driver distraction. The results suggest that participants showed greater lane deviation when changing path and performing a secondary task, compared to the circumstance without performing a secondary task. Besides, differences were also reflected in participants' duration in completing the secondary tasks. Cooper et al. (2009) investigated driver distraction when the tipping point of traffic flow stability is reached. It was concluded that driver distraction was found to affect lane change frequency significantly and average speed.

Harrison & Fillmore (2011) examined the effects of alcohol and driver distraction via a driving simulator study. Forty young adult drivers were recruited using a "divided attention task" as a distracter activity. Performance measures such as standard deviation of the lateral position (SDLP) was used as an indicator of driving impairment. In contrast, divided attention increases the impairing effects of alcohol on driving precision. Young et al. (2011) evaluated lateral control ability via a Lane Change Test (LCT) and event detection parameters to distinguish between visual-manual and cognitive surrogate IVIS tasks with different demand levels. Twenty-seven participants completed the LCT while performing visual search and math problem-solving tasks. Different patterns were observed in terms of the mean deviation and lane excursion between the visual and cognitive tasks. Cades et al. (2017) investigated the effects of Lane Departure Warning (LDW) on driving performance by recruiting participants to perform a non-driving related task designed to simulate cognitive effort while driving. They concluded that cognitive engagement impacts driver control of the vehicle, and the presence of LDW did not reduce the effects of cognitive engagement in a secondary task.

2.3.3 Glance behavior

The eye-tracking system can capture the glance behavior of drivers mounted remotely on the screen of vehicles or a device worn by drivers. Past studies have found that the eye-tracking device is a valid and reliable research tool for measuring the visual workload (Strayer et al., 2014).

Farber et al. (2000) employed the eye glance technique to measure the driver's visual glance behavior by collecting the frequency and duration of eye glances at specific objects. It was concluded that drivers complete the tasks through a series of glances when

the driver performs a secondary task. Curry et al. (2002) used total eyes-off-road-time to measure the visual demand associated with the performance of a secondary task. It was concluded that the visual demand is highly correlated with the number of lane departures when performing secondary tasks. Kircher et al. (2014) conducted a driving simulator study exploring driver glance behavior with intermittent and continuous eco-driving advice. The findings revealed different glance patterns between continuous and intermittent displays. The study also indicated that drivers decrease their glance length to in-vehicle devices when the traffic situation is demanding. As mentioned above, the study conducted by Kountouriotis & Merat (2016) suggests that driver distraction affects gaze behaviors. Pipkorn & Piccinini (2020) analyzed the impact of off-path glances on rear-end conflicts through the naturalistic driving data. They concluded that the combination of short headway with glances transitioning from the road toward the mirror originates "visual mismatches" associated with a rapid change in the kinematic situation, causing the rear-end near-crashes. Starkey et al. (2020) examined the effects of an advisory speed-related smartphone application on driving performance via a driving simulator study. The statistical results indicate no negative impacts on driver behavior by measuring the standard deviation of lane position, glance frequency, and total gaze duration for the application. Besides, the application does not distract drivers if properly configured. Hammond et al. (2019) investigated driver distraction prior to different "safety-critical events". It was observed that drivers are more likely to be engaged in a safety-critical event if their glances away from forward were more than 2 seconds.

2.4 Measurement of collision hazards caused by driver distraction

2.4.1 Reaction time

Janssen et al. (1999) conducted a study to measure drivers' reaction times under the circumstances of using different real-time traffic information systems. They concluded that it is not necessarily to be considered safer by using this type of in-vehicle device than driving with a convenient way of receiving information. Olsson & Burns (2000) measured drivers' visual distraction with a Peripheral Detection Task (PDT), measuring the amount of driver mental workload and visual distraction when driving. Thirteen participants were recruited by driving different road types while performing tasks. The significant differences between different tasks were observed in terms of PDT reaction time and hit rate. A significant difference was observed in reaction time when performing different secondary tasks instead of driving on different road types. The significant difference is also reflected in hit rates among different tasks. They also concluded that the PDT is an effective tool for measuring visual distraction and mental workload in an actual vehicle. Harms & Patten (2003) also employed peripheral detection as a measurement of driver distraction. The study found that PDT impacts the navigation conditions from drivers' reaction times and hit rates. Jahn et al. (2005) investigated workload measures in driving by using peripheral detection. They concluded that the demands of traffic situations have a higher effects of the workload effects than the route guidance systems.

In summary, reaction time has been used as the indicator of collision hazards caused by driver distraction. In order to understand the mechanism of increased collision hazards caused by driver distraction, performance measures from the microscopic perspective should be included in the discussion.

2.4.2 Take-over time (under automated driving)

According to NHTSA, automated driving is expected to increase safety enhancement by eliminating human error, which accounts for 94% of all crashes. As long as the automated vehicle technology has not achieved full automation (Level 5), human drivers are still expected to take over the driving when the automated driving system requests. When driving under Level 1 to Level 4, human drivers' responsibility is shifted from actively operating the vehicle to monitoring the driving environment under both hands-free and feet-free conditions.

A safe and immediate transition from automated to manual driving is highly needed. Therefore, the design of the take-over request is the key to bringing human drivers' attention to the take-over request and, in turn, switching to manual driving. Cabrall et al. (2020) investigated a design of the driver monitoring system that designed in adaptively backing up distracted drivers under automated driving. They conducted a driving simulator study by recruiting ninety-one participants driving with different forms of a driver monitoring system. They have demonstrated preliminary feasibility of the driver monitoring system the incorporate driving context information for distraction assessment. Bieg et al. (2020) examined differences in driver behavior concerning Level 2 and Level 3 automation in a driving simulator experiment with thirty-one professional truck drivers. They concluded that drivers had difficulty adapting their behavior to different demands of Level 2 and Level 3 driving. The driver reactions show potentially critical lapses in attention when driving under Level 2 driving automation. Choi et al. (2020) tested the effects of cognitive and visual workloads after take-over request, respectively. It was

concluded that both cognitive and visual loads affected driving performance after the take-over request, with the effects appearing in different time courses.

In summary, take-over time in automated driving has been used as the measurement for collision hazards caused by distraction. However, with the relationship between take-over time and minimum time-to-collision (TTC) remaining unexplored, the discussion of collision hazards caused by driver distraction in the context of automated driving is incomprehensive.

2.5 Driver distraction under automated driving

Per the definition of driving automation levels, drivers tend to be engaged in non-driving-related tasks while automated driving is in session. Therefore, these non-driving related tasks might cause driver distraction and have an impact on takeover performance as well as driving safety. Choi et al. (2020) investigated the effects of cognitive and visual workloads on driving performance after taking over under automated driving. Participants were asked to complete automated driving on a simulator with and without non-driving related tasks, respectively. The results show that the non-driving related tasks affect driving performance after issuing the takeover request. Du et al. (2019) examined the impact of drivers' emotions on takeover readiness and performance under Level 3 automation. They found that drivers have a better performance in negotiating the driving situations when they were calm. On the contrary, anger results in the "lowest takeover readiness" and the most "aggressive driving style" among all tested emotions. Lee et al. (2020) investigated the takeover quality affected by non-driving related tasks under automated driving. Longitudinal and lateral driving measures were evaluated under three categories of non-

driving related tasks. As a result, the cognitive load of non-driving related tasks had a significant and negative correlation with both longitudinal and lateral measures. Furthermore, they also found that the influence of cognitive distraction on takeover quality is severer compared to other non-driving related tasks (i.e., physical, visual). Wörle et al. (2020) conducted a simulator study to investigate driving's ability to take over the vehicle after engaging in non-driving-related sleeping tasks. The results indicate that the reaction time was extended by approximately 3-second after sleep compared to the wake condition. Wu et al. (2020) explored the effects of non-driving related tasks on driver's drowsiness under Level 3 automation. The eyeblink duration was applied to evaluate drowsiness under automated driving. The results suggest that non-driving-related task engagements extended older drivers' reaction time. Wandtner et al. (2018) evaluated the impact of different non-driving related tasks on takeover performance under automated driving. The research reveals that non-driving related tasks modalities are essential in determining the takeover performance. Yang et al. (2020) investigated glance behaviors in different levels of distraction under automated driving. They measured the "off-road glance duration" under different levels of distraction, suggesting that being eyes-off-the road before a takeover could cause more delay in the urgent takeover reaction than being hands-off-wheel. Klingegård et al. (2020) investigated how well drivers are able to engage in a non-driving-related task while automated driving is in session. They found that drivers' attention shifts from the road ahead towards the non-driving related tasks to a great extent. Lin et al. (2021) investigated the effects of various non-driving related tasks on drivers' readiness in take-over scenarios under Level 3 automation. The hands-on time was evaluated from the perspective of task, time budget, and gender. Liang et al. (2021) used an eye tracking device

to explore how visual engagement in non-driving related tasks affects changes in situation awareness of the driving environment after a takeover request. As a result, they found that time spent on viewing the driving scene is positively correlated to the dispersion of visual attention allocation.

2.6 Current practice in proposing takeover warning systems

As introduced in the previous section, drivers are prone to be engaged in non-driving related tasks under automated driving, which results in driver distraction and might cause safety hazards while driving. Therefore, existing research has proposed in-vehicle systems that can raise driver's situation awareness and bring drivers back in the loop under automated driving. He et al. (2021) tested in-vehicle displays in supporting drivers' readiness in automated vehicles. They evaluated the system with takeover requests and information on automation capability between adding and not-adding surrounding traffic information. As a result, adding the surrounding traffic information leads to more expected driving behaviors. Ma et al. (2021) proposed a two-stage warning system to address situation awareness, driving stress, and takeover performance from the single-stage warning system. They found that the two-stage warning systems increase drivers' situation awareness, reduce physiological stress, and provide better takeover performance. In addition to Ma et al. (2021), Zhang et al. (2021) further explored the optimal time intervals of two-stage warning systems by incorporating the drivers' "neuroticism personality". The results show that drivers in the 5-second time interval had the best takeover preparation. Petermeijer et al. (2017) explored the effects of takeover warning modalities on the takeover process. They found that warnings under the combination of auditory and tactile modalities leads to drivers' quicker reaction in response to a takeover warning compared

to the visual modality. Lu et al. (2019) proposed a monitoring request system before a potential takeover request. They found that drivers spent less time in taking over and a less severe conflict severity when adding the monitoring system. Niu & Ma (2021) established a warning intervention system targeting driver fatigue to investigate whether the driver is ready for taking over the vehicle safely. As a result, issuing the fatigue warning 5-second before the takeover request has greater potential to increase the safety of automated driving than issuing the fatigue warning 10-second before the takeover request. Epple et al. (2018) examined driver behaviors with a two-step takeover request procedure in different modalities, which provides drivers a choice to resume vehicle controls between a warning (first step) and an alarm (second step). The findings suggest that the two-step takeover request can increase drivers' situation awareness.

CHAPTER 3: MODELING VISUAL DISTRACTION UNDER THE AV ENVIRONMENT

3.1 Measure visual distraction under automated driving

3.1.1 Visual distraction: magnitude

In order to measure the magnitude of visual distraction, the first and foremost task is to define the zero point of visual distraction magnitude, which represents no driver distraction if the driver has the fixation point located in this zero point. The road segment type is an important factor that impacts the location of zero point of visual distraction magnitude. For example, when traveling on a tangent segment, drivers are supposed to look ahead for any unexpected driving situations in order to keep a clear vision without being visually distracted. In this case, the zero point of visual distraction magnitude is expected to be higher than the center point of the driver's eye vision. On the other hand, when traveling on a curvy segment, the zero point of visual distraction is dynamic and keeps changing because of the segments. In this research, the main objective is to model HVI-induced visual distraction under automated driving. Moreover, when automated driving (Level 3 or above) is in session, drivers are likely to look around because they are not responsible for performing any driving tasks. Therefore, the center of the driver's vision is used as the driver's visual distraction zero point.

There are two key performance measures regarding eyes off the road: temporal and spatial measures. The temporal measure indicates the duration of the driver's eyes off the road, which is to be discussed in Section 3.1.3. The spatial measure indicates the magnitude (how far away) of the driver's eyes off the road. Therefore, eye tracking data is applicable to collect eye movement data in terms of fixation, including each fixation's location and duration. Figure 3.1 conceptually illustrates the trajectory of eye fixations.

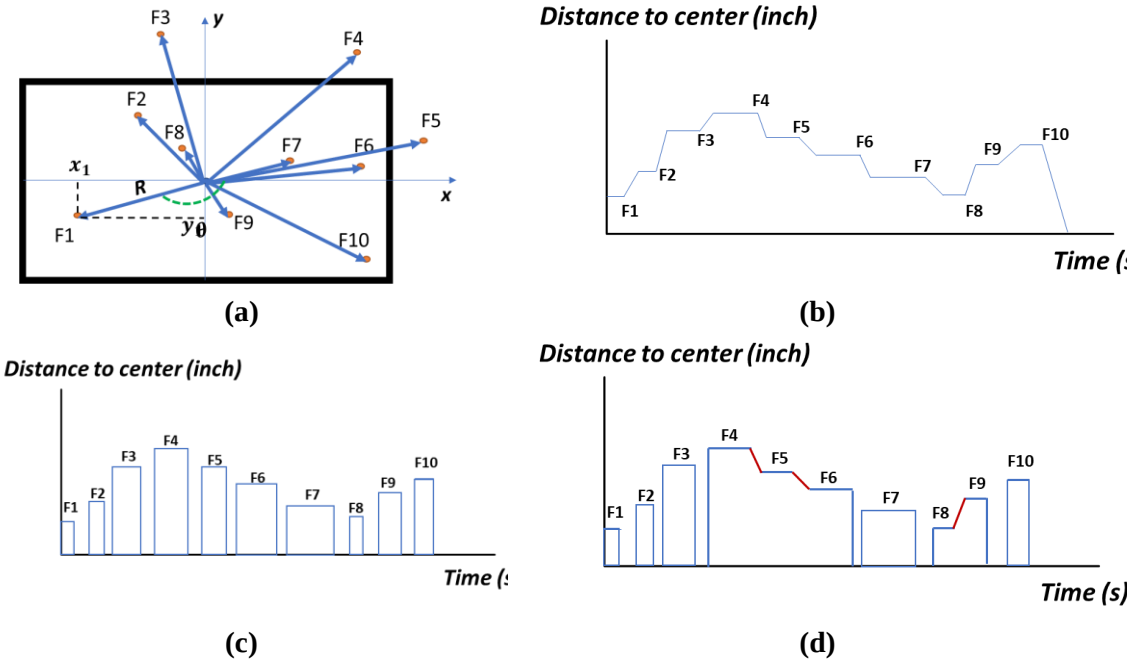

Figure 3. 1 Example of Eye Fixation Movement in (a) Trajectories and Relationship between Distance to Center and Time in (b) Pattern I, (c) Pattern II, and (d) Pattern III.

As illustrated in Figure 3.1(a), green dashed lines represent the eye fixation movement from "F1" to "F10". Given the two-dimension coordinate system, the distance of each fixation (F_i) to the center (represented as a blue dot) can be computed as follows:

$$d_{F_i} = \sqrt{(x_{F_i} - x_0)^2 + (y_{F_i} - y_0)^2} \tag{3.1}$$

Where,

d_{F_i} = Distance of F_i to center ($i = 1,2 \dots, n$);

x_{F_i} = Coordinate of F_i on x-axis;
x_0 = Coordinate of screen center on the x-axis;
y_{F_i} = Coordinate of F_i on y-axis;
y_0 = Coordinate of screen center on the y-axis;

Based on the calculation of d_{F_i}, each fixation's distance to the center of the screen can be calculated. With the eye-tracking system's ability to collect each fixation's duration, a time-discrete relationship can be visualized to describe the relationship between temporal and spatial measurements. In total, there are three potential patterns in representing the relationship.

(1) **Pattern I: Oculate-related events 0% covered between fixations.** According to eye-tracking fixation data, there is a small amount of time being elapsed between fixations (i.e., from "F1" to "F2" as illustrated in Figure 3.1(a)). Moreover, we observed that the driver did not involve in oculate-related events such as blinking or saccades. Therefore, the reason contributing to the time gap between two nearby fixations is the simulation error or eye-tracking running error. However, we do not know the pattern of the distance to center change from the first to the next fixation during the time between two fixations. Therefore, a linear regression was assumed in this case. Figure 3.1(b) illustrates Pattern I based on the fixation movements that illustrated in Figure 3.1(a). The slope is calculated as follows:

$$k_{F_{i,i+1}} = \begin{cases} \dfrac{d_{F_i} - d_{F_{i+1}}}{t_{F_{i+1,Start}} - t_{F_{i,End}}}, \forall d_{F_i} > d_{F_{i+1}} \\ 0, \qquad\qquad \forall d_{F_i} = d_{F_{i+1}} \\ \dfrac{d_{F_{i+1}} - d_{F_i}}{t_{F_{i+1,Start}} - t_{F_{i,End}}}, \forall d_{F_i} < d_{F_{i+1}} \end{cases} \tag{3.2}$$

Where,

$k_{F_{i,i+1}}$ = Slope of the distance to center and time between two nearby fixation points ($i = 1,2 \dots, n$);

$d_{F_i}, d_{F_{i+1}}$ = Distance to center of the two nearby fixation points;
$t_{F_{i+1,Start}}$ = Timestamp of the fixation F_{i+1} starts;
$t_{F_{i,End}}$ = Timestamp of the fixation F_i ends.

(2) P**attern II: Oculate-related events 100% covered between fixations.** In this case, we observed drivers involved in oculate-related events such as blinking that prevents a fixation point on the simulator screen while driving. Therefore, it is unknown regarding the distance to center between fixations, which is considered missing values. Figure 3.1(c) illustrates the relationship between distance to center and time under Pattern 2. Pattern 2 is more like a square-wave pattern.

(3) **Pattern III: Oculate-related events 0%~100% covered between fixations.** Pattern III can be considered as the combination of Pattern I and Pattern II. An example in illustrating Pattern III can be visualized in Figure 3.1(d). As illustrated in Figure 3.1(d), Pattern I is involved between F1 and F2, F2 and F3, F3 and F4, F6 and F7, F7 and F8, as well as F9 and F10. Pattern II covers from F4 to F6, and F8 to F9.

Since the higher distance to the center suggests the higher magnitude of the driver's visual attention away from the center, the distance to the center can be surrogated as the magnitude of driver visual distraction given a certain timestamp (t_i).

Regardless of the distance to the center vs. time pattern, the magnitude of visual distraction can be surrogated as the fixation's distance to the center. Further distance indicates a higher magnitude of visual distraction. Considering a human-machine-interaction has been applied in the driving, meaning the driver received safety messages under the CAV driving environment, Figure 3.2 illustrates the relationship between the magnitude of visual distraction and time with applying HVI session.

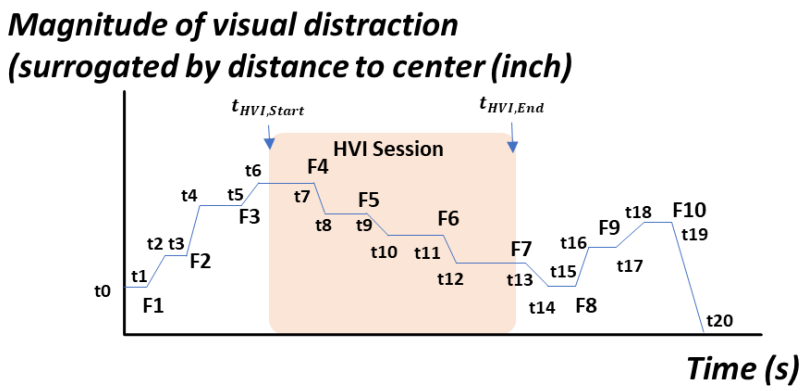

(a)

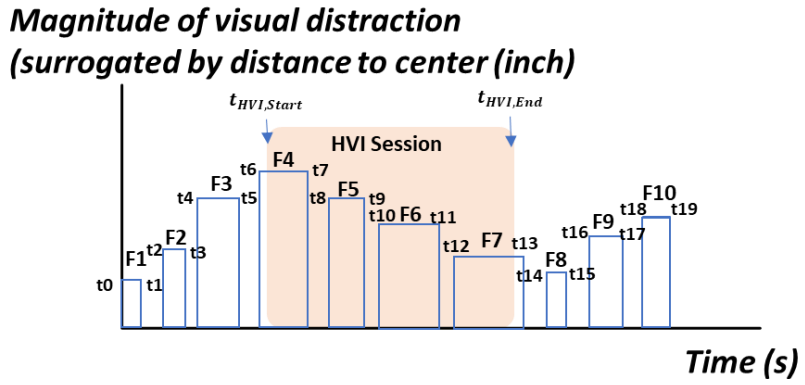

(b)

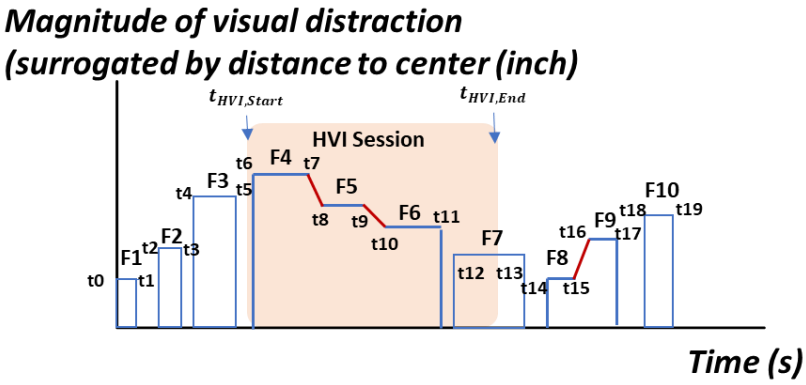

(c)

Figure 3. 2 Magnitude of Visual Distraction and Time under (a) Pattern I; (b) Pattern II; and (c) Pattern III ("t_i" indicates the timestamp for either a starting or ending point of fixation.)

As illustrated in Figure 3.2, when HVI applies to the driving, the driver's fixation position is further away from the center when the HVI session starts (i.e., a takeover

message is just being displayed). However, with the HVI continuing, the driver's visual distraction was reduced, reflected by the fixation gradually getting back to the center.

Moreover, assuming we have collected a number of n fixations during the driving. The intensity of driver distraction is the cumulation of the magnitude of driver distraction during the time period when HVI is in session. Specifically, if the visual distraction follows Pattern I, the intensity of visual distraction can be computed as follows:

$$I_{VD,HVI} = \sum_{i=1}^{n} \int_{t_S}^{t_E} d_i(t)dt \tag{3.3}$$

$$d(t)_{Pattern\ I} = \begin{cases} a_1, t_S \leq t < t_i \\ k_{F_{i,i+1}} * t + b_1, t_i \leq t < t_{i+1} \\ \dots \\ a_n, t_{n-1} \leq t < t_n \end{cases} \tag{3.4}$$

Where,

$I_{VD,HMI}$	=	Intensity of visual distraction under HVI (inch*sec);
$d_i(t)$	=	Distance to center as a function of time given the time period of i, $(i = 1,2, \dots, n)$;
t_S	=	Timestamp of HVI session starts;
t_E	=	Timestamp of HVI session ends;

Equation (3.5) summarizes the distance to the center as a function of time if the magnitude of visual distraction follows Pattern II:

$$d(t)_{Pattern\ II} = \begin{cases} a_1, t_S \leq t < t_i \\ k_{F_{i,i+1}} * t + b_1, t_i \leq t < t_{i+1} \\ 0, t_j \leq t < t_k \\ \dots \\ a_n, t_{n-1} \leq t < t_n \end{cases} \tag{3.5}$$

If the visual distraction follows the Pattern III, the $d_i(t)$ is expressed as the follows:

$$d(t)_{Pattern\ III} = \begin{cases} a_1, t_S \leq t < t_i \\ 0, t_i \leq t < t_{i+1} \\ \dots \\ a_n, t_{n-1} \leq t < t_n \end{cases} \quad (3.6)$$

3.1.2 Visual distraction: direction

In this research, another perspective of modeling visual distraction is proposed to further capture the dynamics of visual distraction, which is the direction of the direction. As mentioned in the previous section, the driver's fixation points can be projected to the Cartesian coordinate system with an x-axis and a y-axis. The driver's fixation points can be described using a different form by converting the Cartesian coordinate system to a polar coordinate system. Figure 3.3 illustrates how to measure a fixation point under a polar coordinate system.

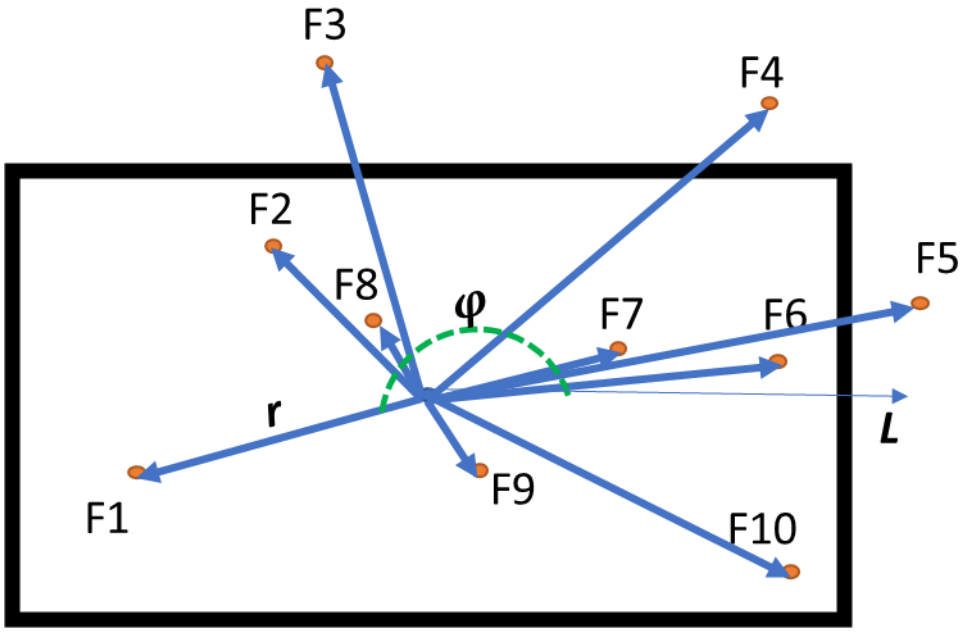

Figure 3. 3 Conceptual Example of Eye Fixation Movement under Polar Coordinate System

As depicted in Figure 3.3, "r" represents the visual distraction magnitude and "φ" represents the angle between "F1" and the polar axis L. The following equations can describe the relation between Cartesian and polar coordinates. Note that "$atan2$" is an arctangent function. Its common variation is based on values of x and y.

$$x = r\cos(\varphi - 180°) \quad (3.7)$$
$$y = r\sin(\varphi - 180°) \quad (3.8)$$
$$r = \sqrt{x^2 + y^2} \quad (3.9)$$
$$\varphi = atan2(y, x) \quad (3.10)$$

Where,

x	=	x coordinates of "F1" under the Cartesian coordinates;
y	=	y coordinates of "F1" under the Cartesian coordinates;
r	=	Visual distraction magnitude;
φ	=	Visual distraction direction.

Under this context, visual distraction direction has been added by converting the fixations under Cartesian coordinates to polar coordinates. Moreover, by using a polar coordinate system, the visual distraction magnitude and direction can be discussed as a group in identifying specific locations of the hotspots of visual distraction magnitude.

3.1.3 Visual distraction: time

Another important indicator for a driver's visual distraction is time. Existing research has not been extensively discussing how visual distraction changes over time. By proposing the visual distraction from the time perspective, this research expects to fill this research gap. Figure 3.4 illustrates the conceptual example of eye fixation in terms of time.

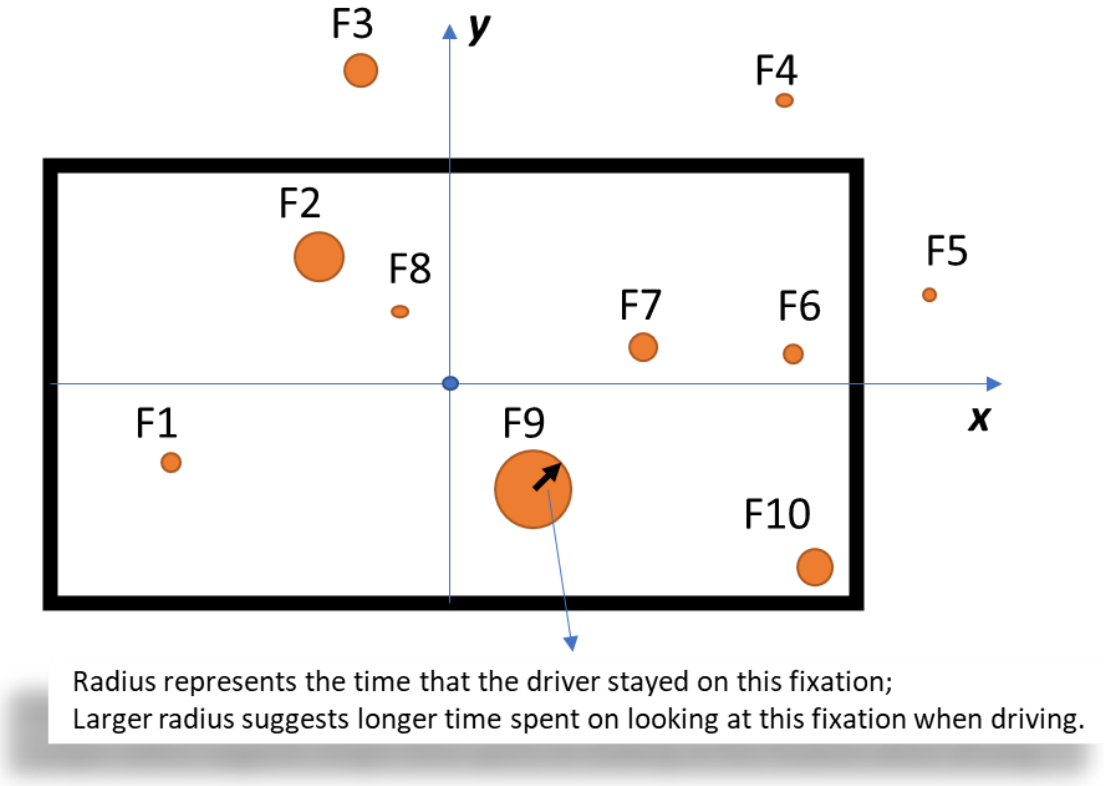

Figure 3. 4 Conceptual Example of Eye Fixation Duration

As illustrated in Figure 3.4, the time spent on each fixation was visualized by a circle, and the radius represented the fixation duration. Larger the radius, the longer time the driver spends on looking at this fixation.

3.1.4 Detailed steps for measuring visual distraction magnitude, direction, and time

In order to achieve the goal for measuring visual distraction in formats of magnitude, direction, and time, a head-mounted eye-tracking device from the Pupil Lab is used to increase the data readiness of measuring visual distraction. The Pupil Lab's eye-tracking device equips a fixed "world camera" that acquires drivers' fixation data points. Figure

3.5(a) illustrates an example of a driver wearing an eye-tracking device while driving on a simulator. The fixation data collected from the eye tracker provides the following variables:

- Fixation ID
- Norm_pos_x: x position in the eye image frame in normalized coordinates.
- Norm_pos_y: y position in the eye image frame in normalized coordinates.
- Duration: the time spent on a fixation point with a unit of milliseconds.

Therefore, for each driver, the steps for measuring visual distraction are summarized as follows:

Step 1: Identify the fixations under the HVI session (i.e., CV safety message display duration, takeover request display duration under automated driving) in the "fixations" dataset.

Step 2: Check the confidence of the fixation data. It is recommended to use the fixation records with a confidence level above 0.6 (Pupil Labs, 2021).

Step 3: Calculate the magnitude of visual distraction by measuring the normalized distance between fixation and screen center. The front camera collects information about where the subject was looking within the world camera's field of view. Since each subject calibrates the eye tracker before starting the experiment, the coordinates representing the center of the screen are different individually. For each participant, it is necessary to manually obtain the fixation that represents the screen center (i.e., Figure 3.5(b)). Note that data will be used only when there is no relative movement between the headset and the screen. In this case, the coordinates of fixation ID 120 are used to represent the screen center coordinates.

(a) **(b)**

Figure 3. 5 Eye-tracking Device in (a) Use of Drivers and (b) Collecting Fixation Data Points

Step 4: Categorize the visual distraction pattern by incorporating the pupil dataset. As introduced above, the relationship between the magnitude of visual distraction and time can be in Pattern I, II, or III based on whether there were oculate-related events such as blinking or saccades involved. Therefore, this step requires checking the pupil's behaviors to decide.

Step 4.1: Retrieve the pupil dataset that matches the timestamps with the fixation dataset.

Step 4.2: Remove records of pupil dataset that the confidence is not above 0.6.

Step 4.3: If pupil diameter with 0 is identified, it should be added into the final dataset for visualizing the magnitude of visual distraction.

Step 5: Compute and visualize the magnitude of visual distraction. After calculating each fixation’s distance to the center screen, the next step is to create the database with timestamps. Figure 3.6(a) illustrates a driver’s magnitude of visual distraction under an HVI session.

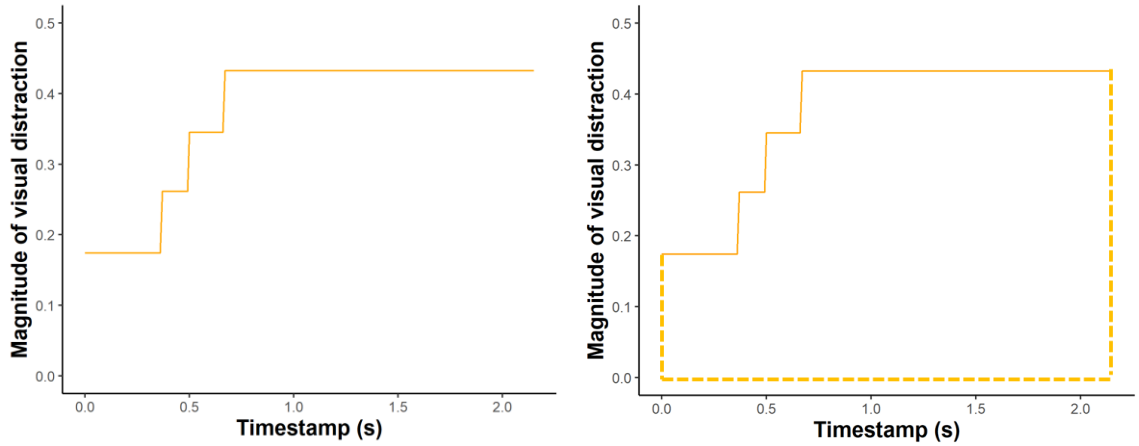

(a) **(b)**

Figure 3. 6 Visual Distraction in (a) Measuring Magnitude and (b) Measuring Intensity

Step 6: Compute and visualize the direction of visual distraction. By employing Equations (3.7) and (3.8), the direction of each fixation point can be calculated based on a fixed direction under an HVI session.

Step 7: Compute and visualize the time of visual distraction.

Step 8: Calculate the intensity of visual distraction in terms of the area from step 5. Figure 3.6(b) illustrates the process of calculating the intensity of visual distraction. Specifically, dashed lines were drawn, and the intensity of visual distraction is the polygon area. The intensity is calculated using Equation (3.3). The calculated intensity of visual distraction will be used as the model input for developing prediction models in sub-module II and modeling with safety performance.

3.2 Models development for predicting driver distraction

In previous modules, the ground truth data for visual and cognitive distraction has been measured. To validate the intensity of driver distraction, Artificial Neural Networks (ANN) are employed in predicting the intensity of visual and cognitive distraction since ANNs have been emerging as an essential tool in the field of transportation (Alwosheel et al., 2021; Servizi et al., 2020; van Cranenburgh & Alwosheel, 2019).

3.2.1 Artificial Neural Networks

ANNs are a research tool inspired by the structure and functional aspects of biological neural systems. The main reasons for ANNs' being employed are that they have strong learning ability with different structures of neurons and a great capacity to predict models (Abiodun et al., 2018; Maind & Wankar, 2014).

ANNs consist of interconnected nodes, also known as neurons, which communicate with each other to perform a classification or regression task. Specifically, an ANN model consists of three layers: input, hidden, and output layers. The input layers include nodes containing the explanatory variables. As illustrated in Figure 2, the explanatory variables in this study are driver information, CAN-BUS information, and HVI characteristics. The output layer contains the ground truth data of the measured driver distraction intensity. The hidden layer consists of many artificial neurons that can transmit a signal to other neurons based on certain activation functions. Each neuron receives model inputs that are multiplied by estimated parameters (weights). The input and output layers are connected by adding to a constant and forming a single input for a pre-defined activation function. In summary, the output can be described as follows:

$$y = g(u) = g(\sum_{i=1}^{I} w_i * v_i + w_b) \tag{3.11}$$

Where,

y = Model output;
$g(u)$ = Activation function;
w_i = Estimated parameter (weight) for model input variable i;
v_i = Model input variable i;
w_b = Constant of the associated weight

As introduced, there are no direct connections between the input nodes and output nodes. An activation function is used in bridging the input and output layers. The activation

functions are in formats of linear, logistic (sigmoid), and hyperbolic tangent (sigmoid). The equations are summarized as follows:

Table 3. 1 Summary of Activation Functions in ANN

Activation function	Equations	
Linear	$g(u)= u$	(3.12)
Logistic (sigmoid)	$g(u) = 1/(1 + exp(-u))$	(3.13)
hyperbolic tangent (sigmoid)	$g(u) = exp(2u) - 1/exp(2u) + 1$	(3.14)

3.2.2 Proposed ANN models for predicting driver distraction

Since the objective of this study is to predict visual and cognitive distraction, two ANN models are developed with targeting visual and cognitive distraction, respectively. Figure 3.7 illustrates a conceptual Artificial Neural Network that captures the relationships between model input variables and visual distraction intensity using visual distraction as an example. In order to complete the ANN modeling process, three components need to be defined. First, the number of hidden layers. Existing research has suggested that multiple hidden layers have a stronger ability to predict the model outputs (Chu et al., 2019; Jahromi et al., 2020). Second, the number of neurons by each hidden layer. The Universal Approximation Theorem (UAT) suggests that ANN can learn more complex functions if more hidden neurons are inserted in the model (Cohen et al., 2018). Third, the activation function. As mentioned in Section 3.2.1, each neuron processes its input through a defined activation function. Potential activation functions include linear, logistic, and hyperbolic tangent.

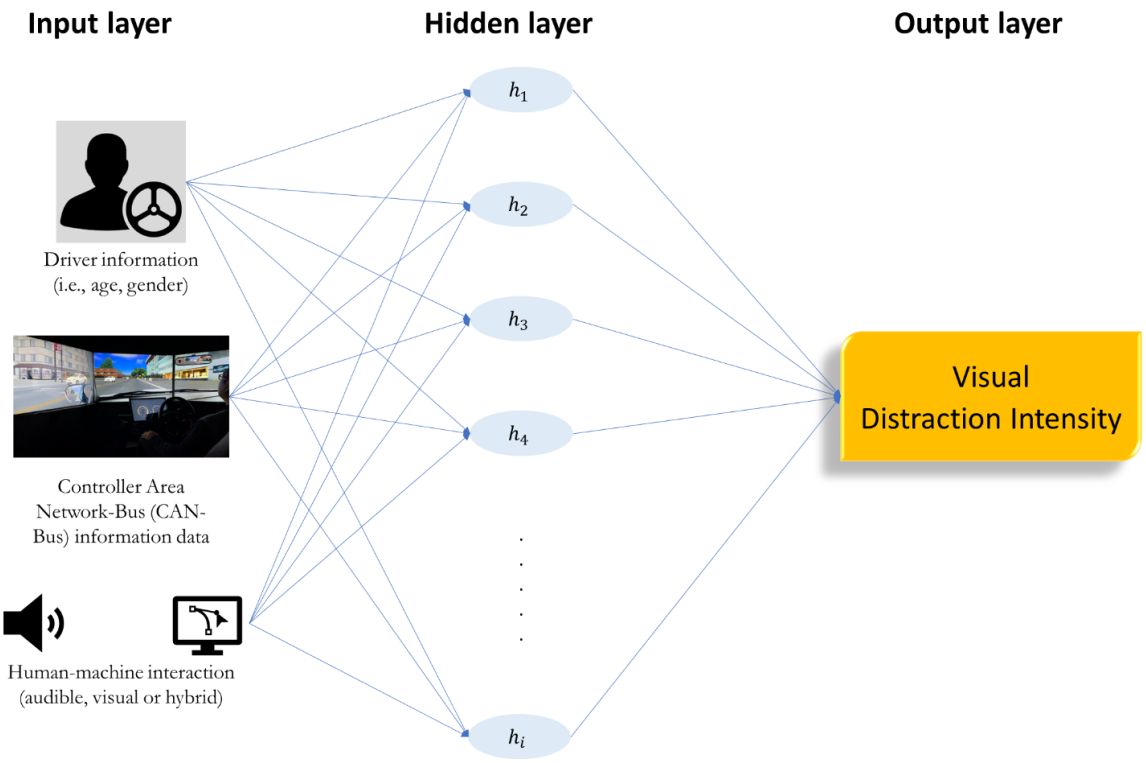

Figure 3. 7 Conceptual Model for Predicting Visual Distraction Intensity

As illustrated in Figure 3.7, the input variables to the Artificial Neural Network (ANN) model are drivers' demographical information (age and gender), HVI characteristics, and takeover time, and the output variable is the visual distraction intensity. Then, the next step is to decide the structure and the number of neurons in the hidden layer. The prediction accuracy of neural network-based models depends upon the number of hidden layers and the number of neurons in each hidden layer (Kumar et al., 2014). Therefore, to obtain the ANN model's optimum structure, several ANN model architectures have been trained and tested by altering the number of hidden layers and numbers of neurons in each layer.

Existing research has suggested that any continuous multivariate function can be implemented by a certain type three-layer neural network (Ismailov, 2020). Therefore, the

number of hidden layers in this research is set to 3. For the number of neurons, the following equation is employed to find the range of numbers of neurons:

$$N_{Neurons} \in [\sqrt{N_{IV} + N_{OV}} + 1, \sqrt{N_{IV} + N_{OV}} + 10] \quad (3.15)$$

Where,

$N_{Neurons}$ = Number of neurons;
N_{IV} = Number of input variables;
N_{OV} = Number of output variables.

In this case, the number of neurons for developing ANN modes in predicting visual or cognitive distraction intensity ranges from 3 to 13. Since the dependent variable (visual or cognitive distraction intensity) is a continuous variable, it is recommended to set the number of neurons on the third hidden layer (closest layer to the output layer) to 1. With the first and the second hidden layer varying the numbers of neurons from 3 to 13, a total of 121 combinations in terms of ANN structures has been performed. The ANN structure with minimum Mean Square Error (MSE) is chosen as the best-fitting model in predicting visual and cognitive distraction intensity, respectively.

On the other hand, if the model is too simple, both the training and testing datasets are likely to be underfitting. Therefore, this type of model has a high bias but low variance (Amiri et al., 2020). To summarize, the best structure is the one that makes the tradeoff and produces the model that is neither too simple nor too complex. Equation (3.14) expresses the best model characteristics:

$$Ideal\ model \overset{def}{\Longrightarrow} \min_{i=1,2,\ldots,121} (MSE_{Test,i} - MSE_{Train,i}) \quad (3.16)$$

Where,

$MSE_{Test,i}$ = Mean Square Error for the testing dataset for model ID = i
$MSE_{Test,i}$ = Mean Square Error for the training dataset for model ID = i

3.3 Data collection

3.3.1 Driving Simulator

A data collection was conducted to validate the proposed methods for measuring and predicting driver distraction by recruiting drivers to try out automated driving under Level 3 (conditional) automation on a driving simulator.

The “miniSim” driving simulator was employed to implement Level 3 automation. Figure 3.8(a) illustrates a participant driving under Level 3 automation on the “miniSim” simulator. The “miniSim” is currently approved and used in Department of Transportation labs, including NHTSA’s miniSim lab located at US DOT’s Turner-Fairbank Highway Research Center (TFHRC) in McLean, VA. MiniSim records high fidelity data with more than 100 variables at 60 Hz. Once driving on the “miniSim”, it will simultaneously collect the driving-related raw data (i.e., speed, lane deviation). Then the raw data can be reduced for further analysis. MiniSim uses high-resolution tiles to create road networks, resulting in very realistic, immersive environments that the user can quickly assemble.

3.3.2 Experimental design and procedure

The ethics application for the study was reviewed and approved by the Institutional Review Board (IRB) at the University of Louisville. Before beginning the study, recruited participants were briefed about the study, which they were required to drive under Level 3 automation. Before starting driving tasks, each participant was asked to complete a questionnaire that collected basic information such as age and gender, representing driver information as one of the model inputs for future analysis.

Then, each participant was introduced to the capabilities and limitations of Level 3 automation based on the definition of driving automation levels (SAE International, 2018),

in which drivers who are sitting behind the steering wheel are not responsible for monitoring the driving environment but responsible for taking over the driving if Level 3 Automated Driving System (ADS) requests.

After participants understood the basic functions of Level 3 automation, they were asked to wear a head-mounted eye tracker from the Pupil Labs to start the driving task. The eye tracker records gaze behaviors at 30 Hz, collecting both the fixation and pupil dilation data to model the visual and cognitive distraction, respectively. Figure 3.8(b) illustrates the eye-tracking device.

(a) **(b)**

Figure 3. 8 The "MiniSim" Driving Simulator in (a) Automated Driving Mode and (b) Adding Eye-tracker.

For the first driving task, each participant was required to drive through a jaywalker scenario under manual driving. The driving performance when participants handling the jaywalker situation was recorded as a benchmark.

For the second driving task, two jaywalker scenarios were popped out when participants were driving under Level 3 automation on the miniSim simulator, and the Level 3 ADS requested participants to take over the driving tasks. The jaywalker scenario was not mentioned in the briefing part to ensure the reliability of the data collection. Two jaywalking scenarios were included because we tested two HVI types: the "visual only"

and “visual + audible”. Note that participants did not drive through these two jaywalking scenarios continuously. In order to avoid any expected behaviors from participants, there are other driving scenarios inserted between the two jaywalking scenarios. For one jaywalker scenario, participants were only notified about the takeover request through the in-vehicle heads-up display. For the other jaywalker scenario, participants were able to hear a chime when the takeover request was displaying simultaneously. Figure 3.9(a) illustrates the concept of jaywalking scenario, and Figure 3.9(b) illustrates the scenario presented in the “miniSim” simulator.

Since drivers are likely to look around because they are not responsible for performing any driving tasks if the automated driving under Level 3 is in session, and the experiment was designed by using a tangent section, this research uses the center of the screen as the visual distraction magnitude zero point.

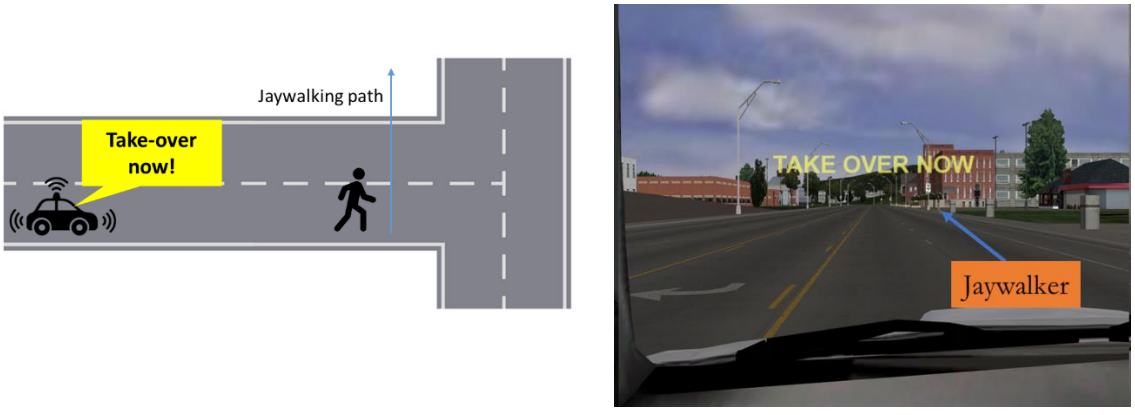

(a) **(b)**

Figure 3. 9 Jaywalking Scenario in (a) Conceptual Format and (b) MiniSim Driving Simulator

In order to complete the prediction models in sub-module III, the model inputs also need the Controller Area Network-Bus (CAN-Bus) information data. In this data collection,

takeover time was selected as the model input representing the CAN-Bus information data, which measures the time elapsed between issuing the takeover request and the driver taking action to control the vehicle. Table 3.2 summarizes all the model inputs needed in completing sub-module III.

Table 3. 2 Model Inputs for Predicting Driver Distraction

Category	Variable name	Variable type	Definition
Driver information	Male	Binary	\
	Age	Continuous	\
Controller Area Network-Bus (CAN-Bus) information data	Takeover time	Continuous	Time spent on taking over the driving.
HVI Characteristics	Visual + Audible	Binary	\

3.3.3 Participants

Seventy-five participants were recruited voluntarily among the nearby counties of the University of Louisville based on the following criteria: possession of a valid U.S. driver's license and low susceptibility to motion sickness when driving on the simulator. All participants have signed a consent form prior to the start of their experiment session. As a result, under each HVI type, twenty-five participants completed the driving task by wearing the eye-tracker and completed the questionnaire.

3.3.4 Performance measures

In addition to measuring visual distraction, two other performance measures are to be collected when participating in the driving simulator experiment.

3.3.4.1 Takeover time

For takeover time, an ADS requests the human driver to take over the driving when an Automated Vehicle (AV) disengagement (i.e., jaywalking). The human driver performs the takeover actions by driving (i.e., applying to the steering wheel, gas pedal, or brake pedal).

Therefore, the takeover time is defined by the duration between the ADS issuing a takeover request and the driver taking over the driving. Figure 3.10 illustrates the definition of takeover time.

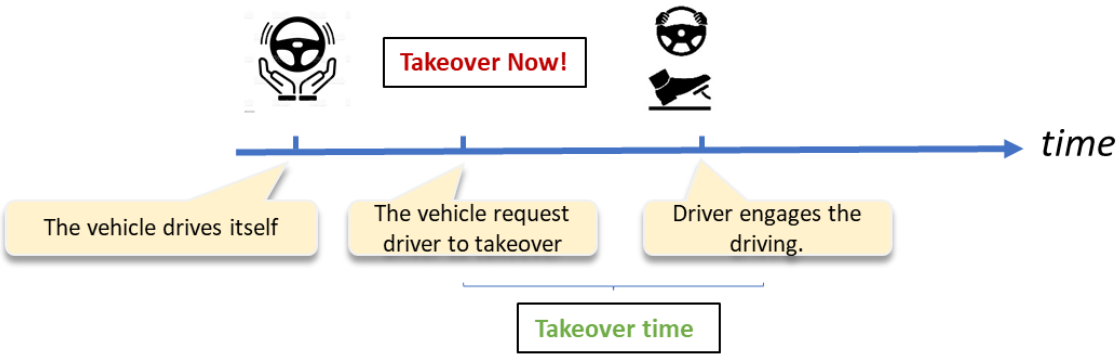

Figure 3. 10 Definition of Takeover Time.

3.3.4.2 Traffic conflict

While driving through the scenario involving a jaywalker, driving performance such as speed and distance was collected to measure the traffic conflicts and conflict severity, which have been considered the valid safety assessment measurements by the Federal Highway Administration (FHWA) (Gettman et al., 2008). Using traffic conflicts and conflict severity is because it is rare to observe AV crashes in the simulation environment. Therefore, in this study, traffic conflicts and conflict severity are analogous to crash frequency and crash severity, respectively.

Furthermore, a traffic conflict can be considered as a more generalized but quantified near miss. According to Surrogate Safety Assessment Model (SSAM), a conflict is defined as an observable situation in which two or more road users approach each other in time and space to such an extent that there is a risk of collision if their movements remain unchanged (Gettman et al., 2008). A conflict is concluded after the time-to-collision value rises back above the critical threshold value. Regarding conflict severity, it is defined as

the minimum time-to-collision (TTC) value observed during the conflict. The lower TTC, the more severe a traffic conflict. TTC is calculated based on two vehicles' current location, speed, and future trajectory at a given constant. Figure 3.11 illustrates how to calculate TTC and introduces the specific thresholds under different collision types. Equation (3.15)

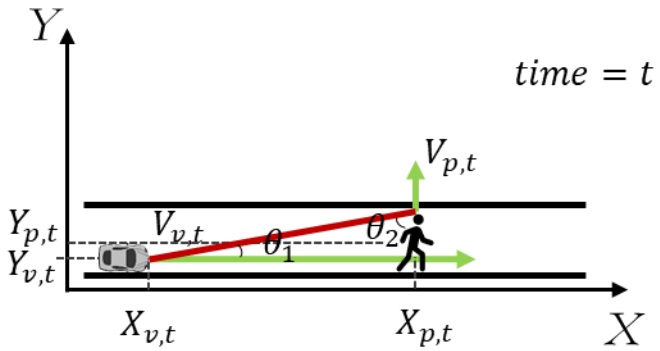

Figure 3. 11 Traffic Conflict Calculation between Vehicle and Jaywalker

$$TTC = \frac{\sqrt{(X_{v,t} - X_{p,t})^2 + (Y_{v,t} - Y_{p,t})^2}}{V_{v,t}\cos(\theta_{1,t}) + V_{p,t}\cos(\theta_{2,t})} \quad (3.17)$$

Where,

$X_{v,t}$ = Position of vehicle on x-axis at time t;
$X_{p,t}$ = Position of jaywalker on x-axis at time t;
$Y_{v,t}$ = Position of vehicle on y-axis at time t;
$Y_{p,t}$ = Position of jaywalker on y-axis at time t;
$V_{v,t}$ = Vehicle speed at time t;
$V_{p,t}$ = Jaywalking speed at time t;
$\theta_{v,t}$ = Relative angle of vehicle to pedestrian at time t;
$\theta_{p,t}$ = Relative angle of pedestrian to vehicle at time t

The collision type between the vehicle and pedestrian is defined as an angled conflict. Per Hirst & Graham (1997), M. Ma & Li (2019), and Tachet et al. (2016), the

threshold of 4-second is used as the minimum TTC to define an angled conflict. In other words, any minimum TTC below 4-second is considered a traffic conflict in this research.

3.4 Results and discussions

3.4.1 Visual distraction magnitude

This section mainly contributes to the literature by discussing how the visual distraction magnitude changes from the temporal perspective. As mentioned in the previous section, drivers experienced two HVI types: “visual only” and “visual + audible”. The real-time visual distraction induced by HVI will be discussed in this section.

Existing studies mainly focus on measuring or detecting visual distraction under specific distracted driving tasks (Aksjonov et al., 2017; Brodeur et al., 2021; Trommler et al., 2021b; Y. Zhang et al., 2021c). This study further discusses the relationship between visual distraction and time horizon.

By employing Equation (3.1), the distance to the center screen can be calculated with given normalized coordinates of a fixation on the x- and y-axis, which is defined as the distance to the center with surrogating the magnitude of visual distraction. As a result, a total of 221 records were collected in capturing driver’s fixation results in both “visual only” and “visual + audible” HVI with facing a jaywalker scenario that requires a takeover action. There were outliers regarding either norm_pos_x or norm_pos_y. The data analysis only includes fixation records with both norm_pos_x and norm_pos_y not being outliers to ensure the data reliability. Therefore, the final sample size for discussing visual distraction magnitude in real-time is set to be 188.

As introduced earlier, the center of the driver’s vision is used as the driver’s visual distraction zero-point under automated driving. Prior to the start of the experiment, each

driver was required to calibrate the eye tracker. The purpose of the calibration is to ensure every driver's glance behavior data were collected in the same coordinate system. Therefore, the collected fixation data by each driver is normalized can be used to perform further analysis. The center of the driver's vision is used to represent the zero point of visual distraction magnitude because drivers are likely to look around if automated driving is in session. Therefore, it is possible that when starting the HVI process by displaying the takeover request on the screen, drivers' fixation locations are randomly distributed. In order to validate this, the initial fixation location by each driver is visualized and illustrated in Figure 3.12.

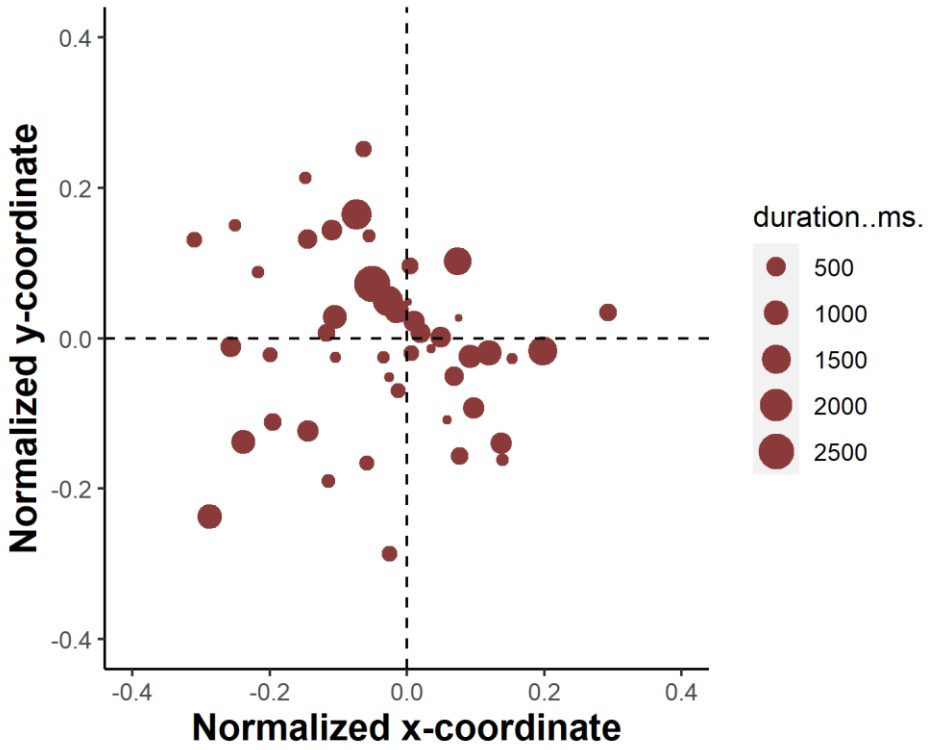

Figure 3. 12 Initial Location of Fixation by Each Driver

As illustrated in Figure 3.12, the x-axis and the y-axis represent the first fixation location by each driver when starting to receive the takeover message. Two dash lines represent the normalized position of the center of the driver's vision. Each point's radius suggests how long the driver looks at this point. Through the two dash lines, Figure 3.12 was divided into four quadrants. The distribution of these initial fixation points under the four-quadrant system is 17%, 26%, 28%, and 30%. Two-tail t-tests were conducted, suggesting no significant differences in the probability of locating the first fixation to any quadrants. In other words, it is safe to validate the hypothesis of using the driver's vision center as the zero point of visual distraction because the initial fixation for each driver is randomly distributed.

Since multiple fixations can be recorded for each driver when under HVI, changes in visual distraction can occur until the driver takes action to take over the vehicle. In this case, a new variable named "trend" is added to the original dataset to capture the changes in visual distraction magnitude during the HVI process. Specifically, for each driver, there are four categories in recording the "trend" variable:

1. "\": Initial fixation record for the driver. This symbol indicates that the driver has more than one fixation record being collected.
2. "+": Visual distraction magnitude was increased based on the previous fixation record for the driver.
3. "-": Visual distraction magnitude was reduced based on the previous fixation record for the driver.
4. "*" Only one fixation record for the driver

Therefore, Table 3.3 summarizes the general statistics of fixation records with the aforementioned variables included. Figure 3.13 illustrates the distribution of fixation points with duration information included under "visual only" and "visual + audible" HVI, respectively.

Table 3. 3 Sample Characteristics of Fixations under HVI (Sample size=188)

Variable		Variable Description	Type	Category	N/ Mean ± Std.Deviation	%/ Range
Variable Category	**Variable name**					
Fixation spatial performance	Norm_pos_x	x position in the eye image frame in normalized coordinates	Continuous	\	-0.004±0.108	-0.310-0.292
	Norm_pos_y	y position in the eye image frame in normalized coordinates	Continuous	\	-0.018±0.106	-0.305-0.252
	Visual distraction magnitude	Surrogated by distance to the center	Continuous	\	0.129±0.081	0-0.373
	Trend	Changes in visual distraction magnitude	Categorical	\	41	21.8
				+	70	37.2
				-	71	37.8
				*	6	3.2
Fixation temporal performance	Duration	time spent on a fixation point with a unit of milliseconds	Continuous	\	470.998±471.882	84-2688

Note that "Mean ± Std.Deviation" and "Range" are summarized if the variable type is continuous. Otherwise, the number of samples and percentage are summarized if it is a categorical variable.

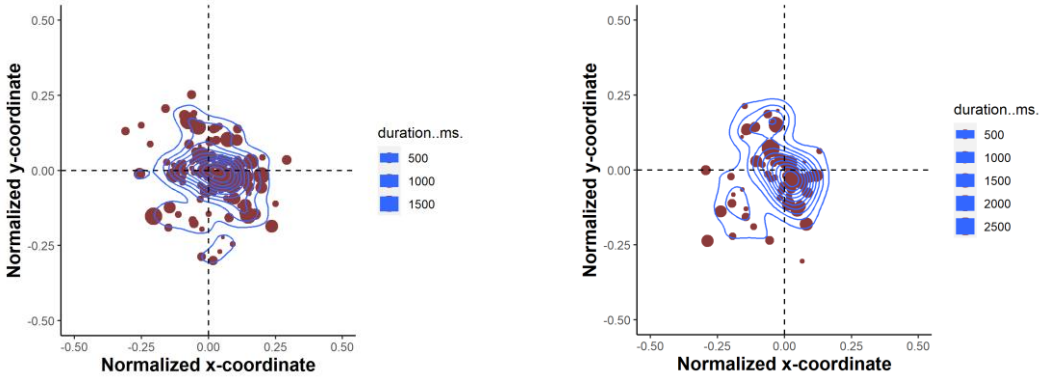

(a) **(b)**

Figure 3. 13 Fixations Distribution under (a) Visual Only and (b) Visual + Audible HVI Types.

As summarized in Table 3.3, there are a limited number of the sample (3.2%) indicating no changes regarding the visual distraction magnitude under either "visual only" or "visual + audible" HVI. Hence, it is necessary to investigate how the magnitude of visual distraction changes during the HVI process. In addition, similar records suggest the increase (N=70) and reduction (N=71) in visual distraction magnitude. The discussion will follow the two major research questions:

- RQ1: When starting the HVI process, are drivers tending to reduce driver distraction by looking towards the center screen? If so, does the reduction is maintained until the driver takes action in responding to the HVI? If not, how long does it keep in a reduction in both HVI types? To what point do the drivers start to look away again?
- RQ2: When starting the HVI process, are drivers increasing their visual distraction by looking away from the center screen? Is it more possible to happen when the HVI is "visual only"? To what point does the driver start to reduce the visual distraction by looking towards the center screen? After reduction, are drivers starting to look away again?

3.4.1.1 Reduction of visual distraction magnitude

In addressing RQ1, the fixation dataset suggests that when starting the "visual only" HVI, 45.5% of drivers start their visual distraction magnitude changes by reducing it. On the other hand, when starting the "visual and audible" HVI, the proportion of drivers starting to reduce their magnitude of visual distraction increases to 52.6%. A two-tail t-test was conducted with the null hypothesis that there are no significant differences in the starting

the change of visual distraction magnitude by reduction under two HVI types. As a result, the null hypothesis is accepted.

For those who started the change of visual distraction magnitude by reduction, 30% of them maintained the reduction of visual distraction magnitude until the driver responded to the "visual only" HVI. When it comes to the "visual and audible" HVI, 40% of drivers did not increase their visual distraction magnitude if their first change of visual distraction magnitude is a reduction. Table 3.4 summarizes the distribution of changes in visual distraction magnitude if drivers' first change of visual distraction magnitude is a reduction. Existing research has mentioned that takeover request modality significantly impacts the takeover readiness and, in turn, takeover time (S. Petermeijer et al., 2017; Politis et al., 2017; Yun & Yang, 2020). In order to theorize this finding, a one-tail t-test was conducted in comparing the number of occurrences in increasing the magnitude of visual distraction between "visual only" and "visual and audible" HVI. The null hypothesis is that there are no significant differences in the number of occurrences regarding increasing visual distraction magnitude. As a result, the t-test results reject the null hypothesis. The occurrences in increasing visual distraction magnitude are 1.9 times per driver under "visual only" HVI, while the occurrences are 0.8 times per driver under "visual and audible" HVI ($t=1.777$, p-value<0.05). Therefore, this study contributes to the literature by revealing why multi-modal takeover warnings are more effective in improving the takeover quality (less takeover time, less traffic conflict). It is safe to conclude that, under "visual and audible" HVI, the takeover readiness is significantly improved because drivers are less likely to pick up their visual distraction magnitude compared to "visual only" HVI.

Regarding the duration in keeping reduction until the driver's next change in visual distraction magnitude, the fixation dataset suggests that drivers spent up to 370 milliseconds in the initial reduction of visual distraction magnitude under "visual only" HVI type while it took drivers up to 580 milliseconds in the initial reduction of visual distraction magnitude under "visual and audible" HVI type. In order to explore whether a significant difference exists in the duration of initial reduction, a two-tail t-test was conducted. The null hypothesis is that it takes a similar amount of time in deceleration until the driver makes another fixation movement. However, the t-test results reject the null hypothesis, suggesting that significantly different patterns of initial reduction regarding visual distraction magnitude were observed between "visual only" and "visual and audible" HVI type (t=-2.0453, p<0.1).

Moreover, this research also explored the relationship between visual distraction reduction rate and time. To compute the reduction rate of visual distraction magnitude, Equation (3.18) was employed and expressed as follows:

$$RR_{HVI=j} = \frac{d_{F_{i+1}} - d_{F_i}}{t};\ \forall d_{F_{i+1}} < d_{F_i} \tag{3.18}$$

Where,

$RR_{HMI=j}$ = The reduction rate of initial visual distraction reduction when HVI type is j (j = "visual only" or "visual and audible") (normalized distance/milliseconds)

d_{F_i} = Distance of F_i to center ($i = 1,2 \dots, n$);

t = Time under initial visual distraction reduction (milliseconds).

Table 3. 4 Distribution of Changes in Visual Distraction Magnitude under (a) "Visual-Only" and (b) "Visual + Audible" HVI

(a)

Driver ID	Initial change of visual distraction magnitude	Total occurrences of reductions in visual distraction magnitude	Total occurrences of increases in reducing visual distraction magnitude
13	-	5	5
26	-	3	4
29	-	3	2
33	-	1	0
41	-	2	2
42	-	1	0
45	-	4	3
50	-	4	2
62	-	5	1
64	-	1	0

(b)

Driver ID	Initial change of visual distraction magnitude	Total occurrences of reductions in visual distraction magnitude	Total occurrences of increases in reducing visual distraction magnitude
15	-	2	1
27	-	1	1
28	-	1	1
37	-	4	0
42	-	1	0
44	-	1	0
45	-	1	1
50	-	1	1
65	-	1	3
67	-	1	0

A model fit test is performed to determine the best-fit model in describing the reduction rate of visual distraction magnitude under "visual only" and "visual and audible" HVI, respectively. Table 3.5 summarizes the result of the test.

As summarized in Table 3.4, each candidate regression model has an $\mathbf{R^2}$ and p-value that obtained from the F test. A higher $\mathbf{R^2}$ suggests that the regression model better explains the reduction rate as a function of time. A lower p-value suggests a more significant effect on the reduction rate of visual distraction magnitude. For the reduction

rate under the "visual only" warning, the inverse regression model has the relatively highest $\mathbf{R^2}$ of 0.706 with indicating the time is significant at the 99.9% confidence level. These values reveal that the inverse model is the best-fit model that describes the relationship between the reduction rate of visual distraction magnitude and time. Therefore, based on the results of the inverse model summarized in Table 3.5, the reduction rate of initial visual distraction induced by "visual only" HVI can be modeled by a function of time, which is presented by the following equation:

$$RR_{visual\ only} = 3.063 * 10^{-5} - \frac{0.088}{t};\ \forall\ t\ \in [0, 370\ ms] \tag{3.19}$$

For the reduction rate under "visual and audible" warning, the inverse regression model also has the relatively highest $\mathbf{R^2}$ of 0.434 with the p-value lower than 0.01. These values imply that the inverse model is the best fit for capturing the relationship between reduction rate under "visual and audible" warning and time. Similar to Equation (3.18), the reduction rate of initial visual distraction induced by "visual and audible" HVI can be expressed as a function of time in the following equation"

$$RR_{visual+audible} = -2.394 * 10^{-7} - \frac{0.038}{t};\ \forall\ t\ \in [0, 580\ ms] \tag{3.20}$$

Table 3. 5 Best Model Fit Analyses for Initial Visual Distraction Reduction Rate under (a) "Visual-Only" and (b) "Visual + Audible" HVI

(a)

Equation	Model Summary					Parameter Estimates			
	R-square	F	df1	df2	Sig.	Constant	b1	b2	b3
Linear	.288	79.726	1	197	.000	-.003	1.559E-5		
Logarithmic	.562	253.090	1	197	.000	-.011	.002		
Inverse	.706	473.144	1	197	.000	3.063E-5	-.088		
Quadratic	.456	82.079	2	196	.000	-.005	5.012E-5	-1.135E-7	
Cubic	.566	84.824	3	195	.000	-.007	.000	-6.248E-7	1.000E-9
Compound[a]	.	.	.	.	.	.000	.000		
Power[a]	.	.	.	.	.	.000	.000		
S[a]	.	.	.	.	.	.000	.000		
Growth[a]	.	.	.	.	.	.000	.000		
Exponential[a]	.	.	.	.	.	.000	.000		
Logistic[a]	.	.	.	.	.	.000	.000		

Note that the dependent variable (reduction rate) contains non-positive values. Therefore, Log transform cannot be applied. The Compound, Power, S, Growth, Exponential, and Logistic models cannot be calculated for this variable.

(b)

Equation	Model Summary					Parameter Estimates			
	R-square	F	df1	df2	Sig.	Constant	b1	b2	b3
Linear	.146	51.742	1	303	.000	-.001	3.199E-6		
Logarithmic	.319	142.102	1	303	.000	-.004	.001		
Inverse	.434	232.606	1	303	.000	-2.394E-7	-.038		
Quadratic	.240	47.693	2	302	.000	-.002	1.115E-5	-1.661E-8	
Cubic	.305	44.060	3	301	.000	-.002	2.587E-5	-8.826E-8	9.073E-11
Compound[a]	.	.	.	.	.	.000	.000		
Power[a]	.	.	.	.	.	.000	.000		
S[a]	.	.	.	.	.	.000	.000		
Growth[a]	.	.	.	.	.	.000	.000		
Exponential[a]	.	.	.	.	.	.000	.000		
Logistic[a]	.	.	.	.	.	.000	.000		

Note that the dependent variable (reduction rate) contains non-positive values. Therefore, Log transform cannot be applied. The Compound, Power, S, Growth, Exponential, and Logistic models cannot be calculated for this variable.

In summary, Figure 3.11 illustrates the reduction rate of HVI-induced initial visual distraction and time. The red circle dots represent ground truth data of the reduction rate due to "visual only" HVI at each timestamp, while the cyan triangle dots represent ground

truth data of the reduction rate due to “visual and audible” HVI at each timestamp. The best-fit models in capturing the relationship between reduction rate and time are also included in Figure 3.14.

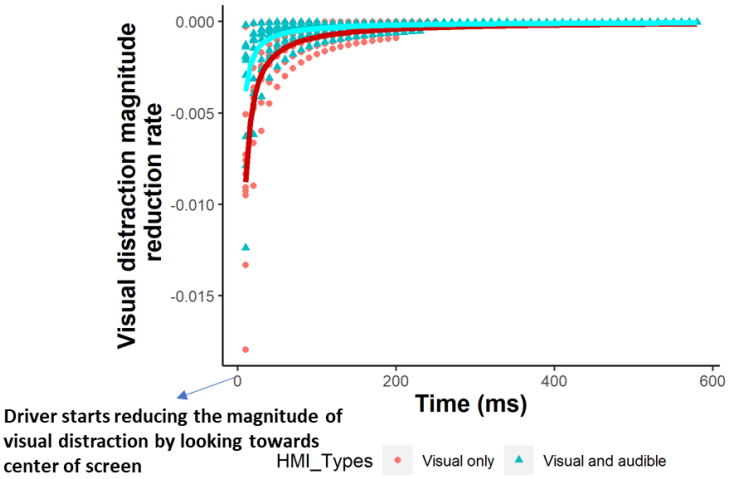

Figure 3. 14 Comparison of Visual Distraction Magnitude Reduction Rate and Time under Different HVI Types

As illustrated in Figure 3.14, during the early stages of reducing visual distraction magnitude, drivers under the “visual only” HVI type show a higher reduction rate in absolute value compared to the “visual and audible” HVI type. Conducting a one-tail t-test, when drivers start to reduce the visual distraction magnitude by looking towards the center screen under the “visual only” warning, drivers show significantly higher visual distraction magnitude reduction rate compared to “visual and audible” ($t=2.589$, $p<0.01$). This finding suggests that HVI types significantly impact how visual distraction changes with time. Drivers are more prepared to reduce visual distraction magnitude under the “visual and audible” HVI type by showing a lower reduction in visual distraction magnitude.

3.4.1.2 Increase of visual distraction magnitude

In addressing RQ2, the fixation dataset suggests that 54.5% of drivers started their changes of visual distraction magnitude by increasing under the "visual only" HVI. On the other hand, 47.4% of drivers first changed visual distraction magnitude towards the positive direction. Therefore, even if the HVI type is "visual and audible", it is possible that drivers tend to increase their visual distraction magnitude by looking away from the center screen. Table 3.6 summarizes the distribution of occurrences in reducing and increasing visual distraction under "visual only" and "visual and audible" warnings if their initial reaction to HVI is increasing the visual distraction magnitude.

Table 3. 6 Distribution of Changes in Visual Distraction Magnitude under (a) "Visual-Only" and (b) "Visual + Audible" HVI (Initial change of visual distraction magnitude is an increase)

(a)

Driver ID	Initial change of visual distraction magnitude	Total occurrences of reductions in visual distraction magnitude	Total occurrences of increases in reducing visual distraction magnitude
11	+	0	1
12	+	2	4
27	+	3	2
28	+	3	3
35	+	2	3
37	+	1	1
43	+	3	3
46	+	0	1
48	+	3	4
63	+	2	3
65	+	1	3
67	+	0	1

(b)

Driver ID	Initial change of visual distraction magnitude	Total occurrences of reductions in visual distraction magnitude	Total occurrences of increases in reducing visual distraction magnitude
11	+	0	2
26	+	1	2
33	+	1	2
41	+	0	1
43	+	1	1
48	+	3	2
62	+	0	1
63	+	1	2
64	+	1	1

As summarized in Table 3.6, after drivers initiated their first change of visual distraction in increasing, the patterns of visual distraction changes are significantly different between "visual only" and "visual and audible" HVI. Specifically, there is an average of 1.67 occurrences per driver in reducing visual distraction magnitude under "visual only" HVI, which is significantly higher compared to 0.89 occurrences of reduction under "visual and audible" HVI ($t=1.651$, p-value<0.1). A potential reason to support this finding is that drivers tend to compensate by checking towards the center screen in case missing any additional information during the HVI process. Choudhary & Velaga (2017b)

and R. Zhou et al. (2016, 2020) also proposed the compensatory beliefs in reducing driver distraction. Hence, this research contributes to the literature by validating compensatory beliefs in the driver distraction field.

On the other hand, for these drivers who initiated their change of visual distraction as an increase, there is an average of 2.41 occurrences per driver in increasing visual distraction magnitude under "visual only" HVI, which is also significantly higher compared to 1.56 occurrences per driver under "visual and audible" HVI. Combining with the previous finding, we can observe that drivers tend to check the center screen back and forth if they are in the "visual only" HVI process as these drivers have significantly more increases and reductions in visual distraction magnitude compared to drivers in "visual and audible" HVI process.

To further validate this observation, Figure 3.15 illustrates the visual distraction magnitude trajectory map due to "visual only" HVI for those who initiate their first change of visual distraction magnitude as an increase. In Figure 3.13, each dot represents the location of each fixation, and the radius of the dot represents the duration of staying in the fixation. The fixation of the two dash lines represents the center screen. As a result, except for drivers with an ID of 11, 46, or 67, most drivers showed multiple occurrences of increasing and reducing visual distraction magnitude. Therefore, this finding further reveals that drivers are more likely to adjust their fixations at multiple attempts for the compensatory reason if the HVI is "visual only". Meanwhile, drivers are more concentrated and prepared if the HVI is "visual and audible" because they showed significantly fewer attempts to look towards or away from the center screen.

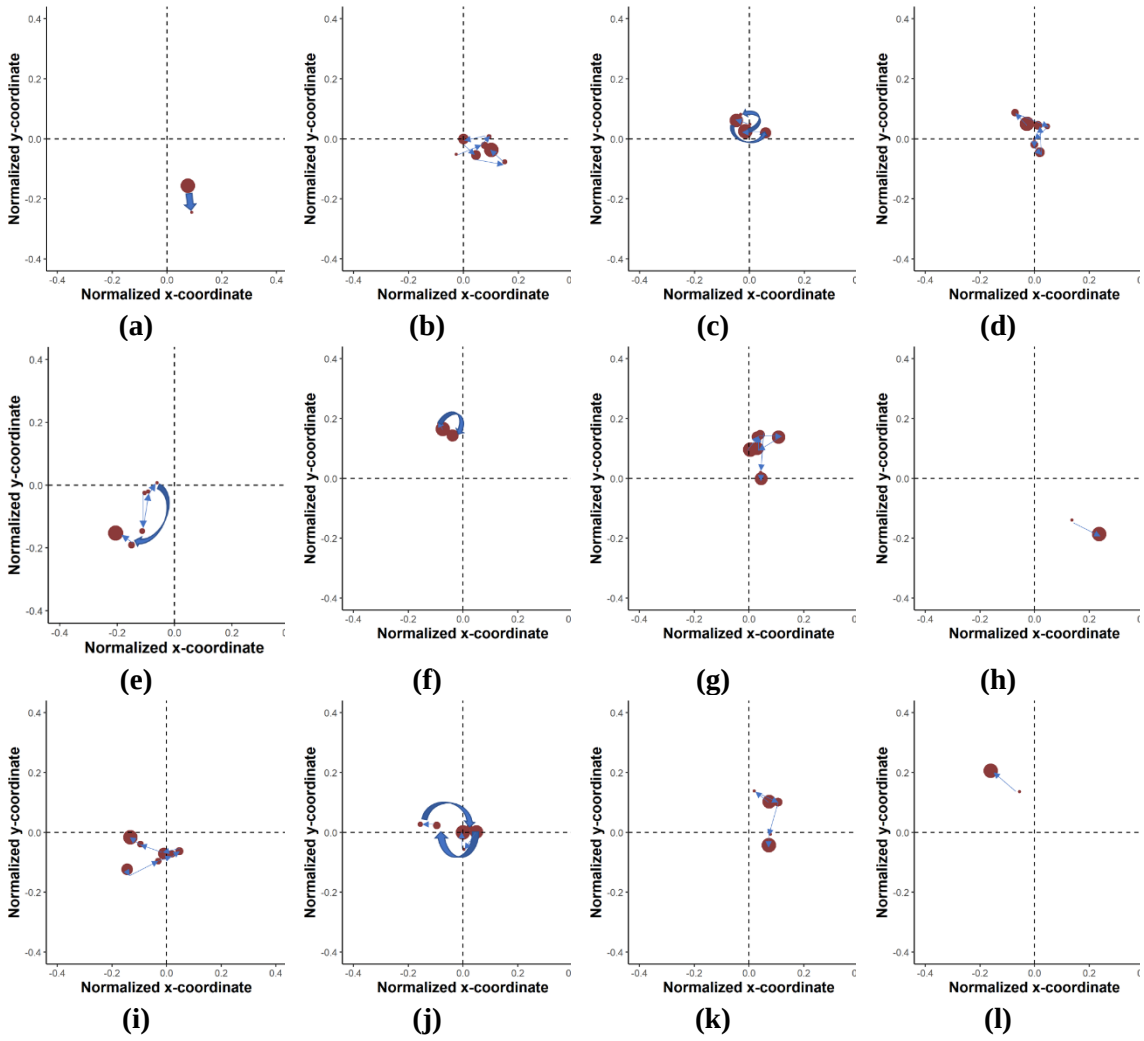

Figure 3. 15 Visual Distraction Magnitude Trajectory Map due to "Visual Only" HVI for (a) Driver ID=11; (b) Driver ID=12; (c) Driver ID=27; (d) Driver ID=28; (e) Driver ID=35; (f) Driver ID=37; (g) Driver ID=43; (h) Driver ID=46; (i) Driver ID=48; (j) Driver ID=63; (k) Driver ID=65; (l) Driver ID=67

Similar to Section 3.4.1.1, this research also explored the relationship between visual distraction increase rate and time. To compute the increase rate of visual distraction magnitude, Equation (3.21) was employed and expressed as follows:

$$IR_{HVI=j} = \frac{d_{F_{i+1}} - d_{F_i}}{t};\ \forall d_{F_{i+1}} > d_{F_i} \tag{3.21}$$

Where,

$IR_{HMI=j}$ = The increase rate of initial visual distraction reduction when HVI type is j (j = "visual only" or "visual and audible") (normalized distance/milliseconds)

d_{F_i} = Distance of F_i to center ($i = 1,2 \ldots, n$);

t = Time under initial visual distraction reduction (milliseconds).

A model fit test is also performed in order to determine the best-fit model in describing the increase rate of visual distraction magnitude under "visual only" and "visual and audible" HVI, respectively. Table 3.7 summarizes the result of the test.

Table 3. 7 Best Model Fit Analyses for Initial Visual Distraction Increase Rate under (a) "Visual-Only" and (b) "Visual + Audible" HVI

(a)

Equation	Model Summary					Parameter Estimates			
	R-square	F	df1	df2	Sig.	Constant	b1	b2	b3
Linear	.143	62.661	1	377	.000	.001	-2.515E-6		
Logarithmic	.407	258.749	1	377	.000	.005	.000		
Inverse	.609	587.522	1	377	.000	1.756E-5	.052		
Quadratic	.280	73.050	2	376	.000	.002	-9.803E-6	1.052E-8	
Cubic	.379	76.362	3	375	.000	.003	-2.328E-5	5.899E-8	-4.321E-11
Compound[a]	.321	178.183	1	377	.000	.001	.997		
Power[a]	.543	447.797	1	377	.000	.021	-.845		
S[a]	.424	277.592	1	377	.000	-8.610	39.983		
Growth[a]	.321	178.183	1	377	.000	-7.334	-.003		
Exponential[a]	.321	178.183	1	377	.000	.001	-.003		
Logistic[a]	.321	178.183	1	377	.000	1.531E3	1.003		

(b)

Equation	Model Summary					Parameter Estimates			
	R-square	F	df1	df2	Sig.	Constant	b1	b2	b3
Linear	.129	46.540	1	314	.000	.001	-1.666E-6		
Logarithmic	.361	177.242	1	314	.000	.004	.000		
Inverse	.583	439.411	1	314	.000	-6.883E-5	.056		
Quadratic	.243	50.127	2	313	.000	.002	-7.315E-6	6.279E-9	
Cubic	.346	54.933	3	312	.000	.003	-1.878E-5	3.717E-8	-2.130E-11
Compound[a]	.538	365.529	1	314	.000	.001	.996		
Power[a]	.774	1.077E3	1	314	.000	.050	-1.084		
S[a]	.515	333.798	1	314	.000	-9.359	55.992		
Growth[a]	.538	365.529	1	314	.000	-7.542	-.004		
Exponential[a]	.538	365.529	1	314	.000	.001	-.004		
Logistic[a]	.538	365.529	1	314	.000	1.885E3	1.004		

The independent variable is time.

As summarized in Table 3.7, each candidate regression model has an $\mathbf{R^2}$ and p-value that obtained from the F test. A higher $\mathbf{R^2}$ suggests that the regression model better explains the increase rate as a function of time. A lower p-value suggests a more significant effect on the increase rate of visual distraction magnitude. For the increase rate under the "visual only" warning, the inverse regression model has the relatively highest $\mathbf{R^2}$ of 0.609

with indicating the time is significant at the 99.9% confidence level. These values reveal that the inverse model is the best-fit model that describes the relationship between increase rate of visual distraction magnitude and time. Therefore, on the basis of the results of the inverse model summarized in Table 3.7, the increase rate of initial visual distraction due to "visual only" HVI can be modeled by a function of time, which is presented by the following equation:

$$IR_{visual\ only} = -1.756 * 10^{-5} + \frac{0.052}{t};\ \forall\, t\ \in [0, 840\ ms] \tag{3.22}$$

For the increase rate under "visual and audible" warning, the power regression model also has the relatively highest $\mathbf{R^2}$ of 0.774 with the p-value lower than 0.01. These values imply that the power model is the best fit model in capturing the relationship between increase rate under "visual and audible" warning and time. Similar to Equation (3.22), the increase rate of initial visual distraction due to "visual and audible" HVI can be expressed as a function of time in the following equation"

$$IR_{visual+audible} = 0.05 * t^{-1.084};\ \forall\, t\ \in [0, 1050\ ms] \tag{3.23}$$

In summary, Figure 3.13 illustrates the increase rate of initial visual distraction induced by both HVI types and time. The red circle dots represent ground truth data of the increase rate due to "visual only" HVI at each timestamp while the cyan triangle dots represent ground truth data of the increase rate due to "visual and audible" HVI at each timestamp. The best-fit models in capturing the relationship between reduction rate and time are also included in Figure 3.16.

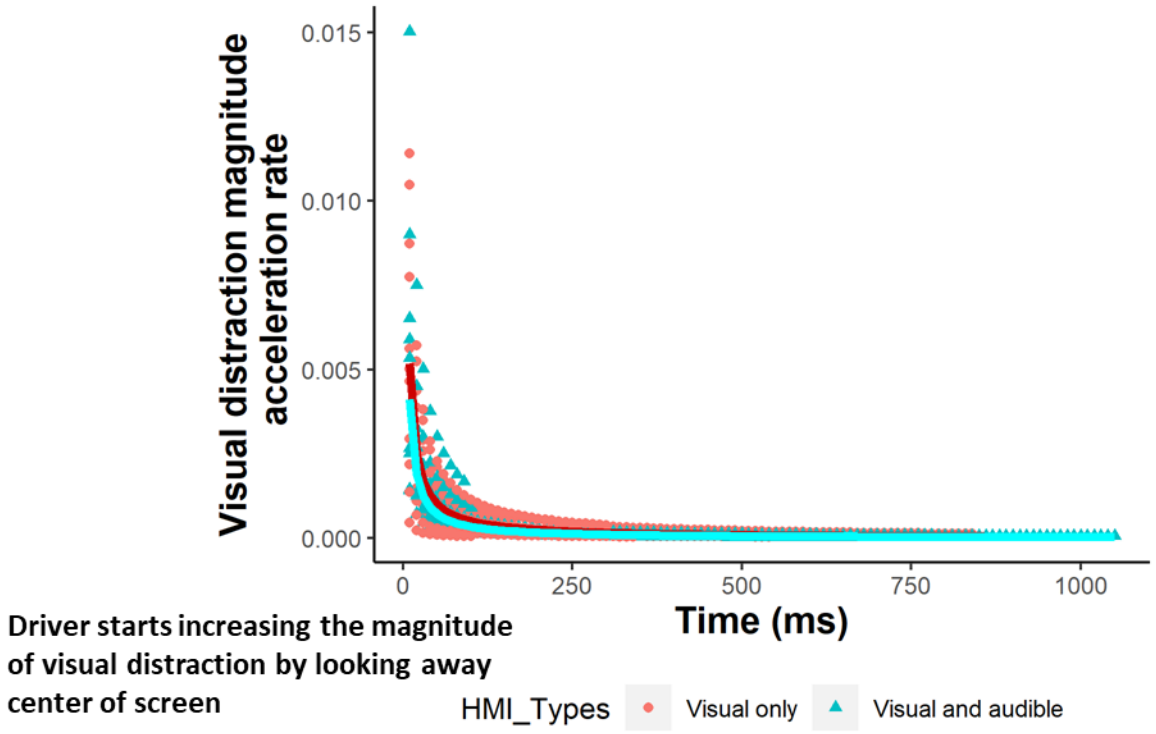

Figure 3. 16 Comparison of Visual Distraction Magnitude Increase Rate and Time under Different HVI Types

As illustrated in Figure 3.16, drivers are starting to increase visual distraction magnitude, regardless of the HVI types, when starting the HVI. Different models were developed in capturing the relationship between time and visual distraction magnitude acceleration rate. On average, drivers under "visual only" spend 315.8 milliseconds on increasing their visual distraction by looking away from the center screen until the next fixation movement, while drivers under "visual and audible" spend 351.1 milliseconds on increasing their visual distraction until the next fixation movement. No significant differences were observed.

3.4.2 Visual distraction direction

By converting the fixation records from Cartesian coordinate system to polar coordinate system, the visual distraction direction was computed and added to the final fixation dataset with 188 sample size. In order to better discuss the visual distraction from the direction perspective, the polar coordinate system was divided into four quadrants based on the angle between the fixed direction axis and the vector of visual distraction. Figure 3.17 illustrates how the polar coordinate system was divided.

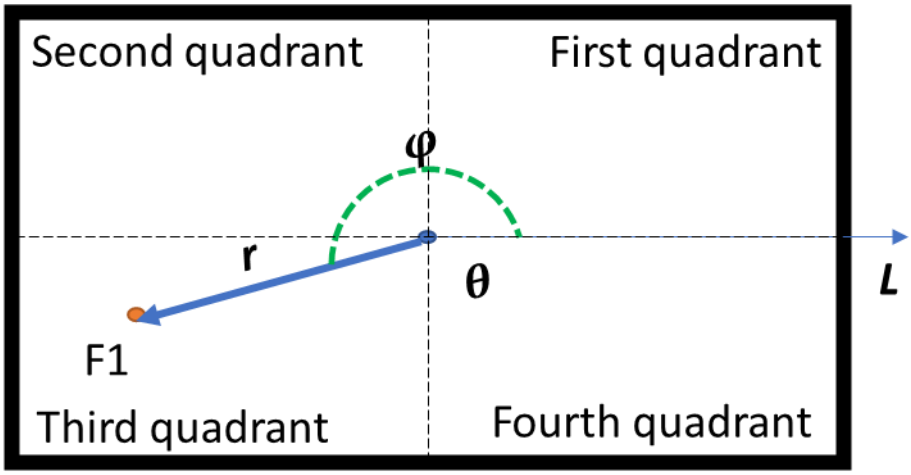

Figure 3. 17 Polar Coordinate System Quadrants

As illustrated in Figure 3.17, the polar coordinate system was divided into four quadrants based on the angle between the visual distraction vectors. An example of fixations "F_1" was given in Figure 16, and $\boldsymbol{\varphi}$ represents the angle between the y-axis and F_1. In this case, the "F_1" has a visual distraction magnitude of "r" with a visual distraction direction at the third quadrant.

Therefore, all participants' fixation records were used to compute the visual distraction direction. Figure 3.18 illustrates the distribution of visual distraction directions under "visual only" and "visual and audible" HVI types.

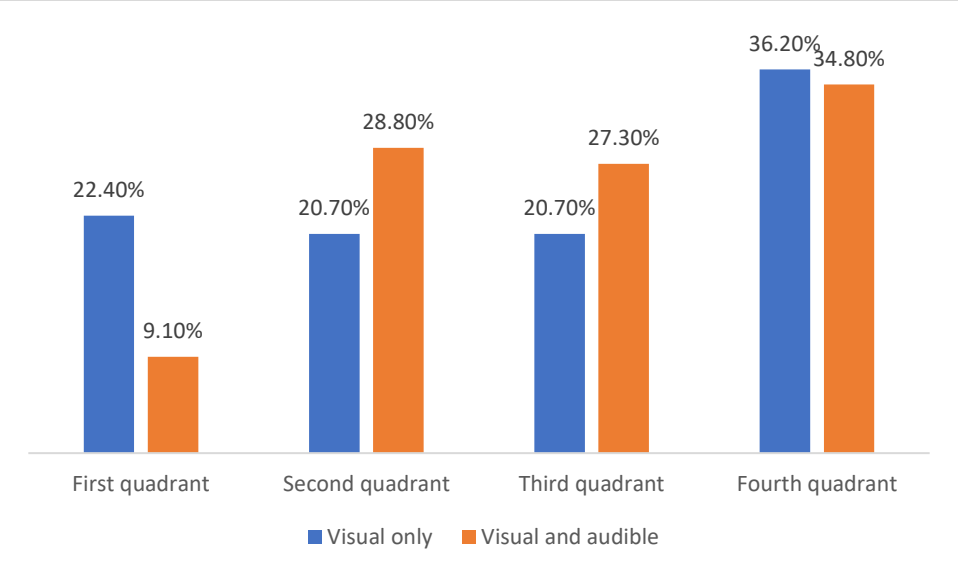

Figure 3. 18 Distribution of Visual Distraction Direction under "Visual Only" and "Visual and Audible" HVI Types

According to Figure 3.18, the same tendency of visual distraction direction for both "visual only" and "visual and audible" HVI types is that drivers have the largest proportion of visual distraction direction located in the lower-right quadrant under both HVI types. However, when drivers in the "visual only" HVI process, the remaining quadrants are close to an evenly distributed situation in terms of fixation location, as the percentage of fixations located in the first, second, and third quadrant is 22.4%, 20.7%, and 20.7%, respectively. On the other hand, drivers have more fixations located in the first quadrant (upper-right quadrant) when receiving messages visually, compared to both receiving messages visually and being alerted audibly (22.4% vs. 9.1%).

To summarize, the distribution of visual distraction direction is different between these two HVI types. To validate this inference, a Wilcoxon test was conducted to determine if the visual distraction directions under two HVI types are different from one another in a statistically significant manner (Happ et al., 2019). As a result, the Wilcoxon test results confirmed that the distributions of visual distraction direction are significantly

different from each other between “visual only” and “visual and audible” HVI types at the 95% confidence interval.

Furthermore, the visual distraction direction was also evaluated from the degree’s perspective. The analysis of degree provides another point of view in understanding visual distraction direction from a continuous perspective rather than a categorical perspective. Table 3.8 summarizes the visual distraction direction in degree under two HVI types.

Table 3. 8 Summary of Visual Distraction Direction (in degree) under “Visual Only” and “Visual and Audible” HVI Types

Variable	Sample size	Visual distraction direction (in degree)			T-test results
		Min.	Mean.	Max.	
“Visual only”	116	1.883	170.442	345.846	t=-2.54,
“Visual and audible”	66	0.199	207.352	352.982	P<0.05*

According to Table 3.8, the average degree of visual distraction direction under visual only is 170.44 degree, which is in the second (lower-right) quadrant, while the average degree of visual distraction direction under visual and audible is 207 degree, which is in the third (lower left) quadrant. A one-tail t-test has been employed to evaluate the significant difference in terms of direction of visual distraction under different HVI types. The result suggests a significant difference, suggesting the visual distraction degree is significantly higher under “visual and audible” HVI type compared to “visual only” HVI type ($t=-2.5398$, $p<0.05$). Therefore, the analysis of visual distraction direction in degree also confirmed the findings from the analysis of visual distraction direction in quadrants.

3.4.3 Visual distraction’s impact on safety

As introduced in the previous section, the visual distraction was extensively modelled from the magnitude and direction perspective. This section mainly discusses the impact of visual distraction on driving safety based on visual distraction magnitude and direction, respectively.

3.4.3.1 Visual distraction intensity and safety

As introduced, drivers have significant difference in terms of visual distraction magnitude and direction between "visual only" and "visual and audible" HVI types. With existing research suggesting that HVI modalities influence driver's takeover time (McDonald et al., 2019; Yoon et al., 2019) and, in turn, affect takeover quality in avoiding collision hazards (W. Zhang et al., 2021), this research reveals the mechanism of how visual distraction magnitude impacts driving safety.

To begin with, a hypothesized model was developed in capturing the relationships among visual distraction magnitude, HVI types, takeover time, and traffic conflicts, which is illustrated in Figure 3.19.

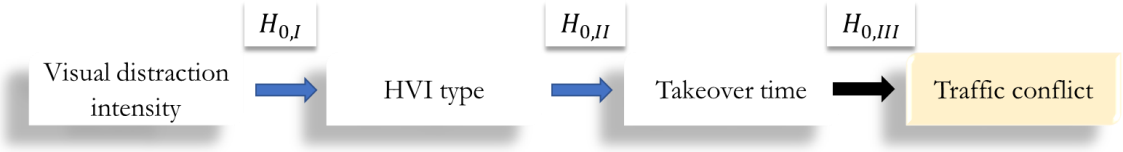

Major hypotheses:

$H_{0,I}$	No significant differences in terms of visual distraction intensity under two HVI types.
$H_{0,II}$	HVI types does not significantly impact takeover time.
$H_{0,III}$	Takeover time does not significantly impact on the probability of having a traffic conflict.

Figure 3. 19 Hypothetical Model in Capturing the Relationship among Visual Distraction Intensity, HVI Types, Takeover Time, and Traffic Conflict.

Table 3.9 summarizes the sample characteristics that prepared for validating the hypothetical model. In order to validate the proposed hypothetical model, a Structural Equation Modeling (SEM) method was employed. This unique discrete choice modeling technique has been widely used in explaining social science problems. SEM is a more advanced statistical model that is capable of estimating interrelationships between "endogenous variables" (direct effects) and "exogenous variables" (indirect effects) in a

simultaneous equation system (Muthén & Muthén, 2011). Furthermore, multi-layers of endogenous variables can be inserted in SEM to reveal how and whether visual distraction magnitude significantly impacts takeover time and the probability of having a traffic conflict under different HVI types. Therefore, SEM is considered a suitable modeling technique in validating the major hypotheses and quantifying the interrelationships among factors introduced in the hypothetical model. The successful applications of SEM in social science have drawn the attention of transportation researchers. For example, researchers have employed SEM to validate the "Technology Acceptance Model," which indicates factors that contribute to Automated Vehicle (AV) acceptance from a psychological perspective (Kapser et al., 2021; T. Zhang et al., 2019).

Table 3. 9 Sample Characteristics for Modeling Visual Distraction Intensity and its Impact on Safety (N=50)

Variable		Description	Type	Category	N/ Mean ± Std.Deviation	Percent (%)/ Range
Category	Name					
Driver distraction intensity	Visual distraction intensity	The total intensity of visual distraction that measured in facing a jaywalker under Level 3-ADS	Continuous	\	0.45±0.60	0.0419~3.6263
HVI Characteristics	Warning Type	Methods to notify drivers regarding a takeover action	Binary Categorical	Visual only	25	50%
				Visual and audible	25	50%
Controller Area Network-Bus (CAN-Bus) information	Takeover time	Time duration from the start of HVI to the moment the driver takes over the driving by applied pedals	Continuous	\	2.29±0.67	1.167~4.667
Safety performance	Traffic conflict	Whether a driver has a traffic conflict after being requested to takeover	Binary Categorical	No conflict	27	54%
				Conflict	23	46%

Figure 3.20 illustrates the final SEM model in capturing the relationships among visual distraction intensity, HVI types, takeover time, and traffic conflicts. The model fits the observed data adequately by the following indices of goodness-of-fits: CFI=1.000, RMSEA=0.000. As this model is estimated using the WLSMV estimator, it produces probit regression coefficients when the endogenous variables are dichotomous, or linear regression coefficients when the endogenous variables are continuous or categorical (Muthén & Muthén, 2011). Table 3.10 summarizes both direct and indirect effects on the probability of having a traffic conflict.

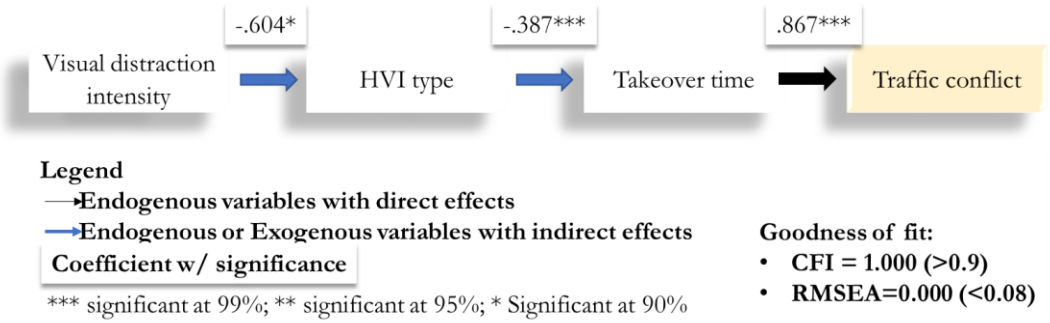

Figure 3. 20 Mechanism of Visual Distraction Intensity Impacting Traffic Conflict

Table 3. 10 Estimated Effects of Direct and Indirect Effects on the Probability of Having a Traffic Conflict

	Direct effects		Indirect effects		Total effects	
	β	**Odds ratio**	***β***	**Odds ratio**	***β***	**Odds ratio**
Visual distraction intensity			0.203	1.225	0.203	1.225
HVI type (visual and audible)			-0.336	0.715	-0.336	0.715
Takeover time	0.867	2.380			0.867	2.380

According to Figure 3.20 and Table 3.10, the mechanism of how visual distraction intensity impacts the probability of having a traffic conflict was revealed and quantified by employing an SEM method. The hypotheses proposed in Figure 3.16 were all rejected. Hence, the visual distraction intensity significantly impacts the takeover time and the probability of having a traffic conflict under different types of HVI.

Specifically, the final SEM model suggests that visual distraction intensity was significantly lower under “visual and audible” HVI type compared to “visual only” HVI type (probit coefficient = -0.604). The analysis of its odds ratio suggests that the visual distraction intensity under “visual and audible” HVI was 39.6% lower than the one under “visual only” HVI, which is consistent with the findings in terms of visual distraction magnitude under these two HVI types. Moreover, the HVI type has a negative impact on

the takeover time (linear coefficient=-0.387), suggesting that drivers spend significantly less time on taking over the vehicle if the HVI type is “visual and audible”, comparing to the circumstance if the HVI type is “visual only”. Combining the aforementioned two observations, it is safe to conclude that the increase in visual distraction intensity positively influences takeover time. The final stage of the SEM model suggests that longer takeover time significantly increase the probability of having a traffic conflict (probit coefficient = 0.867). To summarizes, the final SEM model reveals how visual distraction intensity impacts driving safety in the form of having a traffic conflict.

3.4.3.2 Visual distraction direction and safety

This section mainly discusses how visual distraction direction and safety were connected. The discussion follows the order with analyzing the impact of visual distraction direction on safety from the quadrants’ perspective and then analyzing its impact on safety from the degree perspective.

By linking each driver’s distribution of fixation location with safety performance, it was observed that when having a traffic conflict, drivers have a significant number of fixations staying at the first (upper-right) quadrant, comparing to the number of fixations where there is no traffic conflict ($t=-1.816$, $p<0.1$). Moreover, the number of fixations staying at the second (bottom-right) quadrant also significantly contributes to the probability of having a traffic conflict. The analysis suggests that when having a traffic conflict, drivers have a significant number of fixations staying at the bottom-right corner, comparing to the number of fixations where there is no traffic conflict ($t=-1.59$, $p<0.1$).

Moreover, in order to understand the mechanism of how visual distraction direction impacts the safety performance, a decision tree model was performed. Using a decision

tree to classify a nominal dependent variable is called a classification tree (Ghasemzadeh et al., 2018). The classification can be defined as a procedure for understanding the mechanism for predicting a value in the dependent variable (Han et al., 2011). If the dependent variable is categorical, CART produces a classification tree. If the dependent variable is numerical, CART produces a regression tree. In this study, since the dependent variable is whether having a traffic conflict or not after being requested to takeover. Therefore, a classification tree model was performed with incorporating each driver's age, gender, HVI types, and proportion of fixations staying in each quadrant. Figure 3.21 illustrates the final classification tree model.

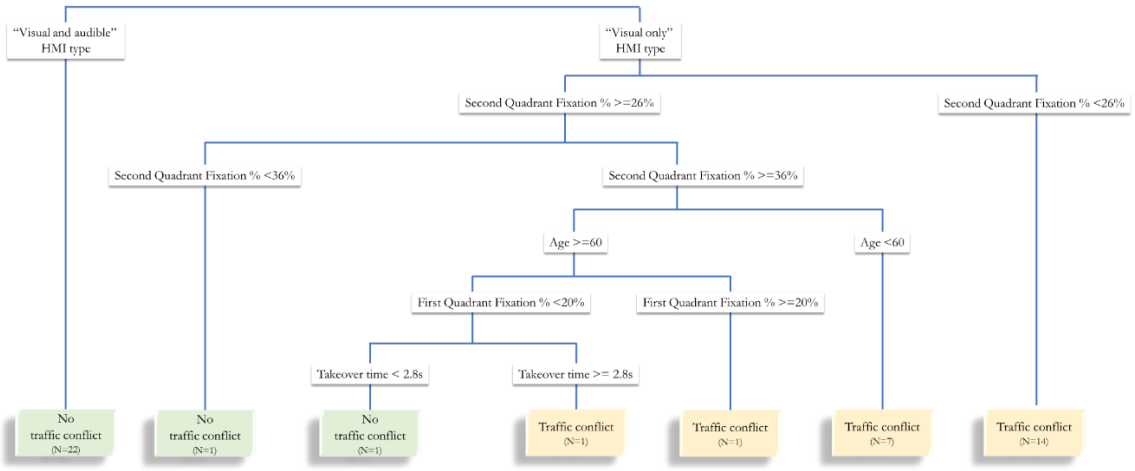

Figure 3. 21 Mechanism of Visual Distraction Direction in Impacting Safety Performance

Figure 3.21 illustrates the final classification tree model in revealing the mechanism of how visual distraction direction impacts the safety performance. The classification tree model has a classification rate of 100%, with driver's age, HVI types, takeover time, and distribution of fixations staying at first as well as second quadrants being identified as contributing factors.

Throughout the classification tree model, there are multiple combinations suggesting the occurrences of traffic conflict. For example, if a driver does not have 26% of the fixations located in the second (upper left) quadrant under the "visual only" HVI type, the probability of having a traffic conflict is 100%. Moreover, drivers who are under 60 with 36% of fixations located in the second quadrant can also result in a traffic conflict under "visual only" HVI. On the other hand, it is still possible that the traffic conflict will not happen under "visual only" HVI, such as (a) having 26%~36% of the fixations located in the second quadrant; and (b) having 36% or above and 20% or lower of fixations located in the second and first quadrant, respectively, with driver's age above 60 and takeover time shorter than 2.8-second.

3.4.4 Predicting visual distraction

The next objective of this research is to develop prediction models that can estimate visual distraction intensity based on drivers' demographical information and Controller Area Network-Bus (CAN-Bus) information data. Previous sub-sections in the "Results" section mainly discuss how driver distraction magnitude changes from the time perspective. In this section, the visual distraction intensity is chosen as the dependent variables, calculated using Equation (3.3), focusing on the entire process of interacting with the jaywalker under Level 3-ADS. Table 3.11 summarizes the sample characteristics for variables included in developing prediction models.

Table 3. 11 Sample Characteristics of Driver Distraction Intensity under HVI (Sample size=50)

Variable		Description	Type	Category	N/ Mean ± Std.Deviation	Percent (%)/ Range
Category	Name					
Demographics	Age	Age of participants	Continuous	\	50.04±14.03	25~73
	Gender	Gender of respondents	Binary Categorical	Male	13	52%
				Female	12	48%
HVI Characteristics	Warning Type	Methods to notify drivers regarding a takeover action	Binary Categorical	Visual only	25	50%
				Visual and audible	25	50%
Controller Area Network-Bus (CAN-Bus) information	Takeover time	Time duration from the start of HVI to the moment the driver takes over the driving by applied pedals	Continuous	\	2.29±0.67	1.167~4.667
Driver distraction intensity	Visual distraction intensity	The total intensity of visual distraction that measured in facing a jaywalker under Level 3-ADS	Continuous	\	0.45±0.60	0.0419~3.6263

Total 50 data sets (samples) that were introduced in Table 3.11 are randomly distributed for training and testing the ANN model at a 70/30 split. The neural network is trained through a number of epochs, and a new set of data is fed into the network during each epoch. Although more complexity of the model can produce better generalization performance, complicated networks can also easily overfit the training data (Amiri et al., 2020). In this case, the testing dataset estimates become worse as the structure learned from the training dataset is top specific, resulting in the overfitting of the model. It has a low bias but high variance.

As a result, when developing the prediction model for estimating visual distraction intensity, it has been observed that the three hidden layer structure with 7 neurons in the first hidden layer, 5 neurons in the second hidden layer, and 1 neuron in the third hidden layer achieves the minimum MSE difference between the testing and training datasets at 0.0831 (MSE in training dataset: 0.0022; MSE in testing dataset: 0.0853). Figure 3.22 illustrates the best-fit models for predicting visual and cognitive distraction.

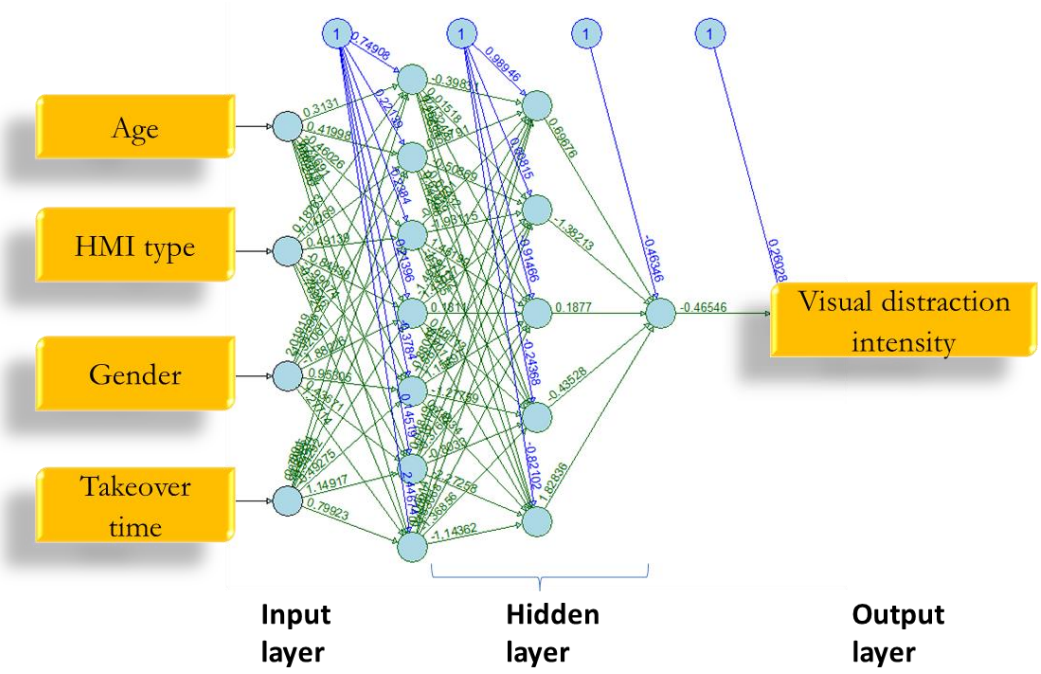

Figure 3. 22 Best-fit ANN Model in Predicting Visual Distraction Intensity

CHAPTER 4: MODELING COGNITIVE DISTRACTION UNDER THE AV ENVIRONMENT

4.1 Modeling cognitive distraction

4.1.1 Cognitive distraction magnitude

Per definition, cognitive distraction is the time that drivers take their minds off. Existing research has been using pupil dilation as a reliable and quantifiable indicator of cognitive load (Beaty & Lucero-Wagnoer, 2000; Gollan et al., 2016; Granholm et al., 1996; Iqbal et al., 2004). Specifically, Pomplun & Sunkara (2003) compared the effects of cognitive workload on pupil dilation. They also confirmed the reliability of using pupil dilation as an indicator for a person's cognitive workload. Pfleging et al. (2016) conducted proof-of-concept research in estimating mental workload by measuring individuals' pupil diameter under different lighting conditions.

Under CAV driving environment, drivers will receive messages from the in-vehicle heads-up or heads-down display, also known as Human-Vehicle Interaction (HVI). Researchers defined this circumstance as a "task-evoked pupil response" (TEPR) (Bradley et al., 2008; Gabay et al., 2011; Jepma & Nieuwenhuis, 2011). This paper will be modeling the HVI-induced cognitive driver distraction under CAV driving environment from pupil dilation.

While the eye-tracking system collects eye movement in temporal and spatial measurements, it also collects gaze behaviors, with pupil dilation being one of the key components. According to Figure 1.2, the pupil dilation data needs to be pre-processed due to possible reasons such as blinking. Moreover, the Pupil Core Eye-tracker sometimes has difficulty detecting the driver's pupil who already wears glasses. These records are to be removed before moving any further.

After records of blinking and pupil not being detected are removed, the next step is to find the baseline pupil diameter since every individual's pupil diameter is different at the baseline level. The baseline pupil diameter is measured at the beginning of the driving without adding any distractions.

In this dissertation, the magnitude of cognitive distraction is measured by the change of pupil diameter compared to the baseline pupil diameter in the format of percentage, which is computed as follows:

$$M_{CD_{t=i}} = \frac{(d_{t=i} - d_0)}{d_0} * 100\% \tag{4.1}$$

Where,

$M_{CD_{t=i}}$ = Intensity of cognitive distraction at the timestamp of i;
$d_{t=i}$ = Pupil diameter at the timestamp of i;
d_0 = Baseline pupil diameter.

Figure 4.1 illustrates the change of pupil diameter change. Moreover, we consider changing pupil diameters based on each eye as the surrogate measurement for cognitive

distraction to reduce human errors. As illustrated in Figure 4.1, unlike visual distraction, cognitive distraction does not show a pattern of time discrete. Therefore, the magnitude of cognitive distraction changes pupil diameter compared to the driver's baseline. According to the driving simulator data, the HVI session can be flagged out.

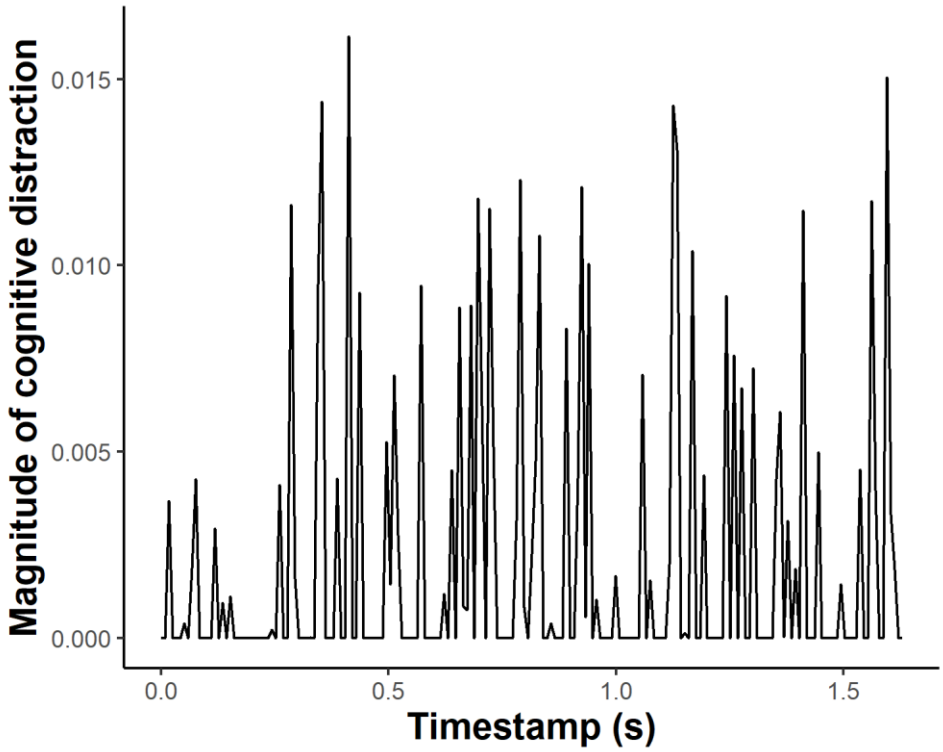

Figure 4. 1 Cognitive Distraction in Measuring Magnitude

Therefore, the intensity of HVI-induced cognitive distraction can be measured using the following equation:

$$I_{CD,HVI} = \int_{t_S}^{t_E} \Delta pd(t)dt \tag{4.2}$$

Where,

I_{CD} = Intensity of cognitive distraction (%*t);
$\Delta pd(t)$ = Pupil diameters change of the left eye as a function of time.

In summary, the magnitude of cognitive distraction can be modeled with following steps:

Step 1: Obtain each driver's baseline pupil diameter in a normal driving session that is not affected by HVI.

Step 2: Retrieve pupil data under the timestamps of the HVI session in the "pupil position" dataset. The retrieved dataset should have the timestamps matched with the ones in the "fixation" dataset.

Step 3: Remove blinking records where suggests the pupil diameter equals 0.

Step 4: Remove pupil data records with a confidence level under 0.6.

Step 5: Select either left or right pupil to continue the measurement of cognitive distraction.

Step 6: Calculate the magnitude of cognitive distraction by using Equation (4.1) under each timestamp.

Step 7: Calculate the intensity of cognitive distraction in terms of the area created in step 6 by referring to the x-axis. Note that unlike the relationship between the magnitude of visual distraction and time illustrated in Figure 4.1, a specific function cannot express the relationship between the cognitive distraction magnitude and time. Therefore, the trapezoidal integration is used to compute the area via MATLAB, which current practice has extensively used (Paraforos & Griepentrog, 2019; Thornton et al., 2015; Y.-D. Wang & Bo, 2013).

4.1.2 Cognitive distraction magnitude and its acceleration rate

In this research, the real-time cognitive distraction is measured by pupil diameter change compared to each driver's baseline pupil diameter in the format of percentage. Unlike visual distraction, the relationship between cognitive distraction and time is time-discrete,

given that every timestamp has a cognitive distraction value matched. Figure 4.2(a) illustrates an example of the relationship between cognitive distraction (in the measurement of pupil diameter change with the format of percentage) and time.

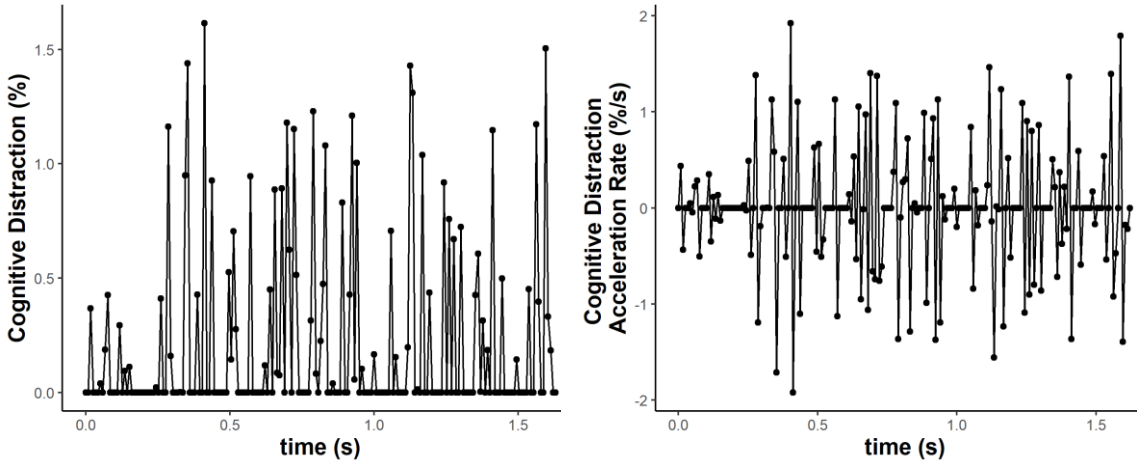

(a) **(b)**

Figure 4. 2 Relationships between (a) Cognitive Distraction and (b) Cognitive Distraction Acceleration Rate with Time (an Example)

As illustrated in Figure 4.2(a), cognitive distraction changes as time increases. By taking the derivative of cognitive distraction with respect to time, the relationship between cognitive distraction acceleration rate (CDAR) and time can be observed, which is illustrated in Figure 4.2(b). Therefore, it can be observed that the CDAR tends to increase, reduce, and then bounce back with a periodic pattern. However, the period in reflecting this tendency is varied. To better observe the frequency of how the cognitive distraction changes over time, a Discrete Fourier Transform (DFT) is used to transform subsequences of the observed time-series data.

The CDAR data reveals a time-series pattern, $t = \{t_0, t_1, \dots, t_n\}$, that can be expressed as a combination of unique circular patterns of varying frequencies, amplitudes, and phases by using a Fourier Transformation (Kluger et al., 2016; X. Wu & Nie, 2011).

Specifically, the cognitive distraction acceleration data was collected in the case of discrete data sampled at a specific frequency. In this case, the Discrete Fourier Transform (DFT) is applied to estimate the frequencies in changing the cognitive distraction.

Assuming a vector set of cognitive distraction acceleration rate, $cdar = \{cdar_0, cdar_1, \dots, cdar_n\}$, samples at discrete time locations of $t = \{t_0, t_1, \dots, t_n\}$. By turning the data vector of CDAR into its sine and cosine through DFT, a frequency domain perspective can be added in exploring the frequency of cognitive distraction accelerates.

The purpose of DFT is to compute a vector set of Fourier coefficients (i.e., $\widehat{cdar_0}, \widehat{cdar_1}, \dots, \widehat{cdar_n}$). With the DFT, the frequency domain will be used to describe the relationship between CDAR and time. For a $\widehat{cdar_k}$,

$$\widehat{cdar_k} = \sum_{j=0}^{n-1} cdar_j e^{-i2\pi jk/n} \tag{4.3}$$

By employing Equation (4.3),

$$\{cdar_0, cdar_1, \dots, cdar_n\} \overset{DFT}{\Longrightarrow} \{\widehat{cdar_0}, \widehat{cdar_1}, \dots, \widehat{cdar_n}\} \tag{4.4}$$

With defining ω_n, the fundamental frequency that is related to the types of sines and cosines can be used to approximate with discrete CDAR in the time domain. The ω_n can be expressed in the following form:

$$\omega_n = e^{-2\pi i/n};\ \forall\ i = \sqrt{-1} \tag{4.5}$$

In this case, the Fourier coefficients (i.e., $\widehat{cdar_0}, \widehat{cdar_1}, \dots, \widehat{cdar_n}$) can be computed using the following equation:

$$\begin{bmatrix} \widehat{cdar_0} \\ \widehat{cdar_1} \\ \widehat{cdar_2} \\ \vdots \\ \widehat{cdar_n} \end{bmatrix} = \begin{bmatrix} 1 & 1 & 1 & \cdots & 1 \\ 1 & \omega_n & \omega_n^2 & \cdots & \omega_n^{n-1} \\ 1 & \omega_n^2 & \omega_n^4 & \cdots & \omega_n^{2(n-1)} \\ \vdots & \vdots & \vdots & \ddots & \vdots \\ 1 & \omega_n^{n-1} & \omega_n^{2(n-1)} & \cdots & \omega_n^{(n-1)^2} \end{bmatrix} \begin{bmatrix} cdar_0 \\ cdar_1 \\ cdar_2 \\ \vdots \\ cdar_n \end{bmatrix} \quad (4.6)$$

MATLAB is used to perform DFT, with an objective of obtaining the maximum frequency of each driver's cognitive distraction along with the CDAR. Figure 4.3 illustrates the flow of DFT analysis.

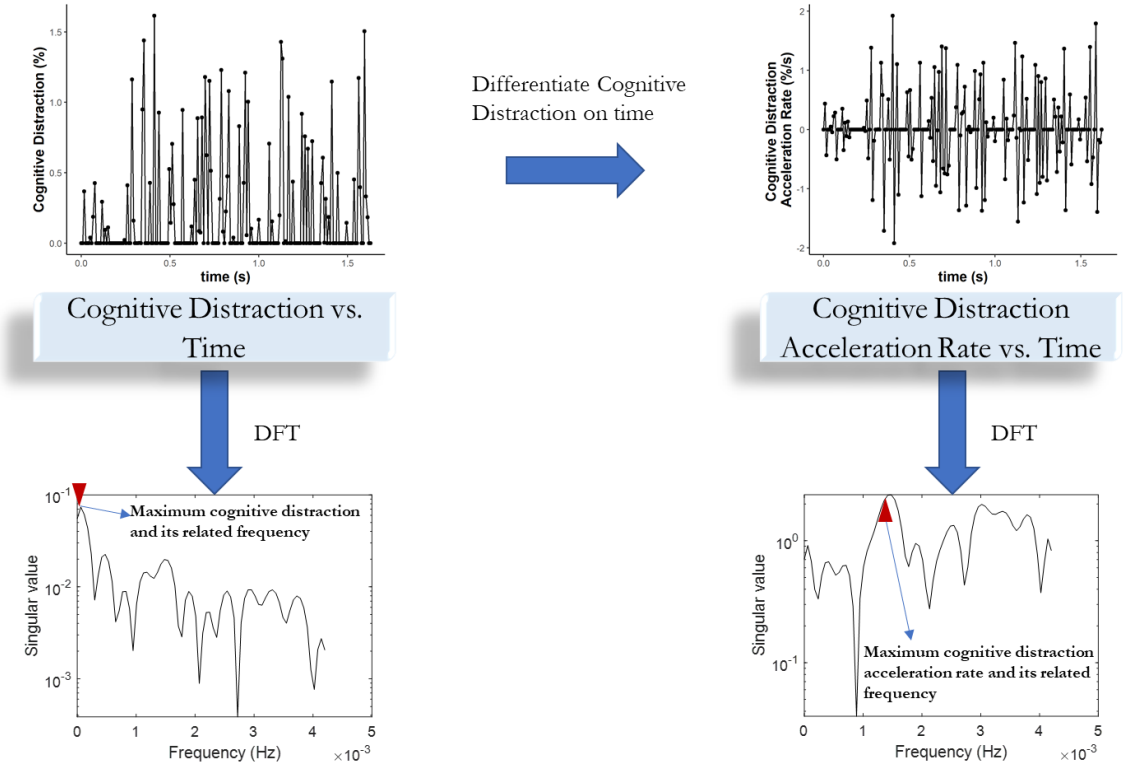

Figure 4. 3 Flow Chart of Performing DFT Analysis with Cognitive Distraction and its Acceleration Rate

4.2 Quantification of cognitive distraction

4.2.1 Factors impacting cognitive distraction and its acceleration rate

As introduced in Section 3.3, participants' pupil dilation was collected by using an eye-tracking device. Pupil dilation was used in modeling a driver's cognitive distraction. In this

research, there were two DFTs performed focusing on cognitive distraction and CDAR, respectively. The frequencies that each driver achieved the maximum cognitive distraction, and its acceleration rate were computed for each driver. By evaluating the drivers with different ages and gender under different HVI types in terms of the computed frequency of achieving maximum cognitive distraction, this research found a significant difference for drivers who are above 60 years old between "visual only" and "visual and audible" HVI types. Table 8 summarizes the differences.

Table 4. 1 Evaluation Results of Frequency in Reflecting Maximum Cognitive Distraction for Drivers above 60 under Two HVI Types

Variable	Sample size	Frequency reflecting maximum cognitive distraction			T-test results
		Min.	Mean.	Max.	
"Visual only" & "Above 60"	8	0.0000	1.597e-05	5.380e-05	T=-1.72, P<0.1*
"Visual and audible" & "Above 60"	8	0.0000	1.063e-04	4.200e-04	

As summarized in Table 4.1, drivers above 60 years old have a significantly lower frequency in achieving the maximum cognitive load under the "visual only" HVI type than the "visual and audible" HVI type. Hence, for drivers who are 60 years old or above, it takes a significantly longer time to reach the maximal cognitive load under the "visual only" HVI type, compared to the "visual and audible" HVI type. A major assumption here is that the quicker the maximal cognitive load, the lower cognitive distraction intensity the driver will obtain during the HVI process. In this case, it can be inferred that drivers who are 60 years old or above have a lower intensity of cognitive distraction if the HVI type is "visual and audible" because maximal cognitive distraction is reached in a significantly shorter period of time compared to "visual only".

To validate this inference, the intensity of cognitive distraction was evaluated for drivers who are 60 years old or above between these two types of HVI. As a result, the

average cognitive distraction intensity is significantly lower under the "visual and audible" HVI, compared to the one under "visual only" HVI ($t=1.404$, $p<0.1$). Table 4.2 summarizes the detailed evaluation results.

Table 4. 2 Evaluation Results of Cognitive Distraction Intensity for Drivers above 60 under Two HVI Types

Variable	Sample size	Intensity of cognitive distraction			T-test results
		Min.	Mean.	Max.	
"Visual only" & "Above 60"	8	0.0096	0.0762	0.2430	T=1.404, P<0.1*
"Visual and audible" & "Above 60"	8	0.0013	0.0343	0.0747	

Therefore, it can be concluded that drivers who are 60 years old or above are significantly reduced in cognitive distraction if the HVI type is "visual and audible", compared to the "visual only" HVI type. The reason is revealed after computing the frequency of reaching maximum cognitive distraction under these two HVI types.

After exploring the cognitive distraction, this research furthers the analysis by evaluating the frequency of achieving maximum CDAR transformed by discrete Fournier. Consequently, it can be concluded that the frequency that corresponds to the maximal of CDAR is significantly larger if the HVI type is "visual only", compared to "visual and audible" ($t=1.9851$, $p<0.05$). Table 4.3 summarizes the evaluation results.

Table 4. 3 Evaluation Results of Cognitive Distraction Acceleration Rate between "Visual Only" and "Visual and Audible" HVI

Variable	Sample size	Frequency reflecting maximum cognitive distraction acceleration rate			T-test results
		Min.	Mean.	Max.	
"Visual only"	25	0.0013	0.0034	0.0042	T=1.9851, P<0.05**
"Visual and audible"	25	0.00005	0.0029	0.0042	

Based on the results from Table 4.3, it can be concluded that the time needed for reaching the maximal CDAR under "visual and audible" is significantly higher than "visual only" HVI. A potential reason is that the situation awareness is relatively higher if the HVI type is a multi-modal (including more than one cue) compared to the uni-modal HVI type

(i.e., visual only), in which the existing studies have supported this inference (Roche et al., 2019; Wright et al., 2017). As a result, drivers are more likely to be well-prepared in handling emergency situations (i.e., takeover) and less likely to heavily increase the cognitive distraction during the "visual and audible" HVI process.

On the other hand, if the HVI is "visual only", drivers' situation awareness is relatively low compared to "visual and audible" HVI. When drivers find out they need to take over the vehicle in response to certain emergencies (i.e., jaywalker) under "visual only", they need an extended time to percept the fact that a takeover is needed and complete the takeover process. The collected data also supports this interpolation, that the takeover time is significantly lower under the "visual and audible" HVI, compared to "visual only" HVI ($t=3.571$, $p<0.01$). Therefore, when the driver realizes that a takeover action is needed, there is a compensation belief reflected in the driver to make up for the potential hazards due to driver distraction. Hence, the action is reflected in the CDAR by increasing the pupil dilation change rate.

4.2.2 Cognitive distraction change after visual distraction reaching the maximum

Gaze behavior data is applied to measure visual and cognitive distraction, respectively. It is worthwhile to investigate the connection between these two types of driver distraction. However, the visual distraction magnitude changes over time. For example, drivers reach their maximum visual distraction at different timestamps. It is a challenge to compare drivers' cognitive distraction if their visual distraction is not generalized. Therefore, this sub-section discusses cognitive distraction and its acceleration rate after the driver's visual distraction reaches maximum.

Figure 4.4 illustrates the cognitive distraction magnitudes' distribution after drivers reach their maximal visual distraction under both “visual only” and “visual and audible” HVI types.

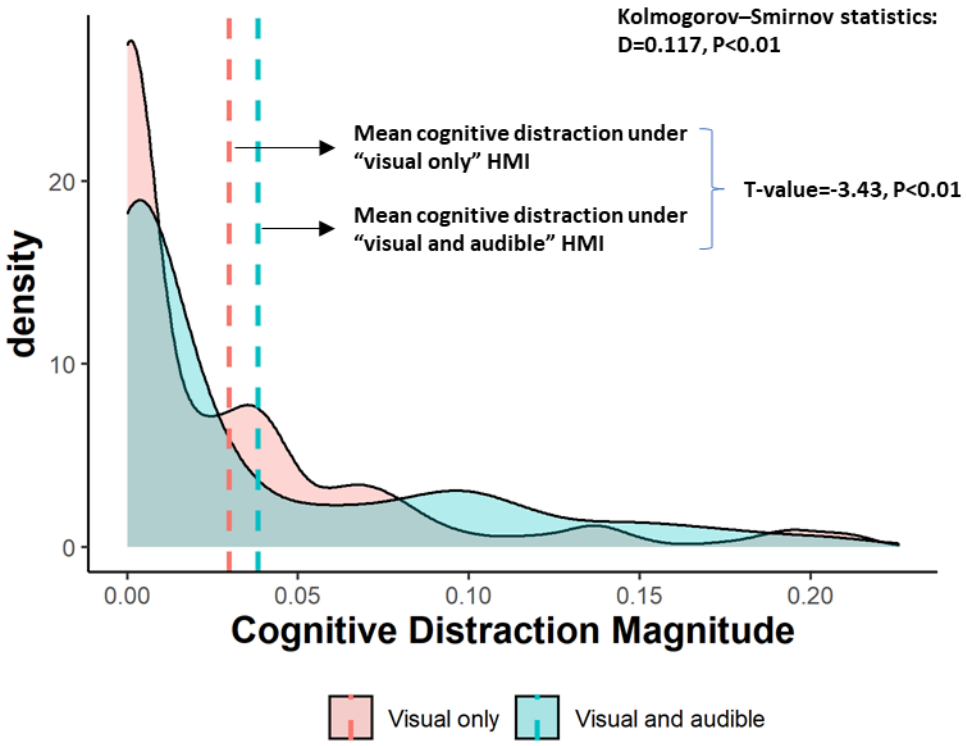

Figure 4. 4 Distribution of Cognitive Distraction Magnitudes after Visual Distraction Magnitude Reaching the Maximum

As illustrated in Figure 4.4, only cognitive distraction magnitudes after drivers reach the maximal visual distraction magnitude are included. The average cognitive distraction magnitudes under these two HVI types are highlighted in Figure 4.4. When visual distraction reaches the maximum, the cognitive distraction is observed with significantly different patterns under different HVI types, according to the Kolmogorov–Smirnov (K-S) test ($D=0.117$, $p<0.01$). Furthermore, after the visual distraction reaches the maximum, the average cognitive distraction under the “visual and audible” HVI type is significantly higher than the one under the “visual only” HVI type ($t=-3.43$, $p<0.01$). A

potential reason is that audio may extend the cognitive workload by maintaining the pupil dilation at a higher level.

Figure 4.5 illustrates the relationship between cognitive distraction magnitude and time under "visual only" and "visual and audible" HVI types to validate this inference. In order to visually assess the relationships of cognitive distraction with respect to time after drivers reach the maximal visual distraction, a Locally Weighted Scatterplot Smoothing (LOESS) smoother is also added in Figure 4.5. Since the nonparametric LOESS technique does not require a priori speciation of data distribution, it is chosen to assist with focusing on foreseeing the trends of how cognitive distraction magnitude changes over time. In each local span defined in LOESS, the neighboring data is processed by a quadratic polynomial to determine the smoothed value (Jacoby, 2000).

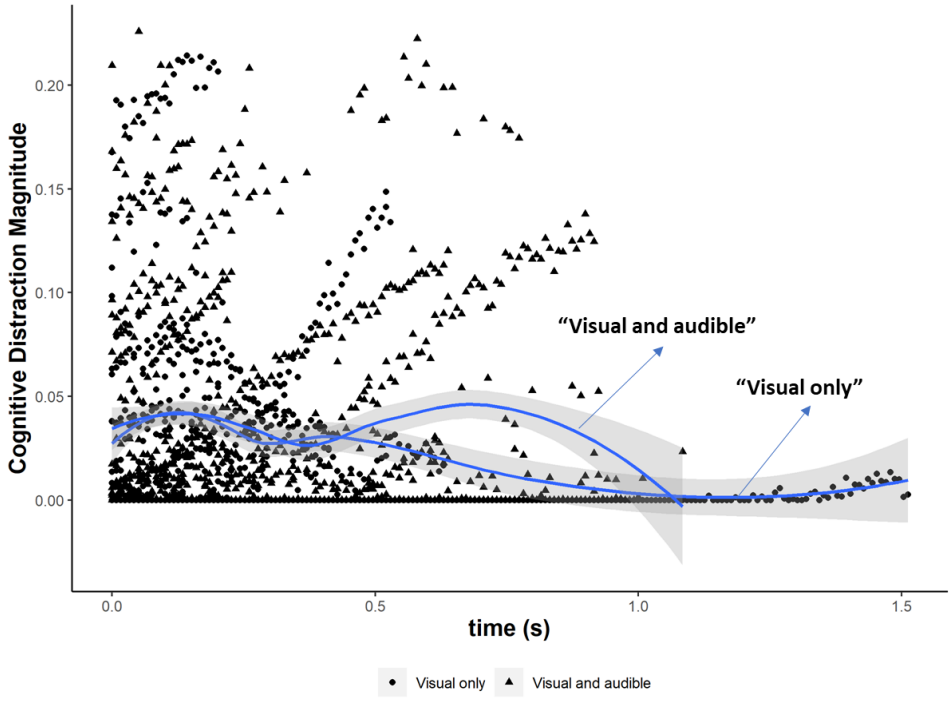

Figure 4. 5 Cognitive Distraction Magnitude vs. Time under "Visual Only" and "Visual and Audible" HVI Types with LOESS Curves at 95% Confidence Interval (Note that "time=0.0s" suggests driver reached the maximum visual distraction).

As illustrated in Figure 4.5, circle dots represent the cognitive distraction under "visual only" after visual distraction reaches the maximum value by each driver, and triangles represent the cognitive distraction under "visual and audible". During the first 0.5 seconds, the cognitive distraction between "visual only" and "visual and audible" are close to evenly distributed. The smoothed curves are highly overlapped between 0-second and 0.5-second. Additionally, a two-tail t-test was conducted with the null hypothesis suggesting that there is no significant difference in terms of the cognitive distraction magnitude between "visual only" and "visual and audible" HVI types at the onset of 0.5-second after drivers reaching their maximal visual distraction. As a result, the null hypothesis is accepted ($t=-0.28$, $p=0.78$), suggesting that although the average cognitive distraction magnitude under "visual and audible" is significantly higher than the one under "visual only" (according to Figure 4.5), it does not reflect on the early stage (0~0.5 seconds) after reaching the maximum visual distraction magnitude.

At the second stage (0.5~1 second), after reaching the maximal visual distraction magnitude, there are fewer records regarding the cognitive distraction magnitude under "visual only" HVI compared to "visual and audible" HVI. Accordingly, the smoothed curves representing these two HVI types also reveal the different relationships between cognitive distraction magnitude and time. A one-tail t-test was conducted, suggesting that cognitive distraction magnitude is significantly higher if the HVI type is "visual and audible" compared to "visual only" ($t=-6.17$, $p<0.01$) during the second stage after reaching the maximal visual distraction magnitude. Therefore, to summarize, the addition of audio significantly extends the cognitive workload after drivers reach the maximal visual distraction magnitude at a later stage. The final stage (1~1.5 seconds) is not discussed here

due to insufficient records of cognitive distraction magnitude under “visual and audible” HVI.

In summary, compared to “visual only” HVI, drivers’ cognitive distraction magnitude is significantly higher under the “visual and audible” HVI. To specify this finding, the analysis is broken down with respect to the driver’s gender and age. Figure 4.6 illustrates the relationship between cognitive distraction magnitude and time among gender and age groups under these two HVI types.

As illustrated in Figure 4.6(a), colors were added to the existing circle dots and triangles with suggesting different age groups, namely “under 40 years old” and “40 years old or above”. There are patterns can be observed between age groups in terms of the cognitive distraction magnitude after drivers reaching the maximal visual distraction magnitude. During the early stages after reaching the maximal visual distraction magnitude (i.e., 0~0.5-second), drivers who are 40 years old or above are more likely to still maintain a high level of cognitive distraction magnitude, as the circle dots and triangles in orange colors dominate the higher level of cognitive distraction magnitude (0.1 and above) in Figure 4.6(a). During the second stage after reaching the maximal visual distraction magnitude (i.e., 0.5~1-second), although younger drivers (under 40 years old) were observed with an uptick in terms of cognitive distraction magnitude, the overall trend suggests that there are older drivers (40 years old or above) maintained the same high level of cognitive distraction magnitude (0.1 and above). Therefore, it is safe to conclude that younger drivers have a lower cognitive workload compared to older drivers after all of them reaching the maximal visual distraction magnitude.

As depicted in Figure 4.6(b), another set of colors were added to the existing circle dots and triangles with indicating female and male drivers. Unlike Figure 4.6(a), the relationship between cognitive distraction magnitude and time suggests different patterns under genders. At the early stages after reaching the maximal visual distraction magnitude (i.e., 0~0.5-second), female drivers have a tendency of maintaining a higher level of cognitive distraction magnitude, as they dominated the higher level of cognitive distraction magnitude (0.1 and above) in Figure 4.6(b), regardless of the HVI types. On the other hand, at the second stage after reaching the maximal visual distraction (i.e., 0.5~1-second), male drivers took the lead in having a higher cognitive distraction compared to female drivers. This finding suggests that female drivers' cognitive workload maintained a higher level than male drivers' after they all reaches the maximum of visual distraction. However, this trend is reversed when they achieve the maximal visual distraction magnitude for a later time frame.

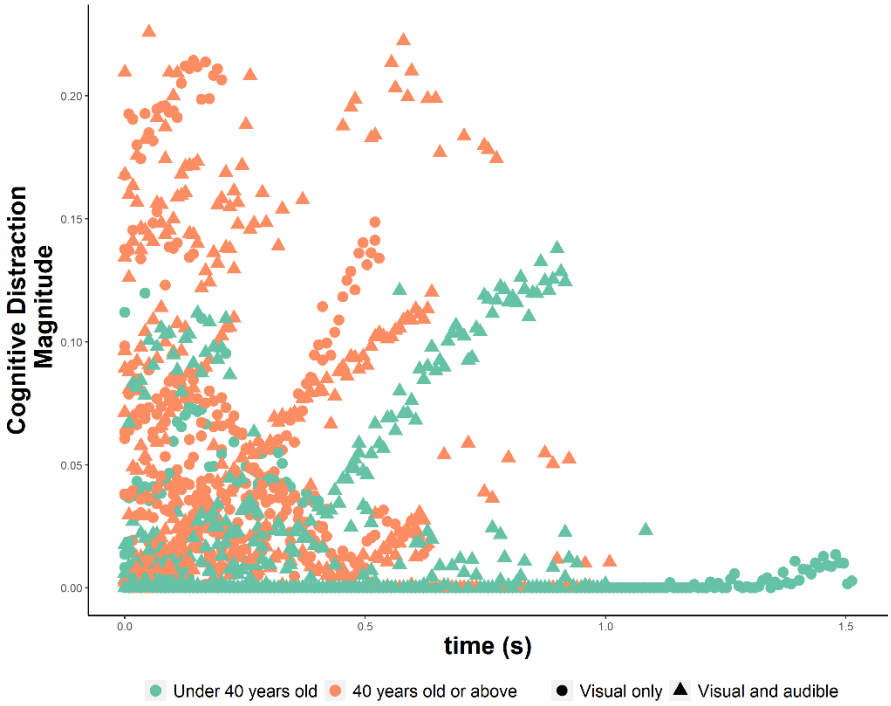

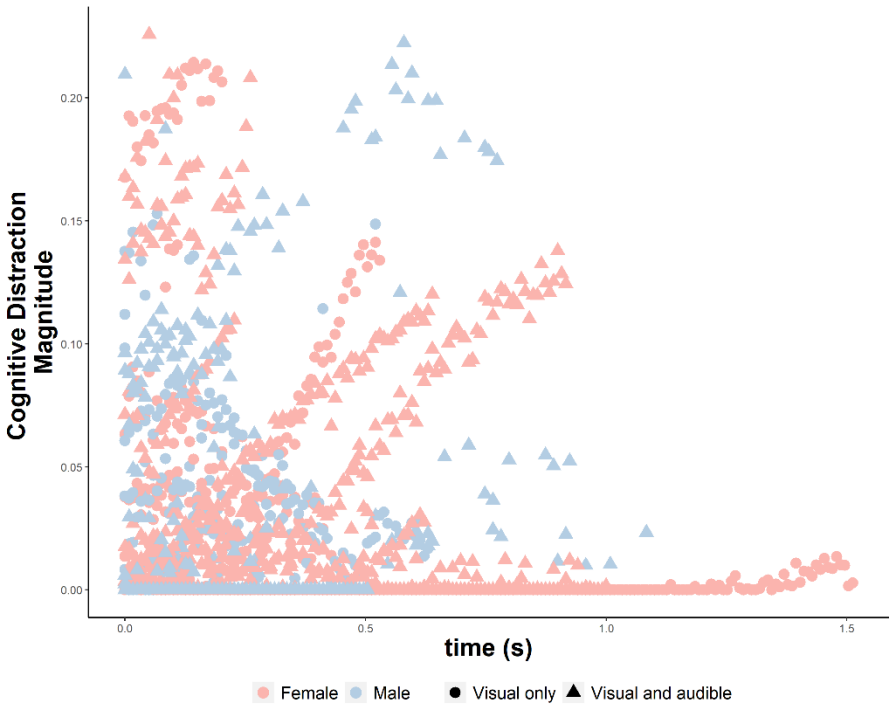

Figure 4. 6 Cognitive Distraction Magnitude vs. Time under "Visual Only" and "Visual and Audible" HVI Types in Comparison of (a) Age, and (b) Gender

Moreover, Figure 4.7 illustrates the relationship between cognitive distraction magnitude and time between female and male drivers under these two HVI types.

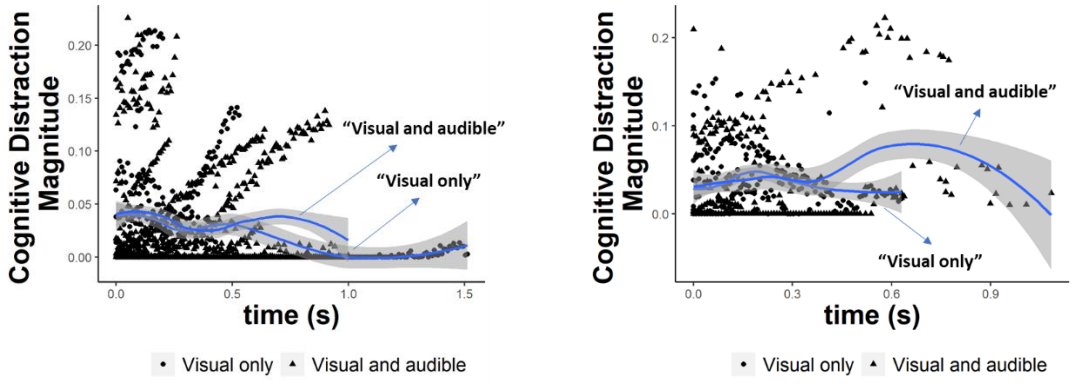

Figure 4. 7 Cognitive Distraction Magnitude vs. Time under "Visual Only" and "Visual and Audible" HVI Types with LOESS Curves at 95% Confidence Interval in terms of (a) Female Drivers and (b) Male Drivers. (Note that "time=0.0s" suggests driver reached the maximum visual distraction).

As illustrated in Figure 4.7, it can be observed that both female and male drivers show higher cognitive distraction under the "visual and audible" HVI in the second stage (female: 0.5~1 second; male: 0.3~0.6 seconds) after reaching maximal visual distraction magnitude, compared to "visual only" HVI.

4.3 Cognitive distraction's impact on safety

As introduced in the previous section, the cognitive distraction was extensively modelled from the magnitude and its acceleration rate, with incorporating human factors. This section mainly discusses the impact of cognitive distraction on driving safety in format of traffic conflicts.

Previous sections suggest that drivers have significant differences in terms of cognitive distraction magnitude between "visual only" and "visual and audible" HVI types. This section uses a similar modeling approach that employed in the previous chapter of revealing why and how visual distraction influences driving safety.

To begin with, a hypothesized model was developed in capturing the relationships among cognitive distraction magnitude, HVI types, takeover time, and traffic conflicts, which is illustrated in Figure 4.8.

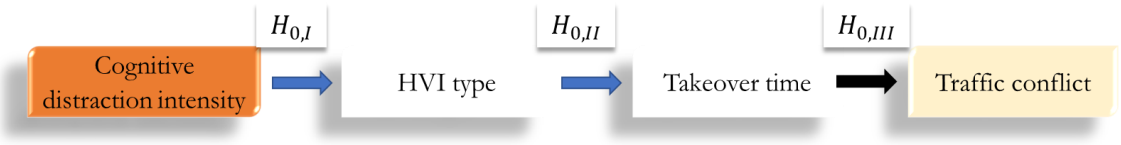

Major hypotheses:

$H_{0,I}$	No significant differences in terms of cognitive distraction intensity under two HVI types.
$H_{0,II}$	HVI types does not significantly impact takeover time.
$H_{0,III}$	Takeover time does not significantly impact on the probability of having a traffic conflict.

Figure 4. 8 Hypothetical Model in Capturing the Relationship among Cognitive Distraction Intensity, HVI Types, Takeover Time, and Traffic Conflict.

Table 4.4 summarizes the sample characteristics that prepared for validating the hypothetical model. In order to validate the proposed hypothetical model, a Structural Equation Modeling (SEM) method was employed. A detailed introduction of SEM methodology has been provided in previous sections. Note that the cognitive distraction intensity was calculated by using Equation (4.2), which integrates the cognitive distraction over the HVI processing time.

Table 4. 4 Sample Characteristics for Modeling Visual Distraction Intensity and its Impact on Safety (N=50)

Variable		Description	Type	Category	N/ Mean ± Std.Deviation	Percent (%)/ Range
Category	Name					
Driver distraction intensity	Cognitive distraction intensity	The total intensity of cognitive distraction that measured in facing a jaywalker under Level 3-ADS	Continuous	\	0.17±0.18	0.0012~0.7578
HVI Characteristics	Warning Type	Methods to notify drivers regarding a takeover action	Binary Categorical	Visual only	25	50%
				Visual and audible	25	50%
Controller Area Network-Bus (CAN-Bus) information	Takeover time	Time duration from the start of HVI to the moment the driver takes over the driving by applied pedals	Continuous	\	2.29±0.67	1.167~4.667
Safety performance	Traffic conflict	Whether a driver has a traffic conflict after being requested to takeover	Binary Categorical	No conflict	27	54%
				Conflict	23	46%

Figure 4.9 illustrates the final SEM model in capturing the relationships among cognitive distraction intensity, HVI types, takeover time, and traffic conflicts. The model fits the observed data adequately by the following indices of goodness-of-fits: CFI=1.000, RMSEA=0.000. As this model is estimated using the WLSMV estimator, it produces probit regression coefficients when the endogenous variables are dichotomous, or linear regression coefficients when the endogenous variables are continuous or categorical (Muthén & Muthén, 2011). Table 4.5 summarizes both direct and indirect effects on the probability of having a traffic conflict.

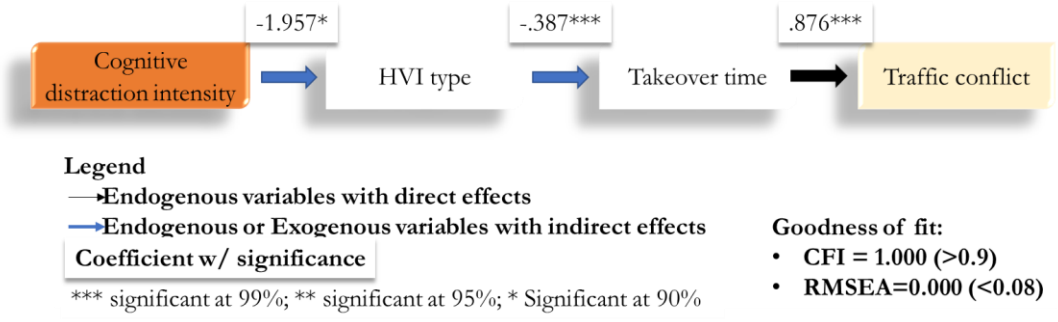

Figure 4. 9 Mechanism of Cognitive Distraction Intensity Impacting Traffic Conflict

Table 4. 5 Estimated Effects of Direct and Indirect Effects on the Probability of Having a Traffic Conflict

	Direct effects		Indirect effects		Total effects	
	β	**Odds ratio**	***β***	**Odds ratio**	***β***	**Odds ratio**
Cognitive distraction intensity			0.663	1.941	0.663	1.941
HVI type (visual and audible)			-0.339	0.712	-0.339	0.712
Takeover time	0.876	2.401			0.876	2.401

According to Figure 4.9 and Table 4.5, the mechanism of how cognitive distraction intensity impacts the probability of having a traffic conflict was revealed and quantified with incorporating HVI types and takeover performance by employing an SEM method.

The hypotheses proposed in Figure 4.8 were all rejected. Therefore, the cognitive distraction intensity significantly impacts the takeover time and the probability of having a traffic conflict under different types of HVI.

Specifically, the final SEM model suggests that cognitive distraction intensity was significantly lower under "visual and audible" HVI type compared to "visual only" HVI type (probit coefficient = -1.957). The analysis of its odds ratio suggests that the cognitive distraction intensity under "visual and audible" HVI was 85.9% lower than the one under "visual only" HVI, which is consistent with the findings in terms of cognitive distraction magnitude under these two HVI types according to the one-tail t-test results ($t=1.39$, $p<0.1$). Moreover, the HVI type has a negative impact on the takeover time (linear coefficient=-0.387), suggesting that drivers spend significantly less time on taking over the vehicle if the HVI type is "visual and audible", comparing to the circumstance if the HVI type is "visual only". Combining the aforementioned two observations, it is safe to conclude that the increase in cognitive distraction intensity positively influences takeover time. The final stage of the SEM model suggests that longer takeover time significantly increase the probability of having a traffic conflict (probit coefficient = 0.867). To summarizes, the final SEM model reveals how cognitive distraction intensity impacts driving safety in the form of having a traffic conflict.

4.4 Predicting cognitive distraction

Similar to Section 3.4.4, this research also develops the prediction model that can estimate cognitive distraction intensity based on drivers' demographical information and Controller Area Network-Bus (CAN-Bus) information data. In this section, the cognitive distraction intensities are chosen as the dependent variables, calculated using Equation (4.2), focusing

on the entire process of interacting with the jaywalker under Level 3-ADS. Table 4.6 summarizes the sample characteristics for variables included in developing prediction models.

Table 4. 6 Sample Characteristics of Driver Distraction Intensity under HVI (Sample size=50)

Variable		Description	Type	Category	N/ Mean ± Std.Deviation	Percent (%)/ Range
Category	Name					
Demographics	Age	Age of participants	Continuous	\	50.04±14.03	25~73
	Gender	Gender of respondents	Binary Categorical	Male	13	52%
				Female	12	48%
HVI Characteristics	Warning Type	Methods to notify drivers regarding a takeover action	Binary Categorical	Visual only	25	50%
				Visual and audible	25	50%
Controller Area Network-Bus (CAN-Bus) information	Takeover time	Time duration from the start of HVI to the moment the driver takes over the driving by applied pedals	Continuous	\	2.29±0.67	1.167~4.667
Driver distraction intensity	Cognitive distraction intensity	The total intensity of cognitive distraction that measured in facing a jaywalker under Level 3-ADS	Continuous	\	0.05±0.05	0.0003~0.2430

Total 50 data sets (samples) that were introduced in Table 4.6 are randomly distributed for training and testing the ANN model at a 70/30 split. The neural network is trained through a number of epochs, and a new set of data is fed into the network during each epoch. Although more complexity of the model can produce better generalization performance, complicated networks can also easily overfit the training data (Amiri et al.,

2020). In this case, the testing dataset estimates become worse as the structure learned from the training dataset is top specific, resulting in the overfitting of the model. It has a low bias but high variance.

As a result, the cognitive distraction intensity prediction model has come up with the three hidden layer structure with 8 neurons in the first hidden layer, 13 neurons in the second hidden layer, and 1 neuron in the third hidden layer, which has achieved the minimum MSE difference between training and testing datasets at -0.0302 (MSE in training dataset: 0.0676; MSE in testing dataset: 0.0364). Figure 4.10 illustrates the best-fit models for predicting visual and cognitive distraction.

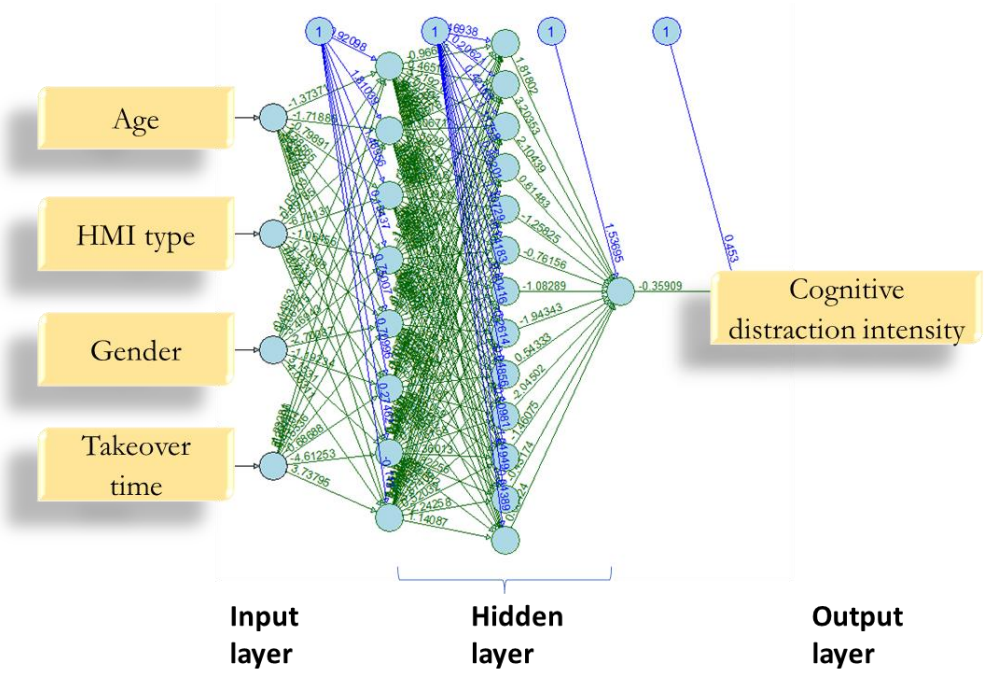

Figure 4. 10 Best-fit ANN Model in Predicting (a) Visual Distraction Intensity and (b) Cognitive Distraction Intensity

CHAPTER 5: OPTIMIZATION FUNCTION DEVELOPMENT IN MAXIMIZING SAFETY BENEFITS UNDER CAV ENVIRONMENT

As introduced the previous chapters, driver distraction exists under automated driving environment. When displaying messages under AV environment, the driver's attention is likely to be diverted depending upon the message location. Therefore, visual distraction exists as there is "a diversion of attention from driving, because the driver is temporarily focusing on an object, person, task or event not related to driving" (Hedlund et al., 2006). In the meantime, cognitive load started to increase in the form of increasing pupil dilation as the driver processes the meaning of the message. However, the displayed messages contain safety-related information that can help drivers with avoiding collision hazards, even though visual and cognitive distraction were generated during the HVI. Therefore, there are trade-offs in designing the HVI in terms of a wide range of parameters (i.e., display location, display modalities, display duration, display transparency) that can maximize the safety benefits and minimize the collision hazards from HVI-induced driver distraction under automated driving. Hence, this section mainly discusses the theoretical modelling of objective functions in maximizing safety benefits under automated driving.

5.1 Objective function and constraint of the optimization

The objective of the optimization is to maximize the safety benefits under CAV environment. For a single vehicle, the safety performance is assessed by the probability of having a traffic conflict. A smaller probability indicates a better safety performance.

Figure 5.1 illustrates a series of situations where in-vehicle heads up display can also cause collision hazards. As illustrated in Figure 5.1(a), the driver is approaching a horizontal curve. There is a message regarding the curve direction and the curve advisory speed being popped up. However, if the message is displayed for a longer period of time (i.e., above 3-second), the driver shifts attentions from the driving environment to the message. Finally, this driver ends up driving into the opposing lane, as illustrated in Figure 5.1(b). Another example is when driving under Level 2 automation on the freeway, which is illustrated in Figure 5.1(c). The AV system requests the driver to take over the driving due to a cut-in vehicle upfront. However, the "take-over" request is displayed in a heads-down position. The driver did not pay attention to the cut-in vehicle but the take-over request. After the driver perceives the meaning of the message, he did not have sufficient time to take over and decelerate. Finally, a near crash or crash is likely to happen on the freeway, which is illustrated in Figure 5.1(c).

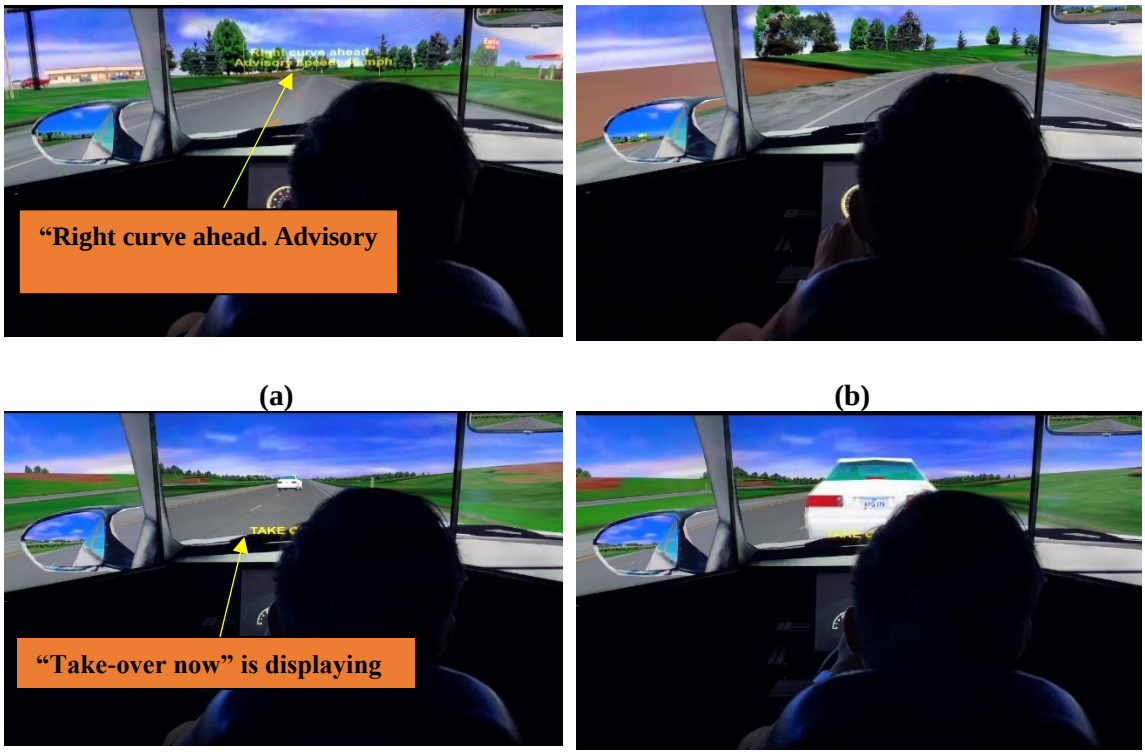

Figure 5. 1 Collision hazards caused by in-vehicle heads-up display in (a) excessive display duration of the information regarding the upcoming curve; (b) run into the opposing lane; (c) "take-over" request displayed in a heads-down position; and (d) collision with the cut-in vehicle

Figure 5.1 introduces two parameters that result in driver distraction under CV and AV driving environment, respectively. Specifically, a longer display duration is meant to be designed in making sure that the driver can completely understand the upcoming horizontal curve. The display location being at a heads-down location is meant to be designed to make sure the popped-up message does not block the driver's view. These decision variables are expected to be optimized in order to achieve maximal safety benefits with popped-up messages in the CV or AV driving environment. Potential parameters that impact driving safety under CAV are summarized in Figure 5.2.

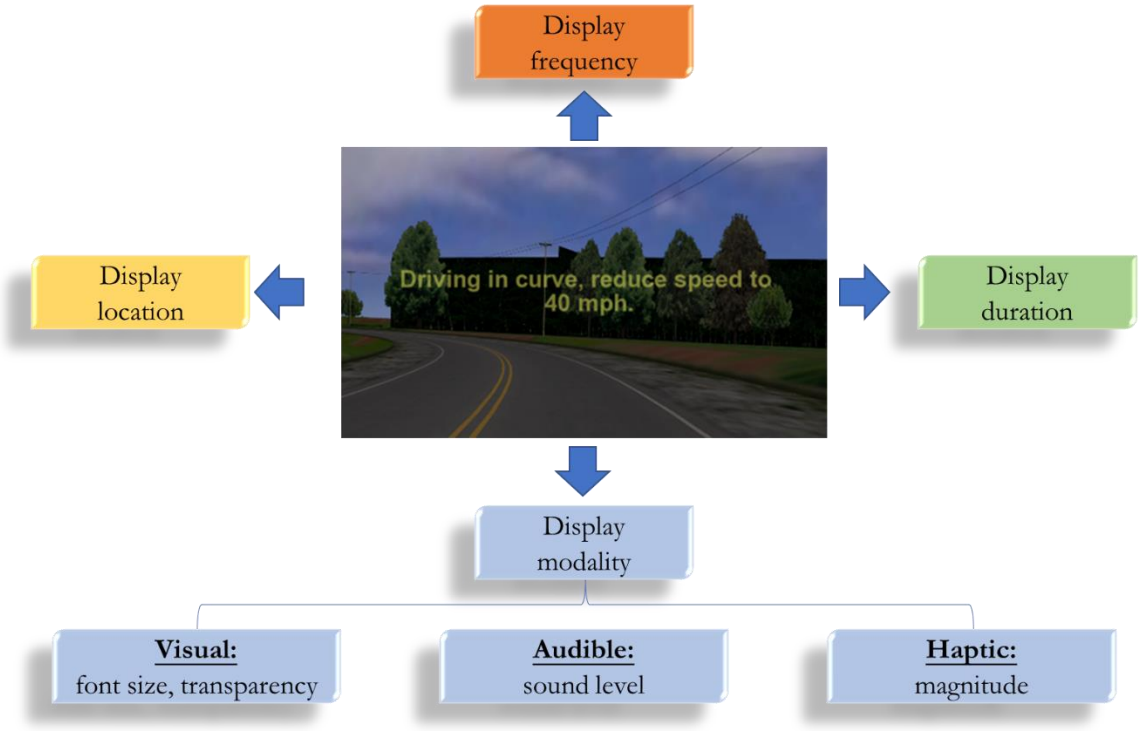

Variable Category	Name	Symbol	Range	Unit	Definition
Display duration	Display duration	δ_{DD}	$(0, +\infty)$	Second	Time interval of the safety message displayed.
Display location	Distance of display location to visual distraction zero point	δ_{DL}	$(0, +\infty)$	\	Location of the safety message displayed (i.e., heads-up display, dashboard).
Display frequency	Display frequency	δ_{DF}	$(0, +\infty)$	Hz	Frequency of the safety message displayed.
Display modality	Font size	δ_{FZ}	$(0, \alpha]$[1]	Inches	When visual warning is applied, the font size of the displaying message.
	Font transparency	δ_{FT}	$(0\%, 100\%]$	\	When visual warning is applied, the transparency of the safety message displayed.
	Sound level	δ_{SL}	$(0\%, 100\%]$	\	When audible warning is applied, the sound level of the audio.
	Haptic magnitude	δ_{HM}	$(0\%, 100\%]$	\	When haptic warning is applied, the amplitude level of the haptic.

Note: 1. $\boldsymbol{\alpha}$ stands for the maximal height of the view, such as the vehicle front view.

Figure 5. 2 Parameters of HVI Design in Developing the Optimization Function

Assuming driver characteristics (i.e., age, gender, driving experience, and psychological variable) are significant in contributing to the collision hazards following a linear regression model, an expected outcome of the modeling results are described in equation (5.1) and (5.2):

$$\begin{aligned} S_{CAV-message} &= TTC_{increased} \\ &= \alpha_{DD}\delta_{DD} + \alpha_{DL}\delta_{DL} + \alpha_{DF}\delta_{DF} + \alpha_{FZ}\delta_{FZ} + \alpha_{FT}\delta_{FT} + \alpha_{SL}\delta_{SL} + \alpha_{HM}\delta_{HM} \\ &\quad + \alpha_a\delta_a + \alpha_g\delta_g + \sum_{i=1}^{i} \alpha_i\delta_a * \delta_{DM} + \in \end{aligned} \tag{5.1}$$

$$\begin{aligned} H_{CAV-message} &= TTC_{decreased} \\ &= \beta_{CAV,VD} VD_{CAV-message}(t) + \beta_{CAV,CD} CD_{CAV-message}(t) + \beta_a\delta_a + \beta_g\delta_g \\ &\quad + \sum_{i=1}^{i} \beta_i\delta_a * \delta_{DM} + \in \end{aligned} \tag{5.2}$$

Where,

$S_{CAV-message}$	=	Safety benefits when driving under CAV;
$H_{CAV-message}$	=	Collision hazards when driving under CAV;
δ_{DD}	=	Display duration (s);
δ_{DL}	=	Display location;
δ_{DF}	=	Display frequency (Hz);
δ_{FZ}	=	Display message font size;
δ_{FT}	=	Display message transparency (%);
δ_{SL}	=	Display sound level;
δ_{HM}	=	Haptic amplitude;
δ_a	=	Driver's age;
δ_g	=	Driver's gender;
$VD_{CAV-message}(t)$	=	Driver visual distraction intensity under CAV;
$CD_{CAV-message}(t)$	=	Driver cognitive distraction intensity under CAV;
t	=	Time spent in interacting with the message under CAV (s).

Since the goal of CAV technology is to bring as many safety benefits as possible to the driver, therefore, the optimization is needed with achieving minimum hazard when driving under CAV. As the driver distraction discussed in this project mainly refers to the issued safety messages, the optimization function can be formulated as:

$$Max(S_{CAV}) = Max(S_{CAV-message} + H_{CAV-message}) \tag{5.3}$$

Subject to:

$\delta_{DD} \in [t_i,\ t_j]$; (5.4)

$\delta_{DL} \in [d_i, d_j]$; (5.5)

$\delta_{DF} \in [\mu\ Hz,\ \tau\ Hz]$ (5.6)

$\delta_{FZ} \in [h_i, h_j]$; (5.7)

$\delta_{FT} \in [\alpha\%,\ \beta\%]$; (5.8)

$\delta_{SL} \in [\delta\%,\ \mu\%]$; (5.9)

$\delta_{HM} \in [\rho\%,\ \sigma\%]$ (5.10)

Where,

$t_i,\ t_j$	=	Time constrains for display duration;
d_i, d_j	=	Distance range of the message display location given the driver's visual cone;
$\mu\ Hz,\ \tau\ Hz$	=	Frequency constrains for display frequency;
h_i, h_j	=	Display message font size range;
$\alpha\%,\ \beta\%$	=	Transparency constrains for displaying messages;
$\delta\%,\ \mu\%$	=	Message alert sound level range;
$\rho\%,\ \sigma\%$	=	Message haptic alert amplitude range.

Potentially, through the optimization, the optimum duration and location of issuing safety warnings can be obtained to achieve the maximum safety benefits when driving under CAV. Therefore, the thresholds of the key parameters in the design of ADAS can be obtained without conducting driving experiments.

5.2 Targeted audience in using specific HVI-warning type to avoid collisions

In this research, the only parameter that included in Figure 5.2 is the takeover warning modality, namely "visual only" and "visual and audible" HVI types. Therefore, the objective of this section is to identify who are suitable for driving under each takeover warning modality, respectively.

In order to tackle this objective, a classification tree model was developed with using the outcome of whether a traffic conflict happened as the model output. It is a binary variable with either "no conflict" or "conflict". For model inputs, the classification tree model includes takeover warning modality, takeover time, and driver's socio-

demographical variables (age and gender). Table 5.1 summarizes the sample characteristics of the model inputs and output for developing the classification tree model.

Table 5. 1 Sample Characteristics for Developing the Classification Tree Model (N=50)

Variable		Description	Type	Category	N/ Mean ± Std.Deviation	Percent (%)/ Range
Category	Name					
Demographics	Age	Age of participants	Continuous	\	50.04±14.03	25~73
	Gender	Gender of respondents	Binary Categorical	Male	26	52%
				Female	24	48%
HVI Characteristics	Warning Type	Methods to notify drivers regarding a takeover action	Binary Categorical	Visual only	25	50%
				Visual and audible	25	50%
Controller Area Network-Bus (CAN-Bus) information	Takeover time	Time duration from the start of HVI to the moment the driver takes over the driving by applied pedals	Continuous	\	2.29±0.67	1.167~4.667
Safety performance	Traffic conflict	Whether a driver has a traffic conflict after being requested to takeover	Binary Categorical	No conflict	27	54%
				Conflict	23	46%

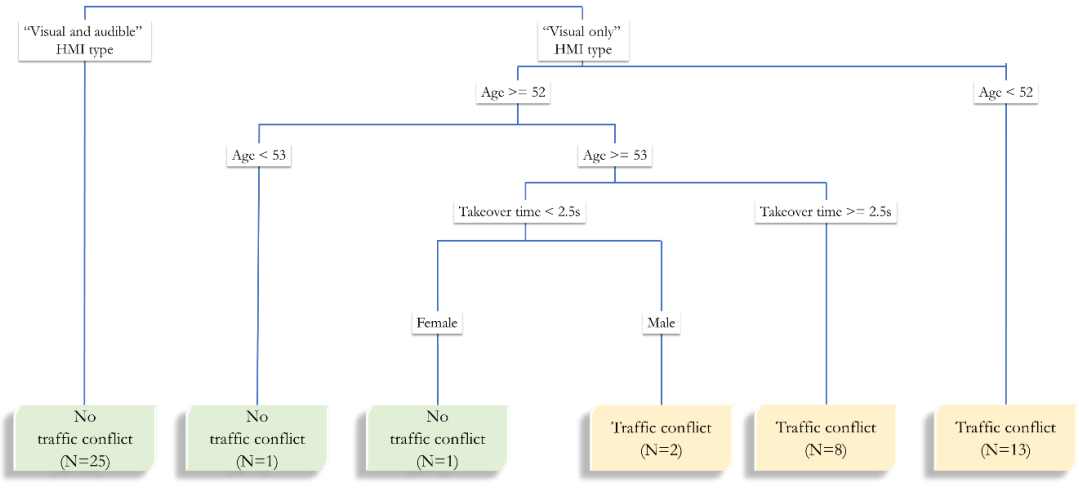

Figure 5. 3 Classification Tree Results for Safety Benefits under Different Takeover Modalities

The classification tree model that depicted in Figure 5.3 has a classification accuracy of 100%. The model classifies every driver into groups of “no traffic conflict” and “traffic conflict” based on drivers’ age, gender, takeover time, and under what type of HVI. As a result, when the HVI type is “visual and audible”, all drivers can take over the driving as requested and avoid a traffic conflict with the jaywalker. On the other hand, when the HVI type is “visual only”, only 2 out of 25 drivers did not run into a traffic conflict with the jaywalker. For unsafe driving situations, it can be observed that drivers under 52 years old 100% have a traffic conflict if the HVI type is “visual only”. For drivers who are 53 years old or above, the probability of having a traffic conflict is 1 if the driver spent more than 2.5-second on taking over the vehicle. Therefore, an optimized takeover time threshold of 2.5-second was discovered by the developed classification tree model for drivers who are 53 years old or above. Moreover, there are two exceptional cases that takeover time under 2.5-second can result in a traffic conflict, in which two male drivers who are 53 years old or above. In other words, as long as a female driver who is 53 years old or above, a traffic conflict does not happen if took over time is under 2.5-second.

CHAPTER 6: AI-DRIVEN, ULTRA-ADVANCED COLLISION AVOIDANCE SYSTEM WITH TARGETING HVI-INDUCED DRIVER DISTRACTION

6.1 Conceptual prototype of AI-driven, Ultra-advanced collision avoidance system under Level 3 automation (AUCAS-L3)

This research aims to design a conceptual prototype of an "add-on" collision avoidance system that can be incorporated with Level 3 automation (AUCAS-L3). The AUCAS-L3 expertise in handling emergency situations. To better explain the functions of AUCAS-L3, a jaywalker situation is chosen since existing research has identified it as one of the most risky driving situations, regardless of manual or automated driving (Lu et al., 2019; S. Wang & Li, 2019a). Figure 6.1 illustrates the conceptual idea of the jaywalking scenario.

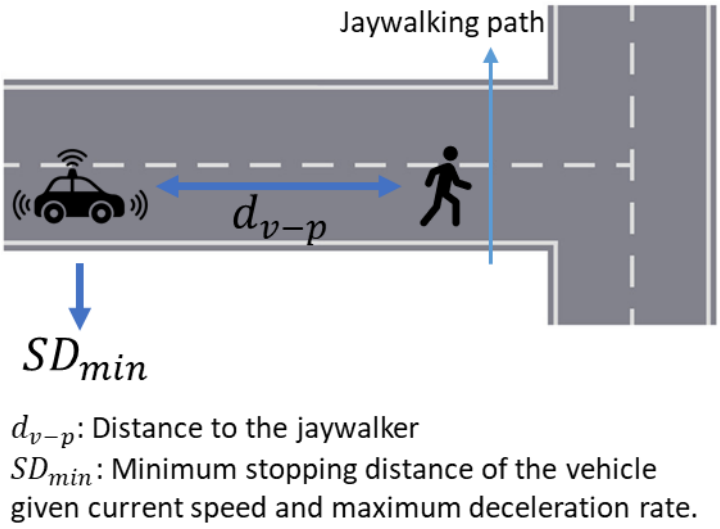

Figure 6. 1 Vehicle Operating under Level 3 ADS Facing a Jaywalker

The AUCAS-L3 works with assuming an obstacle ahead when a vehicle operating under Level 3 is approaching. After detecting the upcoming obstacle (in this research: a jaywalker) by sensors that installed on the vehicle operating under Level 3, the AUCAS-L3 starts to measure and compare the "activate distance", which is defined by the minimum stopping distance (given the vehicle speed and maximum deceleration rate) and the distance to the obstacle. Equation (6.1) explains how the "activate distance" is calculated.

$$d_{activate} = SD_{min} - d_{V-P} \quad (6.1)$$

Where,

$d_{activate}$	=	Activate distance (feet);
SD_{min}	=	Minimum stopping distance (feet);
d_{V-P}	=	Distance between the vehicle and the jaywalker (feet).

By expanding the minimum stopping distance with incorporating vehicle dynamics (i.e., vehicle speed, braking factor, braking force efficiency, rolling resistance coefficient) and factors from pavement condition (i.e., grade, pavement friction), Equation (1) can also be expressed as follows:

$$d_{activate} = SD_{min} - d_{V-O} = \frac{\gamma_b(u_i^2 - u_j^2)}{2g(\eta_b\mu + f_{rl} \pm \sin\theta_g)} - d_{V-P} \quad (6.2)$$

Where:

γ_b	=	Braking factor;
η_b	=	Efficiency of braking force;
f_{rl}	=	Rolling resistance coefficient;
θ_g	=	Grade, degree
μ	=	Pavement friction
u_i	=	Current speed of the approaching vehicle (mi/h);
u_j	=	Advisory speed of the approaching horizontal curve (mi/h);
a_{max}	=	Maximum deceleration rate of the approaching vehicle (feet/sec^2);
g	=	Acceleration of gravity (feet/sec^2);
G	=	Grade, percent.

If the "activate distance" is within a threshold, the AUCAS-L3 will apply the brake pedal by itself without requesting the human driver to do so, given that the crash is about to happen soon. In this research, the threshold is set to 10 feet. Therefore, the AUCAS-L3 will apply the brake pedal when met one of the following two criteria: (1) the driver will not take over when requested, and (2) the driver will have a crash/traffic conflict even if taken over.

Another parameter in developing the AUCAS-L3 is the minimum duration when driver have a traffic conflict after taking over. As mentioned, the AUCAS-L3 has a "built-in" function that can predict whether the driver will have a traffic conflict or not after taking over. Therefore, this prediction model only discusses drivers who do not have a traffic conflict at the timestamp of taking over but have one later on. In other words, those who

have a traffic conflict at the timestamp of taking over or before are not in the discussion of this prediction model. Figure 6.2 illustrates the distribution of time from taking over to the moment before occurring a conflict.

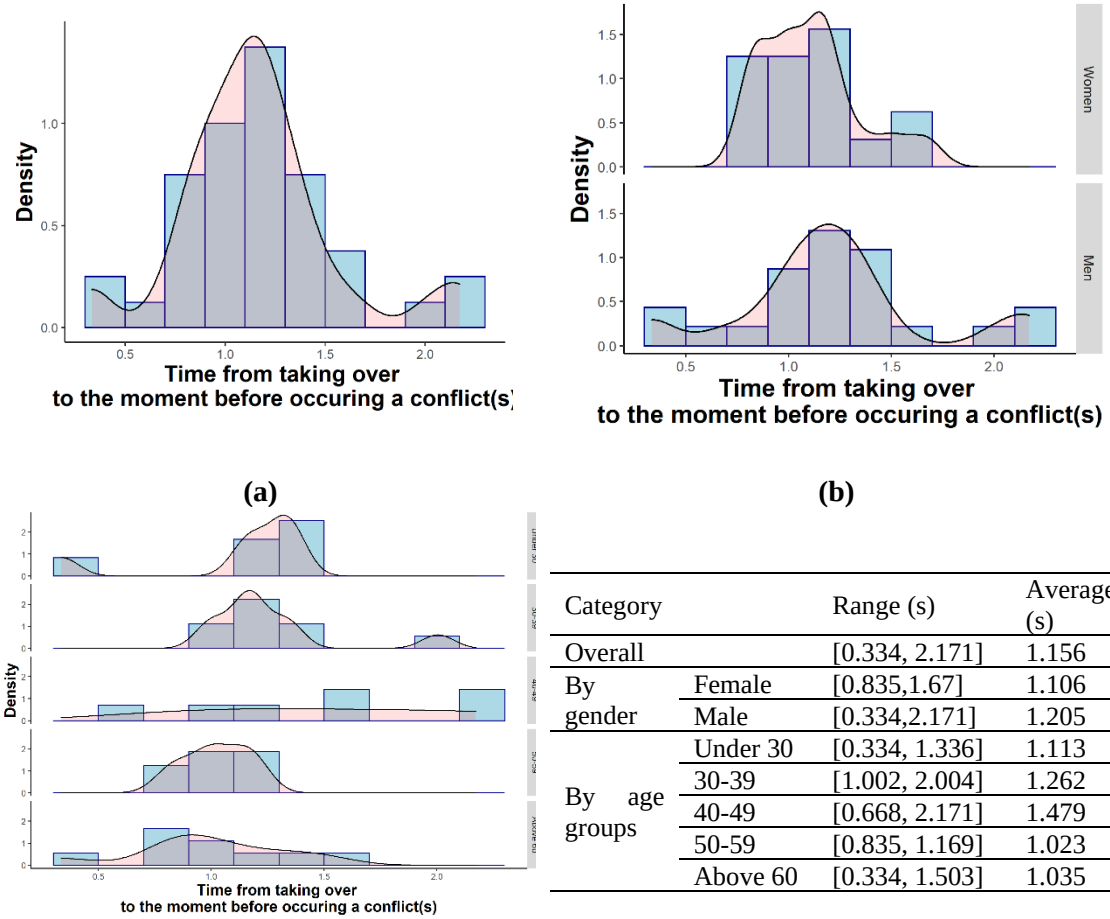

(a) **(b)**

(c) **(d)**

Category		Range (s)	Average (s)
Overall		[0.334, 2.171]	1.156
By gender	Female	[0.835,1.67]	1.106
	Male	[0.334,2.171]	1.205
By age groups	Under 30	[0.334, 1.336]	1.113
	30-39	[1.002, 2.004]	1.262
	40-49	[0.668, 2.171]	1.479
	50-59	[0.835, 1.169]	1.023
	Above 60	[0.334, 1.503]	1.035

Figure 6. 2 Distribution of Duration from Taking Over to the Moment Before Occurring a Conflict in (a) Overall, (b) By Gender, (c) By Age Groups, and (d) Summary of Distribution

As illustrated in Figure 6.2, the minimum duration when the driver has a traffic conflict after taking over is 0.334-second, suggesting that a traffic conflict occurs at the fastest moment after taking over for 0.334-second. To ensure the sample size is sufficient enough in developing the model for predicting whether a traffic conflict happens or not

after taking over, a threshold of 0.3-second is set. Figure 6.3 illustrates the system design for AUCAS-L3.

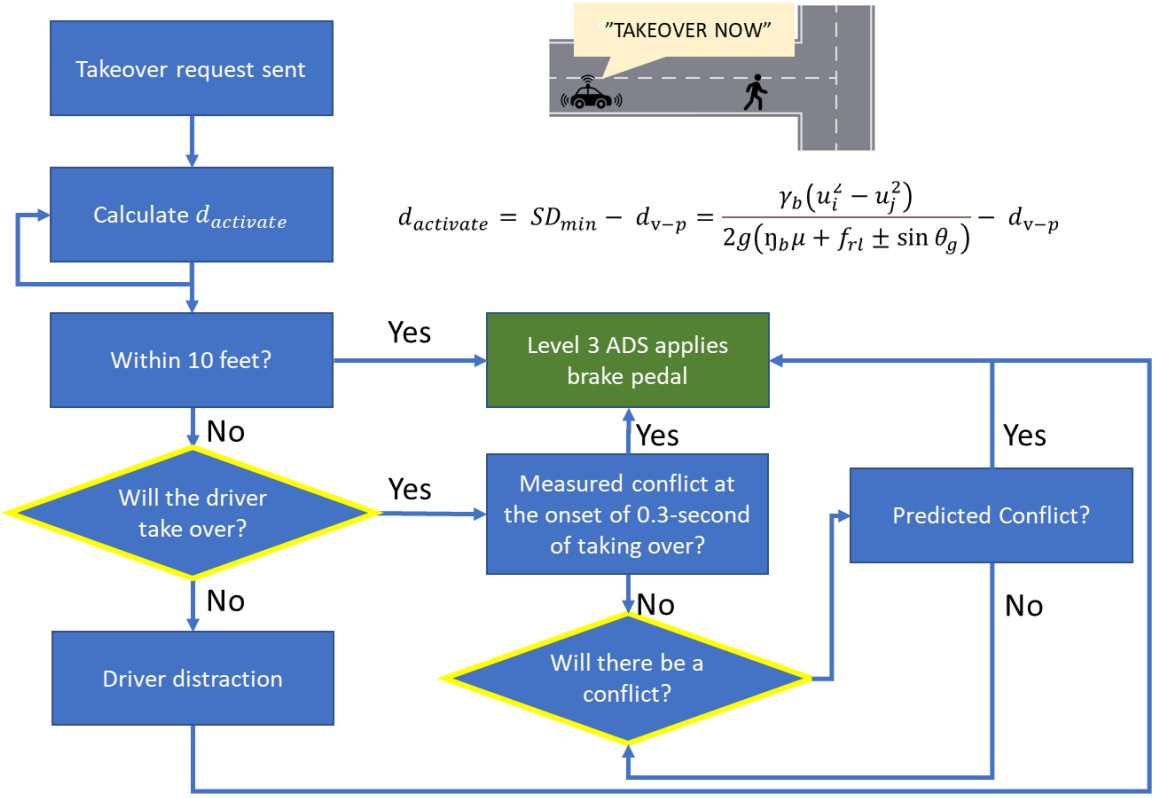

Figure 6. 3 System Design of AUCAS-L3

As illustrated in Figure 6.3, two built-in prediction models are the essential components to design the AUCAS-L3, namely predicting whether the driver will take over and predicting whether there will be a traffic conflict. The reason why predicting drivers' takeover action is necessary is that drivers might not be well-prepared for taking over the driving when ADS requests. In this case, actions are needed by applying the brake pedal before the driver is found to be distraction and will not take over the driving when requested to avoid traffic conflicts. Because there is no driver's input in operating the vehicle (i.e., steering wheel turning angle, brake pedal force, gas pedal position) if automated driving is in session, the built-in model in predicting whether a driver will take over or not focuses

on incorporating driver's age, gender, and takeover warning types as the model inputs. The beauty of this built-in prediction model is that it can predict a takeover action before running into any complex or sudden driving situations (i.e., jaywalking) where a takeover action might be needed.

The second built-in prediction model is to predict whether a traffic conflict will happen if took over. This built-in prediction model does not take those who did not take over into account since they are considered as driver distracted and AUCAS-L3 applies the brake pedal automatically. For those who took over, a traffic conflict can still occur if the driver's takeover time is too long, or the deceleration rate is not large enough. The beauty of the second built-in prediction model is that rather waiting for a traffic conflict to happen and the measuring the conflict severity, it can predict the probability of having a traffic conflict before it actually happens. In this case, the AUCAS-L3 can directly apply the brake pedal in advance if it predicts a traffic conflict will happen. To develop the built-in model in predicting whether a traffic conflict will happen if took over, the model inputs require information regarding driver's input in operating the vehicle since this stage is manual driving. In this case, speed, gas pedal position, brake pedal force, and takeover time are included in the model inputs.

6.2 Findings and discussions for the conceptual prototype of AUCAS-L3

6.2.1 Model 1: Predicting takeover actions

This section presents the modeling results for predicting takeover actions. The detailed methodologies including data collection, performance measures, and modeling approaches are introduced in Chapter 3. As introduced in previous sections, the modeling inputs for predicting takeover actions are driver characteristics including age and gender, as well as

the takeover warning types. The modeling output is whether a driver took over the driving when L3 ADS requests. Table 1 summarizes the general statistics for Model 1. Note that the original sample size for developing the takeover prediction model is 120 given that sixty drivers went through the jaywalker scenario for twice (under "visual only" and "visual and audible", respectively). However, two records are removed in the modeling process due to one participant did not fill out the gender information. In this case, the sample size for predicting takeover actions is 118.

Table 6. 1 Sample Characteristics for Developing Takeover Prediction Model (N=118)

Variable		Description	Type	Category	N/ Mean ± Std.Deviation	Percent (%)/ Range
Category	Name					
Demographics	Age	Age of participants	Continuous	\	49.93±14.30	21~77
	Gender	Gender of respondents	Binary Categorical	Male	25	42.4%
				Female	34	57.6%
HVI Characteristics	Warning Type	Modality to notify drivers regarding a takeover action	Binary Categorical	Visual only	59	50%
				Visual and audible	59	50%
Takeover actions	Takeover or not	Whether the driver takes over the driving when L3 ADS requests	Binary Categorical	Not takeover	9	7.5%
				Takeover	109	92.5%

To begin with, in developing the ANN model for predicting takeover actions, the total sample size (118 records) was divided into a training and a testing dataset by a 70/30 split. Therefore, 83 records are included in the training dataset while 35 records are included in the testing dataset. Then, the model inputs were normalized between 0 and 1, and the model out was classified into two groups (takeover vs. not takeover).

In order to obtain the most accurate model structure, multiple types of neural network topologies and hyperparameters were examined. Figure 6.5 illustrates the best-fit ANN model in predicting takeover actions, along with the model accuracy table.

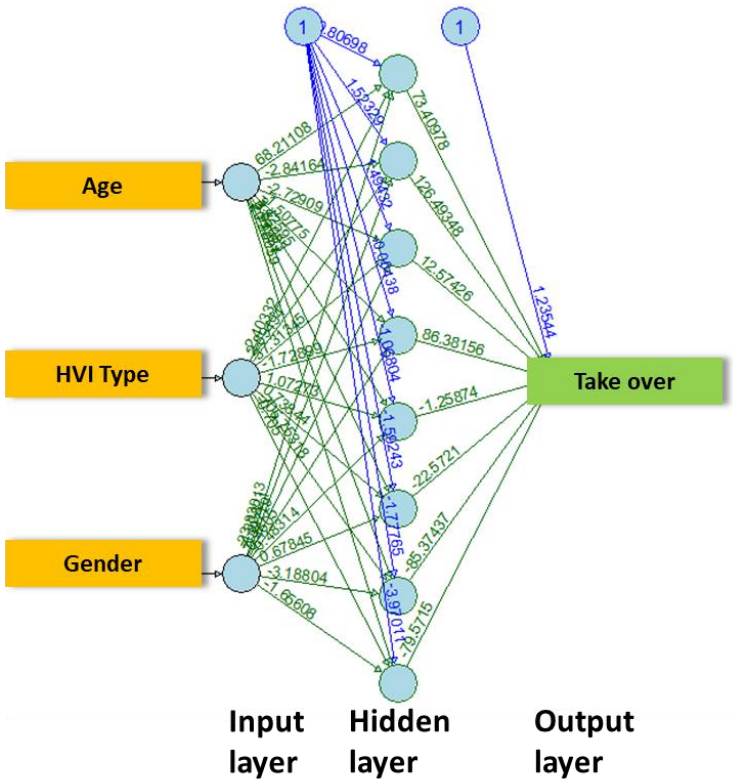

(a)

Accuracy for **training dataset**: 98.8% (82/83)		Ground truth values	
		No takeover	Takeover
Predicted values	No takeover	80% (4/5)	0% (0/78)
	Takeover	20% (1/5)	100% (78/78)

(b)

Accuracy for **testing dataset**: 82.9% (29/35)		Ground truth values	
		No takeover	Takeover
Predicted values	No takeover	50% (2/4)	12.9% (4/31)
	Takeover	50% (2/4)	87.1% (27/31)

(c)

Figure 6. 4 Takeover Action Prediction Model in (a) Visualization; (b) Model Accuracy for Training Dataset; and (c) Model Accuracy for Testing Dataset

As illustrated in Figure 6.4, an ANN structure with a single hidden layer of 8 neurons was developed to predict the takeover actions. The prediction model runs a number of 13,490 epochs for the training purpose. The training dataset has an accuracy performance of 98.8% with only one takeover action being misidentified as a non-takeover action. Although the testing dataset does not have an accuracy performance as good as the

training dataset, it also has a model accuracy above 80%. Additionally, the non-takeover action has been successfully predicted in the testing dataset. To summarize, based on basic driver information and the takeover warning type, the AUCAS-L3 has a robust performance in predicting takeover actions before the driver facing takeover action.

6.2.2 Model 2: Predicting traffic conflicts if took over

After developing the prediction model with targeting takeover actions, this section mainly presents the modeling results for predicting whether a traffic conflict would occur if the human driver took over. As mentioned in previous sections, the model inputs for the second built-in prediction model under AUCAS-L3 have drivers' input in terms of speed, gas pedal position, brake pedal force at the 0.3rd seconds of the time frame after taking over. After removing records for drivers who did not take over and drivers who already had a traffic conflict in the moment of taking over, the final sample size for the second prediction model is 104. Table 6.2 summarizes the sample characteristics for Model 2.

Table 6. 2 Sample Characteristics for Developing Conflict Prediction Model

Variable		Description	Type	Category	N/ Mean ± Std.Deviation	Percent (%)/ Range
Category	Name					
Driver input	Speed	Vehicle travel speed after the driver took over	Continuous	\	31.29±3.14	20.25~35.00
	Gas pedal position	Gas pedal position on a normalized scale from 0~1	Continuous	\	0.02±0.11	0~0.81
	Brake pedal force	Pressure that puts on the brake pedal in (kN)	Continuous	\	24.15±29.29	0~180.00
HVI characteristics	Warning type	Modality to notify drivers regarding a takeover action	Binary Categorical	Visual only	47	45.2%
				Visual and audible	57	54.8%
Traffic conflict	Lead to a conflict	Whether the driver leads to a traffic conflict even if took over	Binary Categorical	No conflict	64	61.5%
				Conflict	40	38.5%

Similarly, in developing the ANN model for predicting whether there is a traffic conflict occurring after took over, the total sample size (104 records) was divided into a training and a testing dataset by a 70/30 split. Therefore, 73 records are included in the training dataset while 31 records are included in the testing dataset. To achieve the best-fit model in predicting the occurrence of a traffic conflict, different ANN structures have been performed with evaluating the model accuracy under both training and testing datasets. Figure 6.5 illustrates the ANN model in predicting whether the driver's input leads to a traffic conflict, along with model accuracy tables.

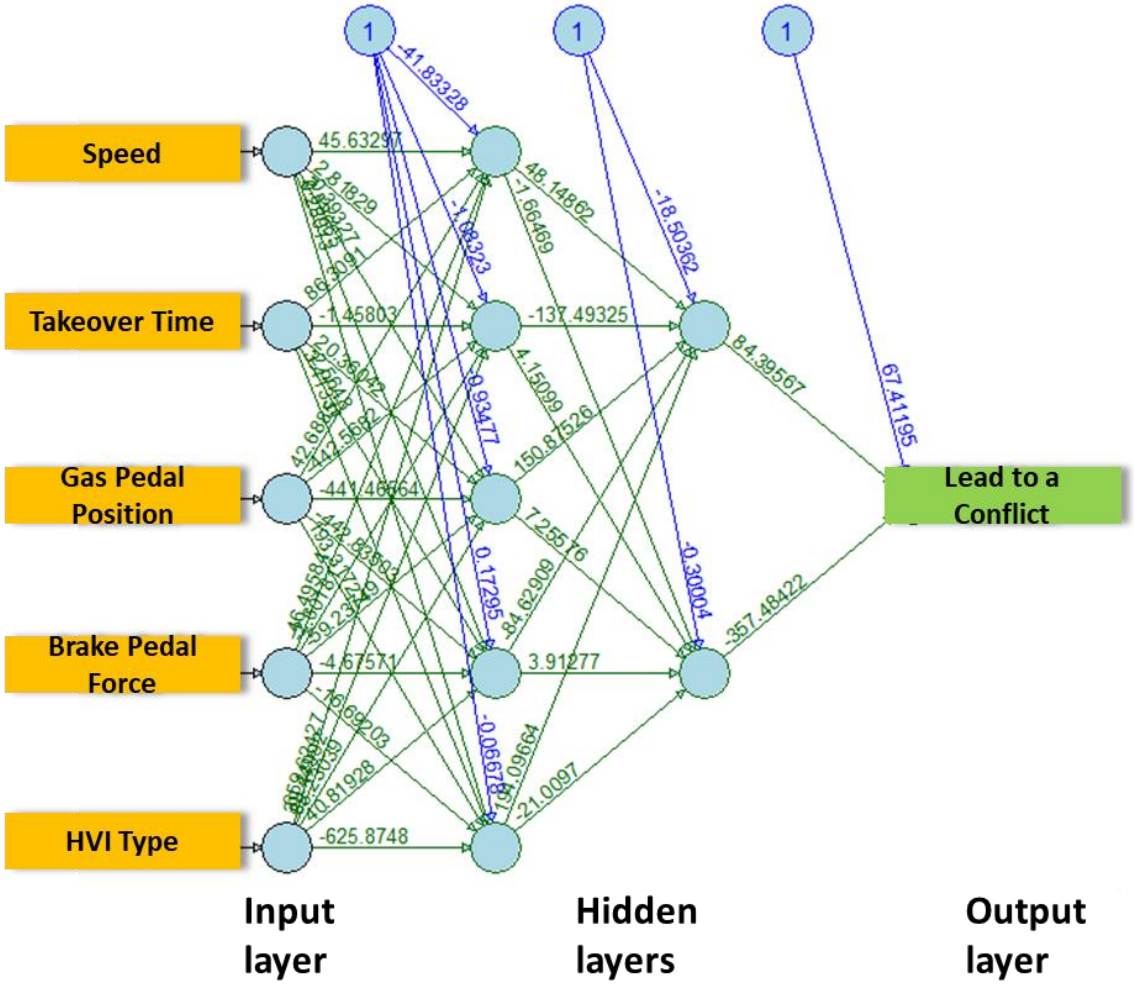

(a)

Accuracy for **training dataset**: 100% (73/73)		Ground truth values	
		No conflict	Conflict
Predicted values	No conflict	100% (44/44)	0% (0/29)
	Conflict	0% (0/44)	100% (29/29)

(b)

Accuracy for **testing dataset**: 93.5% (29/31)		Ground truth values	
		No conflict	Conflict
Predicted values	No conflict	100% (20/20)	18.2% (2/11)
	Conflict	0% (0/20)	81.8% (9/11)

(c)

Figure 6. 5 Conflict Prediction Model in (a) Visualization; (b) Model Accuracy for Training Dataset; and (c) Model Accuracy for Testing Dataset

As illustrated in Figure 6.5, an ANN structure with 2 hidden layers, five neurons on the first hidden layer and two neurons on the second hidden layer, was developed to

predict whether drivers lead to a traffic conflict or not after took over. The prediction model runs a number of 14,899 training epochs. According to Figure 6.5(b) and 6.5(c), both training and testing datasets have a model accuracy above 90%. Therefore, it is safe to conclude that the AUCAS-L3 has been proved in effectively predicting the occurrences of a traffic conflict.

Moreover, this research also calculated how much time can be saved in predicting the occurrences of a traffic conflict in advance based on the ANN modeling results. Figure 6.6 illustrates the distribution of advanced time in predicting a traffic conflict. According to Figure 6.6, the proposed prototype of AUCAS-L3 can predict the occurrence of a traffic conflict in advance of 1.10 seconds on average based on driver actions in terms of speed, gas pedal position, brake pedal force.

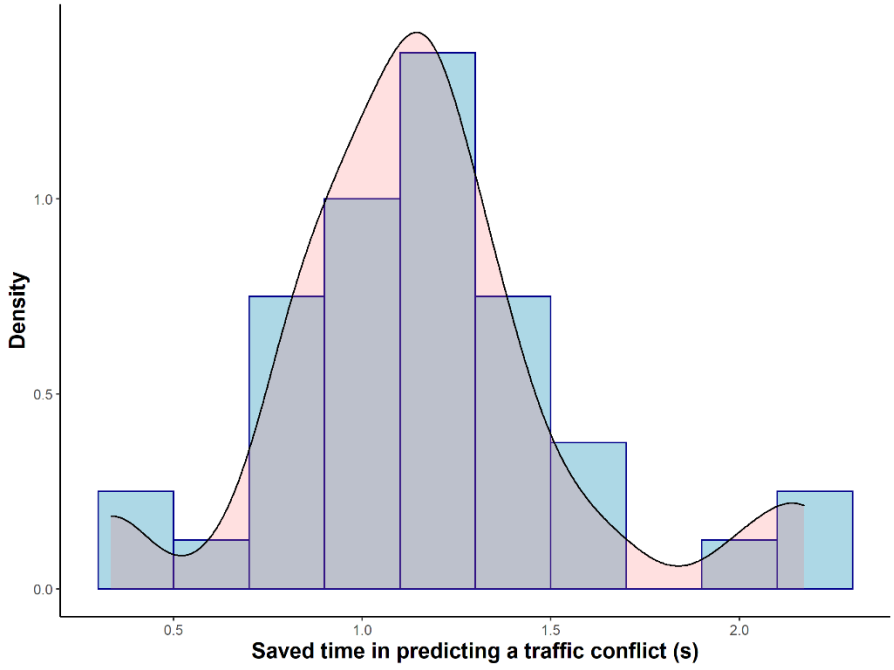

Figure 6. 6 Distribution of Saved Time in Predicting a Traffic Conflict under AUCAS-L3

CHAPTER 7: CONCLUSIONS

7.1 Conclusions of improving the existing methods in quantifying HVI-induced driver distraction under automated driving

This research contributes to the literature by improving the existing methods in quantifying Human-Vehicle Interaction-induced (HVI-induced) visual and cognitive distraction. Moreover, this research fills the research gap of lacking discussion of how visual and cognitive distraction magnitude changes continuously over time due to different HVI types ("visual only", "visual and audible"). In addition to the visual distraction, this research also improves the existing methods in quantifying HVI-induced cognitive distraction by incorporating the driver's pupil dilation performance. More importantly, this research quantitatively described the magnitude of HVI-induced distraction under automated driving from the binary perspective to the non-binary perspective. Specific methods were developed to target visual and cognitive distraction, respectively. Also, this research adds the measurement of visual distraction from one-dimension (magnitude-only) to two-dimension (magnitude and direction) by utilizing polar coordinates. The highlight of the conclusions in AV distraction modeling is summarized as follows:

- Only a limited sample (3.2%) suggests no visual distraction magnitude changes under the HVI. The majority of drivers vary their visual distraction magnitude while

interacting with Level 3 ADS. Moreover, the changes of visual distraction are non-linear and dispersed with respect to both duration and magnitude.

- At the beginning of interacting with the safety message displaying, most drivers initiate a change to visual distraction by looking away or looking towards the zero point of the visual distraction magnitude. Different patterns are observed between "visual only" and "visual and audible" HVI types in increasing or reducing visual distraction at the initial stage.
- If drivers started the change of visual distraction by a reduction, the occurrences of picking up the visual distraction magnitude are significantly fewer under the "visual and audible" HVI type, compared to the "visual only" HVI type. This finding suggests that drivers are more concentrated and maintain a higher level of takeover readiness when the HVI warning is multi-modal (visual and audible), compared to a single modal (visual only).
- If drivers made the initial move of changing visual distraction by a reduction, a significant difference is observed in the duration of the initial reduction between "visual only" and "visual and audible" HVI types. Moreover, the initial reduction rate of the visual distraction magnitude was modeled as a function of time. Two inverse models are chosen as the best fit models in capturing the relationship between visual distraction reduction rate and time under "visual only" and "visual and audible" HVI types, respectively.
- If drivers' initial change of visual distraction is a reduction, it is observed that drivers reflected a higher visual distraction reduction rate under "visual only" HVI compared to "visual and audible" HVI. This finding suggests that drivers are less likely to heavily

reduce their visual distraction magnitude if the HVI type is “visual and audible”, compared to the circumstance that the HVI type is “visual only”, which also confirms the previous finding that drivers are more concentrated under “visual and audible” HVI type.

- If drivers began their change of visual distraction by an increase, significantly higher occurrences of reducing visual distraction magnitude are observed when the HVI type is “visual only”, compared to “visual and audible”. This finding is interesting because it validates the compensatory beliefs in reducing driver distraction proposed by past studies. Under this context, drivers who interact with the machine (L3-ADS) with “visual only” present a compensatory belief by frequently looking towards the zero point of visual distraction.
- If drivers are observed with an increase of visual distraction to start their interaction process with the machine, they also show a significantly higher occurrence in increasing visual distraction magnitude under “visual only” HVI than “visual and audible” HVI. This finding delivers similar messages from the previous conclusions suggesting drivers are more concentrated when the HVI type is “visual and audible” than the “visual only” HVI type. Moreover, drivers under the “visual only” HVI type have a compensatory belief as mentioned above and show a pattern of frequently changing visual distraction magnitude, which can be considered as a sign of low takeover readiness and less concentration.
- Furthermore, the initial increase rates under two HVI types are also modeled with respect to time. The initial increase rate under “visual only” and “visual and audible”

HVI is captured as a function of time with an inverse model a power model, respectively.

- This research also contributes to the literature by exploring a new visual distraction indicator, namely the visual distraction direction. By splitting the driver's view into four quadrants with every 90-degree turn, it can be concluded that distributions of visual distraction direction are significantly different between "visual only" and "visual and audible" HVI types. By using a fixed axis as the visual distraction degree zero point, this research also suggests a significant difference in terms of visual distraction direction between these two HVI types.
- From the human factor's perspective, older drivers (i.e., 60 years old or above) show significant differences in terms of the frequency of achieving maximal cognitive distraction between "visual only" and "visual and audible" HVI types. This research suggests that older drivers tend to have a lower cognitive distraction intensity if the HVI type is "visual and audible" than "visual only" HVI. The underlying reason is that older drivers spend significantly less time reaching the maximal cognitive distraction magnitude under "visual and audible" HVI compared to "visual only" HVI. Once reaching the maximum of cognitive distraction magnitude, the cognitive distraction intensity maintains. Therefore, this research strongly recommends that drivers who are 60 years old or above use "visual and audible" HVI type under CAV driving environment for less cognitive distraction.
- From the perspective of how cognitive distraction changes over time, it is observed that the frequency corresponding to the maximal Cognitive Distraction Acceleration Rate (CDAR) is significantly larger if the HVI type is "visual only" than the HVI type being

"visual and audible". This finding suggests that drivers under "visual and audible" HVI are less likely to increase their cognitive distraction heavily and frequently than "visual only" HVI. In other words, drivers are more well-prepared in interacting with the machine (L3-ADS) during the "visual and audible" HVI process compared to the "visual only" HVI process. Previous conclusions have confirmed that drivers' situation awareness is relatively low under "visual only" HVI than "visual and audible" HVI. When drivers find out they need to take over the vehicle in response to certain emergencies (i.e., jaywalker), they need an extended period of time to percept the fact that a takeover is needed, and in turn, complete the takeover process. Therefore, when a driver realizes that a takeover action is needed under "visual only" HVI, there is a compensation belief reflected in the driver in order to make up for the potential hazards due to driver distraction. Hence, the action is reflected in the CDAR by increasing the pupil dilation change rate.

- When visual distraction reaches the maximum, the cognitive distraction is observed with significantly different patterns under different HVI types. Furthermore, after the visual distraction reaches the maximum, the average cognitive distraction under the "visual and audible" HVI type is significantly higher than the "visual only" HVI type. A potential reason is that the addition of audio may extend the cognitive workload by maintaining the pupil dilation at a higher level. The extension of the cognitive workload does not happen immediately, right after the visual distraction achieves maximum. This research suggests that cognitive distraction magnitude is significantly higher if the HVI type is "visual and audible" than "visual only" after reaching the maximal visual distraction magnitude from 0.5-second to 1-second. Specifically, both female and male

drivers show significantly higher cognitive distraction under the “visual and audible” HVI in the second stage (female: 0.5~1 second; male: 0.3~0.6 seconds) after reaching maximal visual distraction magnitude, compared to “visual only” HVI.

7.2 Conclusions of AV distraction prediction model

This research has shown how Artificial Neural Networks (ANN) can be employed to investigate the heterogeneity of visual and cognitive distraction among drivers. Particularly, the best-fit ANNs model in predicting visual and cognitive distraction intensity is obtained by proposing a novel ANN topology seeking the minimal values of the Mean Square Error (MSE) between training and testing datasets. Based on the results, it is expected that ANNs provide a valuable addition to the toolbox to predict driver distraction intensity. Therefore, this research contributes to the literature by developing an AI-driven, non-intrusive, video-recording free driver distraction monitoring system that includes both visual and cognitive distraction and focuses on driver’s demographical characteristics, HVI characteristics, and driving performance.

7.3 Conclusions of revealing the dynamic nature of collision hazards of HVI-induced driver distraction under automated driving

This research theoretically explained why HVI-induced distraction under automated driving influences driving safety by mathematically describing the relationships among distraction intensity, warning types, takeover time, and traffic conflict. The highlight of the conclusions can be summarized as follow:

- From the perspective of how visual distraction influences driving safety under automated driving, this research reveals how and why visual distraction significantly impacts the probability of having a traffic conflict in a quantitative manner. As a result,

the visual distraction intensity significantly impacts the takeover time and the probability of having a traffic conflict under different types of HVI. Moreover, the mechanism of how visual distraction direction impacts safety performance was revealed in a hierarchy structure. An interesting finding of this research is that it is still possible that the traffic conflict will not happen, even if the HVI type is "visual only". These circumstances are (a) having 26%~36% of the fixations located in the upper-left (second) quadrant; and (b) having 36% or above and 20% or lower of fixations located in the upper-left (second) and upper-right (first) quadrant, respectively, with driver's age above 60 and takeover time shorter than 2.8-second. The results can be beneficial to AV manufacturers for developing a non-intrusive eye-tracking system that can be installed on the car front window. The system can monitor the driver's fixation direction and takeover time to provide safety enhancements if any hazard collision happens.

- Similar to visual distraction, this research also revealed how cognitive distraction impacts driving safety, suggesting the underlying reasons through a quantitative manner. As a result, the cognitive distraction intensity significantly increases the probability of having a traffic conflict because it impacts the takeover time and different types of HVI.

7.4 Conclusions of the targeted audiences in achieving safety benefits under specific HVI warning types

This research established an optimization function of achieving the maximum safety benefits induced by driver distraction under HVI of automated driving. Constrains are proposed in related to the parameters in designing HVI. Moreover, this research identified

the targeted audience for using specific HVI warning modality in order to avoid traffic conflicts. As a result, this research recommends using “visual and audible” in any case to avoid traffic conflicts. More importantly, this research does not recommend drivers under 52 years old to have the HVI type as “visual only”. In addition, this research also obtains an optimized takeover time threshold in avoiding traffic conflicts. Drivers above 53 years old are not recommended for “visual only”, if the takeover time is above 2.5-second. However, there are exceptions that takeover time under 2.5-second can lead to a traffic conflict if the driver is male and above 53 years old. This research does not recommend male drivers above 53 years old use “visual only” HVI type with caution due to a sample size issue.

7.5 Conclusions of the ultimate solution (AUCAS-L3) in offsetting the collision hazards due to driver distraction under automated driving

In order to address the collision hazards due to driver distraction, this research contributes to the literature by designing a conceptual prototype of an AL-driven, Ultra-advanced collision avoidance system that can be incorporated with Level 3 automation (AUCAS-L3). Unlike the collision-actuated avoidance systems (i.e., forward collision warning/avoidance system) in the current vehicle market, the AUCAS-L3 specializes in handling emergencies that can apply brake pedal for drivers under certain situations, including the absence of taking over due to driver distraction and the occurrences of collision hazards even if taking over the driving. Two prediction models were developed to predict whether a driver will take over the driving as requested and whether a traffic conflict will happen even if taken over, employing deep learning-based ANN modeling techniques. As a result, the developed model for predicting whether the driver takeover or

not has yielded a prediction accuracy of 98.8% and 82.9% in training and testing datasets, respectively. Moreover, the developed model for predicting whether a traffic conflict will happen even if it took over has yielded a prediction accuracy for 100% in the training dataset and 93.5% in the testing dataset. More importantly, the proposed prototype of AUCAS-L3 can predict the occurrence of a traffic conflict in advance of 1.10 seconds on average based on driver actions in terms of speed, gas pedal position, brake pedal force. To summarize, the AUCAS-L3 has been proved as a conceptual prototype that can be added to the Level 3 automation system in addressing collision hazards due to driver distraction, which can benefit AV manufacturers in developing the driver distraction protection system.

7.6 Limitations and future research recommendations

Although this research contributes to the literature by offering a path to model visual and cognitive distraction incorporating from temporal and spatial perspectives, this study has limitations.

First, in this research, the investigation of HVI design is limited to one parameter, namely the HVI modality ("visual only" vs. "visual and audible"). Although this research has identified a targeted audience for either recommending or not recommending the use of each HVI modality, it is expected to include more parameters into field testing or testing in a simulation environment for future research, such as multiple groups of message transparency, different durations of the displayed messages, and different locations of the displayed messages.

Second, this research has defined the center screen as the zero point of the visual distraction magnitude when modeling visual distraction. The underlying reasons are (a)

drivers tend to randomly look around when automated driving is in session, and (b) the driving simulator experiment was conducted on a tangent segment as the popped-out message is also located in the center of the screen. Under this context, the absolute visual distraction has the same value as the relative visual distraction. It is recommended for future research to focus on defining the visual distraction magnitude zero-point since it depends upon the road segment type (whether it is a tangent segment or a curvy segment) and driving mode (manual driving or automated driving).

REFERENCES

Abiodun, O. I., Jantan, A., Omolara, A. E., Dada, K. V., Mohamed, N. A., & Arshad, H. (2018). State-of-the-art in artificial neural network applications: A survey. *Heliyon*, *4*(11), e00938.

Aksjonov, A., Nedoma, P., Vodovozov, V., Petlenkov, E., & Herrmann, M. (2017). A method of driver distraction evaluation using fuzzy logic: Phone usage as a driver's secondary activity: Case study. *ICAT 2017 - 26th International Conference on Information, Communication and Automation Technologies, Proceedings*, *2017-Decem*(October), 1–6. https://doi.org/10.1109/ICAT.2017.8171599

Aksjonov, A., Nedoma, P., Vodovozov, V., Petlenkov, E., & Herrmann, M. (2019). Detection and Evaluation of Driver Distraction Using Machine Learning and Fuzzy Logic. *IEEE Transactions on Intelligent Transportation Systems*, *20*(6), 2048–2059. https://doi.org/10.1109/TITS.2018.2857222

Alwosheel, A., van Cranenburgh, S., & Chorus, C. G. (2021). Why did you predict that? Towards explainable artificial neural networks for travel demand analysis. *Transportation Research Part C: Emerging Technologies*, *128*(January 2020), 103143. https://doi.org/10.1016/j.trc.2021.103143

Amiri, A. M., Sadri, A., Nadimi, N., & Shams, M. (2020). A comparison between Artificial Neural Network and Hybrid Intelligent Genetic Algorithm in predicting the severity of fixed object crashes among elderly drivers. *Accident Analysis and Prevention*,

138(January), 105468. https://doi.org/10.1016/j.aap.2020.105468

Angell, L. S., Auflick, J., Austria, P. A., Kochhar, D. S., Tijerina, L., Biever, W., Diptiman, T., Hogsett, J., & Kiger, S. (2006). *Driver workload metrics task 2 final report*.

Beaty, J., & Lucero-Wagnoer, B. (2000). *The Pupillary System, Handbook of Psychophysiology, 2a Edição*. Cambridge University Press. pg.

Beirness, D. J., Simpson, H. M., & Desmond, K. (2002). *The road safety monitor 2002: Risky driving*.

Bieg, H.-J., Daniilidou, C., Michel, B., & Sprung, A. (2020). Task load of professional drivers during level 2 and 3 automated driving. *D. de Waard, A. Toffetti, L. Pietrantoni, T. Franke, JF. Petiot, C. Dumas, A. Botzer, L. Onnasch, I. Milleville, and F*, 41–52.

Biondi, F. N., Balasingam, B., & Ayare, P. (2020). On the cost of detection response task performance on cognitive load. *Human Factors*, 0018720820931628.

Bradley, M. M., Miccoli, L., Escrig, M. A., & Lang, P. J. (2008). The pupil as a measure of emotional arousal and autonomic activation. *Psychophysiology*, *45*(4), 602–607.

Brands, B., Mann, R. E., Wickens, C. M., Sproule, B., Stoduto, G., Sayer, G. S., Burston, J., Pan, J. F., Matheson, J., & Stefan, C. (2019). Acute and residual effects of smoked cannabis: Impact on driving speed and lateral control, heart rate, and self-reported drug effects. *Drug and Alcohol Dependence*, *205*, 107641.

Brodeur, M., Ruer, P., Léger, P. M., & Sénécal, S. (2021). Smartwatches are more distracting than mobile phones while driving: Results from an experimental study. *Accident Analysis and Prevention*, *149*(August 2020). https://doi.org/10.1016/j.aap.2020.105846

Bruyas, M.-P., & Dumont, L. (2013). *Sensitivity of Detection Response Task (DRT) to the*

driving demand and task difficulty.

Burns, P. C., Parkes, A., Burton, S., Smith, R. K., & Burch, D. (2002). *How Dangerous is Driving with a Mobile Phone?: Benchmarking the Impairment to Alcohol* (Vol. 547). TRL Crowthorne.

Cabrall, C. D. D., Stapel, J. C. J., Happee, R., & de Winter, J. C. F. (2020). Redesigning today's driving automation toward adaptive backup control with context-based and invisible interfaces. *Human Factors*, *62*(2), 211–228.

Cades, D. M., Crump, C., Lester, B. D., & Young, D. (2017). Driver distraction and advanced vehicle assistive systems (ADAS): investigating effects on driver behavior. In *Advances in Human Aspects of Transportation* (pp. 1015–1022). Springer.

Choi, D., Sato, T., Ando, T., Abe, T., Akamatsu, M., & Kitazaki, S. (2020). Effects of cognitive and visual loads on driving performance after take-over request (TOR) in automated driving. *Applied Ergonomics*, *85*, 103074.

Choudhary, P., & Velaga, N. R. (2017a). Modelling driver distraction effects due to mobile phone use on reaction time. *Transportation Research Part C: Emerging Technologies*, *77*, 351–365. https://doi.org/10.1016/j.trc.2017.02.007

Choudhary, P., & Velaga, N. R. (2017b). Modelling driver distraction effects due to mobile phone use on reaction time. *Transportation Research Part C: Emerging Technologies*, *77*, 351–365. https://doi.org/10.1016/j.trc.2017.02.007

Choudhary, P., & Velaga, N. R. (2020). Impact of distraction on decision making at the onset of yellow signal. *Transportation Research Part C: Emerging Technologies*, *118*, 102741.

Christian, M., & Krause, F. (2017). *Modeling Driver Distraction*.

Chu, Y., Fei, J., & Hou, S. (2019). Adaptive global sliding-mode control for dynamic systems using double hidden layer recurrent neural network structure. *IEEE Transactions on Neural Networks and Learning Systems*, *31*(4), 1297–1309.

Cohen, D., Foley, J., Zamani, H., Allan, J., & Croft, W. B. (2018). Universal approximation functions for fast learning to rank: Replacing expensive regression forests with simple feed-forward networks. *The 41st International ACM SIGIR Conference on Research & Development in Information Retrieval*, 1017–1020.

Conti-Kufner, A. S. (2017). *Measuring cognitive task load: An evaluation of the Detection Response Task and its implications for driver distraction assessment*. Technische Universität München.

Cooper, J. M., Vladisavljevic, I., Medeiros-Ward, N., Martin, P. T., & Strayer, D. L. (2009). An investigation of driver distraction near the tipping point of traffic flow stability. *Human Factors*, *51*(2), 261–268.

Cunningham, M. L., & Regan, M. A. (2018). Driver distraction and inattention in the realm of automated driving. *IET Intelligent Transport Systems*, *12*(6), 407–413. https://doi.org/10.1049/iet-its.2017.0232

Curry, R., Greenberg, J., & Blanco, M. (2002). An alternate method to evaluate driver distraction. *ITS America 12th Annual Meeting and Exposition: Securing Our FutureIntelligent Transportation Society of America (ITS America)*.

Dogan, E., Honnêt, V., Masfrand, S., & Guillaume, A. (2019). Effects of non-driving-related tasks on takeover performance in different takeover situations in conditionally automated driving. *Transportation Research Part F: Traffic Psychology and Behaviour*, *62*, 494–504. https://doi.org/10.1016/j.trf.2019.02.010

Du, N., Ayoub, J., Zhou, F., Pradhan, A. K., Robert, L., Tilbury, D., Pulver, E., & Yang, X. J. (2019). Examining the impacts of drivers' emotions on takeover readiness and performance in highly automated driving. *Proceedings of the Human Factors and Ergonomics Society Annual Meeting*, *63*(1), 2076–2077. https://doi.org/10.1177/1071181319631391

Du, N., Yang, X. J., & Zhou, F. (2020). Psychophysiological responses to takeover requests in conditionally automated driving. *Accident Analysis & Prevention*, *148*, 105804.

Engström, J., Johansson, E., & Östlund, J. (2005). Effects of visual and cognitive load in real and simulated motorway driving. *Transportation Research Part F: Traffic Psychology and Behaviour*, *8*(2), 97–120.

Engström, J., Larsson, P., & Larsson, C. (2013). *Comparison of static and driving simulator venues for the tactile detection response task*.

Engström, J., Markkula, G., Victor, T., & Merat, N. (2017). Effects of cognitive load on driving performance: The cognitive control hypothesis. *Human Factors*, *59*(5), 734–764.

Epple, S., Roche, F., & Brandenburg, S. (2018). The sooner the better: Drivers' reactions to two-step take-over requests in highly automated driving. *Proceedings of the Human Factors and Ergonomics Society Annual Meeting*, *62*(1), 1883–1887.

Farber, E., Foley, J., & Scott, S. (2000). Visual attention design limits for ITS in-vehicle systems: The Society of Automotive Engineers standard for limiting visual distraction while driving. *Transportation Research Board Annual General Meeting*, 2–3.

Foley, J. P. (2008). Now you see it, now you don't: Visual occlusion as a surrogate distraction measurement technique. *Driver Distraction: Theory, Effects, and*

Mitigation, 123–134.

Gabay, S., Pertzov, Y., & Henik, A. (2011). Orienting of attention, pupil size, and the norepinephrine system. *Attention, Perception, & Psychophysics*, *73*(1), 123–129.

Gao, J., & Davis, G. A. (2017). Using naturalistic driving study data to investigate the impact of driver distraction on driver's brake reaction time in freeway rear-end events in car-following situation. *Journal of Safety Research*, *63*, 195–204.

Gettman, D., Pu, L., Sayed, T., Shelby, S. G., & Energy, S. (2008). *Surrogate safety assessment model and validation*. Turner-Fairbank Highway Research Center.

Ghasemzadeh, A., Hammit, B. E., Ahmed, M. M., & Young, R. K. (2018). Parametric ordinal logistic regression and non-parametric decision tree approaches for assessing the impact of weather conditions on driver speed selection using naturalistic driving data. *Transportation Research Record*, *2672*(12), 137–147.

Gollan, B., Haslgrübler, M., & Ferscha, A. (2016). Demonstrator for extracting cognitive load from pupil dilation for attention management services. *Proceedings of the 2016 ACM International Joint Conference on Pervasive and Ubiquitous Computing: Adjunct*, 1566–1571.

Granholm, E., Asarnow, R. F., Sarkin, A. J., & Dykes, K. L. (1996). Pupillary responses index cognitive resource limitations. *Psychophysiology*, *33*(4), 457–461.

Green, P. (2004). *Driver distraction, telematics design, and workload managers: Safety issues and solutions*. SAE Technical Paper.

Guo, H., Boyle, L. N., Jenness, J. W., & Lee, J. D. (2020). Tactile detection response task: Metrics for assessing drivers' cognitive workload. *Transportation Research Part F: Traffic Psychology and Behaviour*, *70*, 98–108.

Hammond, R. L., Soccolich, S. A., & Hanowski, R. J. (2019). The impact of driver distraction in tractor-trailers and motorcoach buses. *Accident Analysis & Prevention*, *126*, 10–16.

Han, J., Pei, J., & Kamber, M. (2011). *Data mining: concepts and techniques*. Elsevier.

Hansen, J. H. L., Busso, C., Zheng, Y., & Sathyanarayana, A. (2017). Driver modeling for detection and assessment of driver distraction: Examples from the UTDrive test bed. *IEEE Signal Processing Magazine*, *34*(4), 130–142.

Happ, M., Bathke, A. C., & Brunner, E. (2019). Optimal sample size planning for the Wilcoxon-Mann-Whitney test. *Statistics in Medicine*, *38*(3), 363–375.

Haque, M. M., & Washington, S. (2015). The impact of mobile phone distraction on the braking behaviour of young drivers: a hazard-based duration model. *Transportation Research Part C: Emerging Technologies*, *50*, 13–27.

Harms, L., & Patten, C. (2003). Peripheral detection as a measure of driver distraction. A study of memory-based versus system-based navigation in a built-up area. *Transportation Research Part F: Traffic Psychology and Behaviour*, *6*(1), 23–36.

Harrison, E. L. R., & Fillmore, M. T. (2011). Alcohol and distraction interact to impair driving performance. *Drug and Alcohol Dependence*, *117*(1), 31–37.

He, D., & Donmez, B. (2019). Influence of driving experience on distraction engagement in automated vehicles. *Transportation Research Record*, *2673*(9), 142–151.

He, D., Kanaan, D., & Donmez, B. (2021). In-vehicle displays to support driver anticipation of traffic conflicts in automated vehicles. *Accident Analysis & Prevention*, *149*, 105842.

Hedlund, J., Simpson, H. M., & Mayhew, D. R. (2006). *International conference on*

distracted driving: Summary of proceedings and recommendations: October 2-5, 2005.

Hirst, S., & Graham, R. (1997). Ergonomics and Safety of Intelligent Driver Interfaces. *The Format and Perception of Collision Warnings*.

Hurtado, S., & Chiasson, S. (2016). An eye-tracking evaluation of driver distraction and unfamiliar road signs. *Proceedings of the 8th International Conference on Automotive User Interfaces and Interactive Vehicular Applications*, 153–160.

Iio, K., Guo, X., & Lord, D. (2021). Examining driver distraction in the context of driving speed: An observational study using disruptive technology and naturalistic data. *Accident Analysis and Prevention*, *153*(December 2020), 105983. https://doi.org/10.1016/j.aap.2021.105983

Innes, R. J., Evans, N. J., Howard, Z. L., Eidels, A., & Brown, S. D. (2019). A broader application of the detection response task to cognitive tasks and online environments. *Human Factors*, 0018720820936800.

Iqbal, S. T., Zheng, X. S., & Bailey, B. P. (2004). Task-evoked pupillary response to mental workload in human-computer interaction. *CHI'04 Extended Abstracts on Human Factors in Computing Systems*, 1477–1480.

Iranmanesh, S. M., Nourkhiz Mahjoub, H., Kazemi, H., & Fallah, Y. P. (2018). An adaptive forward collision warning framework design based on driver distraction. *IEEE Transactions on Intelligent Transportation Systems*, *19*(12), 3925–3934. https://doi.org/10.1109/TITS.2018.2791437

Ismailov, V. (2020). A three layer neural network can represent any discontinuous multivariate function. *ArXiv Preprint ArXiv:2012.03016*.

Jacoby, W. G. (2000). Loess:: a nonparametric, graphical tool for depicting relationships between variables. *Electoral Studies*, *19*(4), 577–613.

Jahn, G., Oehme, A., Krems, J. F., & Gelau, C. (2005). Peripheral detection as a workload measure in driving: Effects of traffic complexity and route guidance system use in a driving study. *Transportation Research Part F: Traffic Psychology and Behaviour*, *8*(3), 255–275.

Jahromi, A. N., Hashemi, S., Dehghantanha, A., Choo, K.-K. R., Karimipour, H., Newton, D. E., & Parizi, R. M. (2020). An improved two-hidden-layer extreme learning machine for malware hunting. *Computers & Security*, *89*, 101655.

Janssen, W. H., Kaptein, N., & Claessens, M. (1999). Behavior and safety when driving with in-vehicle devices that provide real-time traffic information. *Proceedings of the Sixth World Congress on Intelligent Transport Systems, Toronto*, 22.

Jenness, J. W., Lattanzio, R. J., O'Toole, M., & Taylor, N. (2002). Voice-activated dialing or eating a cheeseburger: which is more distracting during simulated driving? *Proceedings of the Human Factors and Ergonomics Society Annual Meeting*, *46*(4), 592–596.

Jepma, M., & Nieuwenhuis, S. (2011). Pupil diameter predicts changes in the exploration–exploitation trade-off: Evidence for the adaptive gain theory. *Journal of Cognitive Neuroscience*, *23*(7), 1587–1596.

Kapser, S., Abdelrahman, M., & Bernecker, T. (2021). Autonomous delivery vehicles to fight the spread of Covid-19–How do men and women differ in their acceptance? *Transportation Research Part A: Policy and Practice*.

Kashevnik, A., Shchedrin, R., Kaiser, C., & Stocker, A. (2021). Driver Distraction

Detection Methods: A Literature Review and Framework. *IEEE Access*, 60063–60076. https://doi.org/10.1109/ACCESS.2021.3073599

Kircher, K., Fors, C., & Ahlstrom, C. (2014). Continuous versus intermittent presentation of visual eco-driving advice. *Transportation Research Part F: Traffic Psychology and Behaviour*, *24*, 27–38.

Klingegård, M., Andersson, J., Habibovic, A., Nilsson, E., & Rydström, A. (2020). Drivers' ability to engage in a non-driving related task while in automated driving mode in real traffic. *IEEE Access*, *8*, 221654–221668.

Kluger, R., Smith, B. L., Park, H., & Dailey, D. J. (2016). Identification of safety-critical events using kinematic vehicle data and the discrete fourier transform. *Accident Analysis and Prevention*, *96*, 162–168. https://doi.org/10.1016/j.aap.2016.08.006

Kountouriotis, G. K., & Merat, N. (2016). Leading to distraction: Driver distraction, lead car, and road environment. *Accident Analysis & Prevention*, *89*, 22–30.

Kountouriotis, G. K., Spyridakos, P., Carsten, O. M. J., & Merat, N. (2016). Identifying cognitive distraction using steering wheel reversal rates. *Accident Analysis & Prevention*, *96*, 39–45.

Kret, M. E., & Sjak-Shie, E. E. (2019). Preprocessing pupil size data: Guidelines and code. *Behavior Research Methods*, *51*(3), 1336–1342. https://doi.org/10.3758/s13428-018-1075-y

Kujala, T., Kircher, K., & Ahlström, C. (2021). A review of occlusion as a tool to assess attentional demand in driving. *Human Factors*, 00187208211010953.

Kumar, P., Nigam, S. P., & Kumar, N. (2014). Vehicular traffic noise modeling using artificial neural network approach. *Transportation Research Part C: Emerging*

Technologies, *40*, 111–122.

Kuo, J., Koppel, S., Charlton, J. L., & Rudin-Brown, C. M. (2015). Evaluation of a video-based measure of driver heart rate. *Journal of Safety Research*, *54*, 55-e29.

Lansdown, T. C., Brook-Carter, N., & Kersloot, T. (2004). Distraction from multiple in-vehicle secondary tasks: vehicle performance and mental workload implications. *Ergonomics*, *47*(1), 91–104.

Lee, J. D., Young, K. L., & Regan, M. A. (2008). Defining driver distraction. *Driver Distraction: Theory, Effects, and Mitigation*, *13*(4), 31–40.

Lee, S. C., Yoon, S. H., & Ji, Y. G. (2020). Effects of Non-Driving-Related Task Attributes on Takeover Quality in Automated Vehicles. *International Journal of Human-Computer Interaction*, *00*(00), 1–9. https://doi.org/10.1080/10447318.2020.1815361

Lee, S. C., Yoon, S. H., & Ji, Y. G. (2021). Effects of non-driving-related task attributes on takeover quality in automated vehicles. *International Journal of Human–Computer Interaction*, *37*(3), 211–219.

Li, G., Yan, W., Li, S., Qu, X., Chu, W., & Cao, D. (2021). A Temporal-Spatial Deep Learning Approach for Driver Distraction Detection Based on EEG Signals. *IEEE Transactions on Automation Science and Engineering*.

Li, N., & Boyle, L. N. (2020). Allocation of driver attention for varying in-vehicle system modalities. *Human Factors*, *62*(8), 1349–1364.

Li, P., Yang, Y., Grosu, R., Wang, G., Li, R., Wu, Y., & Huang, Z. (2021). Driver Distraction Detection Using Octave-Like Convolutional Neural Network. *IEEE Transactions on Intelligent Transportation Systems*.

Li, Q., Hou, L., Wang, Z., Wang, W., Zeng, C., Yuan, Q., & Cheng, B. (2021). Drivers ’

visual-distracted take-over performance model and its application on adaptive adjustment of time budget. *Accident Analysis and Prevention*, *154*(January), 106099. https://doi.org/10.1016/j.aap.2021.106099

Li, Z., Bao, S., Kolmanovsky, I. V., & Yin, X. (2018). Visual-Manual distraction detection using driving performance indicators with naturalistic driving data. *IEEE Transactions on Intelligent Transportation Systems*, *19*(8), 2528–2535. https://doi.org/10.1109/TITS.2017.2754467

Liang, N., Yang, J., Yu, D., Prakah-Asante, K. O., Curry, R., Blommer, M., Swaminathan, R., & Pitts, B. J. (2021). Using eye-tracking to investigate the effects of pre-takeover visual engagement on situation awareness during automated driving. *Accident Analysis & Prevention*, *157*, 106143.

Liang, Y., & Lee, J. D. (2010). Combining cognitive and visual distraction: Less than the sum of its parts. *Accident Analysis & Prevention*, *42*(3), 881–890.

Liang, Y., & Lee, J. D. (2014). A hybrid Bayesian Network approach to detect driver cognitive distraction. *Transportation Research Part C: Emerging Technologies*, *38*, 146–155. https://doi.org/10.1016/j.trc.2013.10.004

Lin, Q.-F., Lyu, Y., Zhang, K.-F., & Ma, X.-W. (2021). Effects of non-driving related tasks on readiness to take over control in conditionally automated driving. *Traffic Injury Prevention*, 1–5.

Lin, Q., Li, S., Ma, X., & Lu, G. (2020). Understanding take-over performance of high crash risk drivers during conditionally automated driving. *Accident Analysis and Prevention*, *143*(May), 105543. https://doi.org/10.1016/j.aap.2020.105543

Lu, Z., Zhang, B., Feldhütter, A., Happee, R., Martens, M., & De Winter, J. C. F. (2019).

Beyond mere take-over requests: The effects of monitoring requests on driver attention, take-over performance, and acceptance. *Transportation Research Part F: Traffic Psychology and Behaviour*, *63*, 22–37.

Ma, M., & Li, Z. (2019). *A Proactive Approach for Intersection Safety Visualization based on Real-Time Radar Sensor Data*.

Ma, S., Zhang, W., Yang, Z., Kang, C., Wu, C., Chai, C., Shi, J., Zeng, Y., & Li, H. (2021). Take over gradually in conditional automated driving: the effect of two-stage warning systems on situation awareness, driving stress, takeover performance, and acceptance. *International Journal of Human–Computer Interaction*, *37*(4), 352–362.

Maind, S. B., & Wankar, P. (2014). Research paper on basic of artificial neural network. *International Journal on Recent and Innovation Trends in Computing and Communication*, *2*(1), 96–100.

Makhtar, A. K., & Sulaiman, M. I. (2020). Development of Heart Rate Monitoring System to Estimate Driver's Mental Workload Level. *IOP Conference Series: Materials Science and Engineering*, *834*(1), 12057.

Mase, J. M., Chapman, P., Figueredo, G. P., & Torres, M. T. (2020). A hybrid deep learning approach for driver distraction detection. *2020 International Conference on Information and Communication Technology Convergence (ICTC)*, 1–6.

Masood, S., Rai, A., Aggarwal, A., Doja, M. N., & Ahmad, M. (2020). Detecting distraction of drivers using Convolutional Neural Network. *Pattern Recognition Letters*, *139*, 79–85. https://doi.org/10.1016/j.patrec.2017.12.023

McDonald, A. D., Alambeigi, H., Engström, J., Markkula, G., Vogelpohl, T., Dunne, J., & Yuma, N. (2019). Toward Computational Simulations of Behavior During Automated

Driving Takeovers: A Review of the Empirical and Modeling Literatures. *Human Factors, 61*(4), 642–688. https://doi.org/10.1177/0018720819829572

McDonald, A. D., Ferris, T. K., & Wiener, T. A. (2020). Classification of Driver Distraction: A Comprehensive Analysis of Feature Generation, Machine Learning, and Input Measures. *Human Factors*, *62*(6), 1019–1035. https://doi.org/10.1177/0018720819856454

Morgenstern, T., Wögerbauer, E. M., Naujoks, F., Krems, J. F., & Keinath, A. (2020). Measuring driver distraction – Evaluation of the box task method as a tool for assessing in-vehicle system demand. *Applied Ergonomics*, *88*(May), 1–11. https://doi.org/10.1016/j.apergo.2020.103181

Muthén, L. K., & Muthén, B. O. (2011). Mplus user's guide. 1998–2011. *Los Angeles, California: Muthén and Muthén*.

National Transportation Safety Board. (2018). *Preliminary Report Highway: HWY18MH010*. https://www.ntsb.gov/investigations/AccidentReports/Pages/HWY18MH010-prelim.aspx

Naujoks, F., Purucker, C., Wiedemann, K., & Marberger, C. (2019). Noncritical State Transitions During Conditionally Automated Driving on German Freeways: Effects of Non–Driving Related Tasks on Takeover Time and Takeover Quality. *Human Factors*, *61*(4), 596–613. https://doi.org/10.1177/0018720818824002

Niu, J., & Ma, C. (2021). Is it Good or Bad to Provide Driver Fatigue Warning During Take-Over in Highly Automated Driving? *Transportation Research Record*, 03611981211046920.

Olsson, S., & Burns, P. C. (2000). Measuring driver visual distraction with a peripheral detection task. *Obtained from August*.

Oviedo-Trespalacios, O., Haque, M. M., King, M., & Washington, S. (2016). Understanding the impacts of mobile phone distraction on driving performance: A systematic review. *Transportation Research Part C: Emerging Technologies*, *72*, 360–380.

Paraforos, D. S., & Griepentrog, H. W. (2019). Tractor fuel rate modeling and simulation using switching Markov chains on CAN-Bus data. *IFAC-PapersOnLine*, *52*(30), 379–384.

Petermeijer, S., Doubek, F., & De Winter, J. (2017). Driver response times to auditory, visual, and tactile take-over requests: A simulator study with 101 participants. *2017 IEEE International Conference on Systems, Man, and Cybernetics, SMC 2017*, *2017-Janua*, 1505–1510. https://doi.org/10.1109/SMC.2017.8122827

Petermeijer, S. M., Cieler, S., & de Winter, J. C. F. (2017). Comparing spatially static and dynamic vibrotactile take-over requests in the driver seat. *Accident Analysis and Prevention*, *99*, 218–227. https://doi.org/10.1016/j.aap.2016.12.001

Pfleging, B., Fekety, D. K., Schmidt, A., & Kun, A. L. (2016). A model relating pupil diameter to mental workload and lighting conditions. *Proceedings of the 2016 CHI Conference on Human Factors in Computing Systems*, 5776–5788.

Pipkorn, L., & Piccinini, G. B. (2020). The role of off-path glances: A quantitative analysis of rear-end conflicts involving Chinese professional truck drivers as the striking partners. *Journal of Safety Research*, *72*, 259–266.

Politis, I., Brewster, S., & Pollick, F. (2017). Using multimodal displays to signify critical

handovers of control to distracted autonomous car drivers. *International Journal of Mobile Human Computer Interaction (IJMHCI)*, *9*(3), 1–16.

Pomplun, M., & Sunkara, S. (2003). Pupil dilation as an indicator of cognitive workload in human-computer interaction. *Proceedings of the International Conference on HCI*, *273*.

Przybyla, J., Taylor, J., Jupe, J., & Zhou, X. (2015). Estimating risk effects of driving distraction: A dynamic errorable car-following model. *Transportation Research Part C: Emerging Technologies*, *50*, 117–129.

Pupil Labs. (2021). *User Guide*. https://docs.pupil-labs.com/core/

Ranney, T A, Garrott, W. R., & Goodman, M. J. (2001). NHTSA driver distraction research: Past, present, and future (No. 2001-06-0177). *SAE Technical Paper*.

Ranney, Thomas A, Baldwin, G. H., Smith, L. A., Mazzae, E. N., & Pierce, R. S. (2014). *Detection response task (DRT) evaluation for driver distraction measurement application*.

Reed, M. P., & Green, P. A. (1999). Comparison of driving performance on-road and in a low-cost simulator using a concurrent telephone dialling task. *Ergonomics*, *42*(8), 1015–1037.

Roche, F., Somieski, A., & Brandenburg, S. (2019). Behavioral changes to repeated takeovers in highly automated driving: effects of the takeover-request design and the nondriving-related task modality. *Human Factors*, *61*(5), 839–849.

SAE International. (2016). Taxonomy and definitions for terms related to driving automation systems for on-road motor vehicles. *SAE International,(J3016)*.

SAE International. (2018). Surface Vehicle. *SAE International*, *724*, 1–5.

Servizi, V., Petersen, N. C., Pereira, F. C., & Nielsen, O. A. (2020). Stop detection for smartphone-based travel surveys using geo-spatial context and artificial neural networks. *Transportation Research Part C: Emerging Technologies*, *121*, 102834.

Standardization, I. O. for. (2016). *Road vehicles—Transport information and control systems—Detection-response task (DRT) for assessing attentional effects of cognitive load in driving*. Author Geneva, Switzerland.

Starkey, N. J., Charlton, S. G., Malhotra, N., & Lehtonen, E. (2020). Drivers' response to speed warnings provided by a smart phone app. *Transportation Research Part C: Emerging Technologies*, *110*, 209–221.

Stojmenova, K., & Sodnik, J. (2018a). Detection-response task—uses and limitations. *Sensors*, *18*(2), 594.

Stojmenova, K., & Sodnik, J. (2018b). Validation of auditory detection response task method for assessing the attentional effects of cognitive load. *Traffic Injury Prevention*, *19*(5), 495–500.

Strayer, D. L., Cooper, J. M., Turrill, J., Coleman, J. R., & Hopman, R. J. (2015). Measuring Cognitive Distraction in the Automobile III. *AAAFoundation.Org*, *October*, 202–638. https://doi.org/10.3390/cryst7120370

Strayer, D. L., Turrill, J., Coleman, J. R., Ortiz, E. V, & Cooper, J. M. (2014). Measuring Cognitive Distraction in the Automobile II: Assessing In-Vehicle Voice-Based Interactive Technologies. *AAAFoundation.Org*, *October*, 202–638.

Sullivan, H. W., Boudewyns, V., O'Donoghue, A., Marshall, S., & Williams, P. A. (2017). Attention to and distraction from risk information in prescription drug advertising: An eye-tracking study. *Journal of Public Policy & Marketing*, *36*(2), 236–245.

Swathi, V., Akhilesh, D., Kumar, G. S., & Vathsala, A. V. (2021). Real-Time Driver Distraction Detection Using OpenCV and Machine Learning Algorithms. In *Smart Computing Techniques and Applications* (pp. 35–46). Springer.

Tachet, R., Santi, P., Sobolevsky, S., Reyes-Castro, L. I., Frazzoli, E., Helbing, D., & Ratti, C. (2016). Revisiting street intersections using slot-based systems. *PloS One*, *11*(3), e0149607.

Thornton, G. M., Bailey, S. J., & Schwab, T. D. (2015). Time-dependent damage in predictions of fatigue behaviour of normal and healing ligaments. *Mechanics of Time-Dependent Materials*, *19*(3), 335–349.

Tijerina, L. (2000). Issues in the evaluation of driver distraction associated with in-vehicle information and telecommunications systems. *Transportation Research Inc*, *12*, 54–67.

Topolšek, D., Areh, I., & Cvahte, T. (2016). Examination of driver detection of roadside traffic signs and advertisements using eye tracking. *Transportation Research Part F: Traffic Psychology and Behaviour*, *43*, 212–224.

Treat, J. R. (1980). A study of precrash factors involved in traffic accidents. *HSRI Research Review*.

Trommler, D., Morgenstern, T., Wögerbauer, E. M., Naujoks, F., Krems, J. F., & Keinath, A. (2021a). The box task-a method for assessing in-vehicle system demand. *MethodsX*, *8*, 101261.

Trommler, D., Morgenstern, T., Wögerbauer, E. M., Naujoks, F., Krems, J. F., & Keinath, A. (2021b). The box task - a method for assessing in-vehicle system demand. *MethodsX*, *8*. https://doi.org/10.1016/j.mex.2021.101261

van Cranenburgh, S., & Alwosheel, A. (2019). An artificial neural network based approach to investigate travellers' decision rules. *Transportation Research Part C: Emerging Technologies*, *98*(September 2017), 152–166. https://doi.org/10.1016/j.trc.2018.11.014

Wakabayashi, D. (2018). *Self-Driving Uber Car Kills Pedestrian in Arizona, Where Robots Roam*. https://www.nytimes.com/2018/03/19/technology/uber-driverless-fatality.html

Wali, B., Santi, P., & Ratti, C. (2021). Modeling consumer affinity towards adopting partially and fully automated vehicles – The role of preference heterogeneity at different geographic levels. *Transportation Research Part C: Emerging Technologies*, *129*(January), 103276. https://doi.org/10.1016/j.trc.2021.103276

Wandtner, B., Schömig, N., & Schmidt, G. (2018). Effects of Non-Driving Related Task Modalities on Takeover Performance in Highly Automated Driving. *Human Factors*, *60*(6), 870–881. https://doi.org/10.1177/0018720818768199

Wang, S., & Li, Z. (2019a). Exploring causes and effects of automated vehicle disengagement using statistical modeling and classification tree based on field test data. *Accident Analysis and Prevention*, *129*. https://doi.org/10.1016/j.aap.2019.04.015

Wang, S., & Li, Z. (2019b). Exploring the mechanism of crashes with automated vehicles using statistical modeling approaches. *PLoS ONE*, *14*(3). https://doi.org/10.1371/journal.pone.0214550

Wang, Y.-D., & Bo, L. (2013). Integrations between Visual Basic and MATLAB. *2013 5th International Conference and Computational Intelligence and Communication*

Networks, 604–606.

Wörle, J., Metz, B., Othersen, I., & Baumann, M. (2020). Sleep in highly automated driving: Takeover performance after waking up. *Accident Analysis & Prevention*, *144*, 105617.

Wright, T. J., Agrawal, R., Samuel, S., Wang, Y., Zilberstein, S., & Fisher, D. L. (2017). Effects of alert cue specificity on situation awareness in transfer of control in level 3 automation. *Transportation Research Record*, *2663*(1), 27–33.

Wu, X., & Nie, Y. (2011). Application of discrete Fourier transform to find reliable shortest paths. *Transportation Research Record*, *2263*(1), 82–91.

Wu, Y., Kihara, K., Hasegawa, K., Takeda, Y., Sato, T., Akamatsu, M., & Kitazaki, S. (2020). Age-related differences in effects of non-driving related tasks on takeover performance in automated driving. *Journal of Safety Research*, *72*, 231–238.

Yang, S., Kuo, J., & Lenné, M. G. (2020). Effects of distraction in on-road level 2 automated driving: impacts on glance behavior and takeover performance. *Human Factors*, 0018720820936793.

Yannis, G., Laiou, A., Papantoniou, P., & Gkartzonikas, C. (2016). Simulation of texting impact on young drivers' behavior and safety on motorways. *Transportation Research Part F: Traffic Psychology and Behaviour*, *41*, 10–18.

Yekhshatyan, L., & Lee, J. D. (2013). Changes in the correlation between eye and steering movements indicate driver distraction. *IEEE Transactions on Intelligent Transportation Systems*, *14*(1), 136–145. https://doi.org/10.1109/TITS.2012.2208223

Yoon, S. H., Kim, Y. W., & Ji, Y. G. (2019). The effects of takeover request modalities on highly automated car control transitions. *Accident Analysis and Prevention*, *123*(November 2018), 150–158. https://doi.org/10.1016/j.aap.2018.11.018

Young, K. L., Lenné, M. G., & Williamson, A. R. (2011). Sensitivity of the lane change test as a measure of in-vehicle system demand. *Applied Ergonomics*, *42*(4), 611–618.

Yun, H., & Yang, J. H. (2020). Multimodal warning design for take-over request in conditionally automated driving. *European Transport Research Review*, *12*(1). https://doi.org/10.1186/s12544-020-00427-5

Zhang, T., Tao, D., Qu, X., Zhang, X., Lin, R., & Zhang, W. (2019). The roles of initial trust and perceived risk in public's acceptance of automated vehicles. *Transportation Research Part C: Emerging Technologies*, *98*(June 2018), 207–220. https://doi.org/10.1016/j.trc.2018.11.018

Zhang, W., Zeng, Y., Yang, Z., Kang, C., Wu, C., Shi, J., Ma, S., & Li, H. (2021). Optimal Time Intervals in Two-Stage Takeover Warning Systems With Insight Into the Drivers' Neuroticism Personality. *Frontiers in Psychology*, *12*.

Zhang, Y., Chen, Y., & Gao, C. (2021a). Deep unsupervised multi-modal fusion network for detecting driver distraction. *Neurocomputing*, *421*, 26–38. https://doi.org/10.1016/j.neucom.2020.09.023

Zhang, Y., Chen, Y., & Gao, C. (2021b). Deep unsupervised multi-modal fusion network for detecting driver distraction. *Neurocomputing*, *421*, 26–38. https://doi.org/10.1016/j.neucom.2020.09.023

Zhang, Y., Chen, Y., & Gao, C. (2021c). Deep unsupervised multi-modal fusion network for detecting driver distraction. *Neurocomputing*, *421*, 26–38.

Zhang, Z., Velenis, E., Fotouhi, A., Auger, D. J., & Cao, D. (2020). Driver distraction detection using machine learning algorithms: an experimental approach. *International Journal of Vehicle Design*, *83*(2–4), 122–139.

Zhao, Z., Xia, S., Xu, X., Zhang, L., Yan, H., Xu, Y., & Zhang, Z. (2020). Driver Distraction Detection Method Based on Continuous Head Pose Estimation. *Computational Intelligence and Neuroscience, 2020*.

Zhou, F., Yang, X. J., & Winter, J. De. (2021). *Using Eye-tracking Data to Predict Situation Awareness in Real Time during Takeover Transitions in Conditionally Automated Driving*. 1–12.

Zhou, R., Yu, M., & Wang, X. (2016). Why do drivers use mobile phones while driving? The contribution of compensatory beliefs. *PloS One*, *11*(8), e0160288.

Zhou, R., Zhang, Y., & Shi, Y. (2020). Driver's distracted behavior: The contribution of compensatory beliefs increases with higher perceived risk. *International Journal of Industrial Ergonomics*, *80*, 103009.

LIST OF ACRONYMS

ADAS	Advanced Driver-Assistance Systems
ADS	Automated Driving System
AI	Artificial Intelligence
ANN	Artificial Neural Network
AV	Automated Vehicle
AUCAS-L3	AI-driven, Ultra-advanced collision avoidance system under Level 3
CAN-Bus	Control Area Network-Bus
CART	Classification and Regression Tree
CAV	Connected & Automated Vehicle
CDAR	Cognitive Distraction Acceleration Rate
CFI	Comparative Fit Index
CV	Connected Vehicle
DFT	Discrete Fourier Transform
DRT	Detection Response Task
EEG	Electroencephalogram
FHWA	Federal Highway Administration
HMI	Human-Machine Interface
HVI	Human-Vehicle Interaction

LOESS	Locally Weighted Scatterplot Smoothing
MSE	Mean Square Error
NDRT	Non-Driving Related Tasks
NTSB	National Transportation Safety Board
RDDQPS	Real-time Driver Distraction Quantification & Prediction System
RMSEA	Root Mean Square Error of Approximation
SA	Situation Awareness
SAE	Society of Automotive Engineers
SEM	Structural Equation Modeling
SSAM	Surrogate Safety Assessment Model
TEPR	Task-Evoked Pupil Response
TFHRC	Turner-Fairbank Highway Research Center
TTC	Minimum Time-To-Collision
UAT	Universal Approximation Theorem
V2I	Vehicle-to-Infrastructure
WLSMV	Weighted Least Square Mean and Variance adjusted

CURRICULUM VITA

NAME: Song Wang

ADDRESS: Civil and Environmental Engineering Department
218 Eastern Pkwy,
Louisville, KY 40208

DOB: Chongqing, China – May 4, 1990

EDUCATION & TRAINING:

B.S. in Civil Engineering
Chongqing Jiaotong University
2009-2013

M.Sc. in Civil Engineering
Chongqing Jiaotong University
2003-2016

Exchange program in Civil Engineering
Nottingham Trent University
February-May 2015

Ph.D. Transportation Engineering
University of Louisville
2016-2021

AWARDS:

- **2020,** Doctoral Dissertation Completion Award at University of Louisville, Louisville, KY.
- **2018~2021**, Graduate Student Council Travel Funds at University of Louisville, Louisville, KY.
- **2017**, 3rd Place in Student Competition of International Highway Engineering Exchange Program, Covington, KY.
- **2016~2017**, Grosscurth fellowship, University of Louisville, Louisville, KY

PROFESSIONAL SOCIETIES: Chinese Overseas Transportation Association (COTA)

PUBLICATIONS:

- **Published:**
  1. **Wang, S.**, Wang, Y., Zheng, Q., & Li, Z. (2020). Guidance-oriented advanced curve speed warning system in a connected vehicle environment. *Accident Analysis & Prevention, 148*, 105801.

  2. **Wang, S.**, & Li, Z. (2019). Exploring causes and effects of automated vehicle disengagement using statistical modeling and classification tree based on field test data. *Accident Analysis & Prevention, 129*, 44-54.

  3. **Wang, S.**, & Li, Z. (2019). Exploring the mechanism of crashes with automated vehicles using statistical modeling approaches. *PloS one*, *14*(3), e0214550.

  4. **Wang, S.**, & Li, Z. (2019). Roadside sensing information enabled horizontal curve crash avoidance system based on connected and autonomous vehicle technology. *Transportation Research Record*, 0361198119837957.

- **Under review:**
  1. **Wang, S.**, Li, Z., Wang, Y., & Wyatt, D. A. (2021). What Makes Education More Effective in Improving People's Acceptance of Automated Driving? – An Exploration on Kentucky Survey Data using the Structural Equation Modeling Approach. *Transport Policy*

- **Ready to submit:**
  1. **Wang, S.,** Cui, Y., Wei, H., Li, Z. (2021). Why Do Drivers Running the Yellow light? Characterizing Direct and Indirect Factors Impacting Driver's Yellow-light Stop/Go Behavior using Structural Equation Modeling. *Science Advances*

  2. **Wang, S.**, Li, Z., Wang, Y., & Wyatt, D. A. (2021). Why Do Age and Gender Influence the Acceptance of Automated Vehicle? – Unveiling the Hidden Mediating Effects from the Built Environment and

Personal Factors. *Transportation Research Part A: Policy and Practice*

3. **Wang, S.**, Li, Z., Wang, Y., & Zheng, Q. (2021). How People with Disabilities Accept and Benefit from Automated Driving? –Views from People with Disabilities and General Public. *Journal of Sustainability City and Society*

- **Conference Publications:**
  1. **Wang, S.** and Li, Z. (2019). Roadside Sensing Information Enabled Horizontal Curve Crash Avoidance System Based on Connected and Autonomous Vehicle Technology. *The 98th Annual Meeting of Transportation Research Board*, Washington D.C.

  2. **Wang, S.**, Li, Z., Wang, Y., Yao, Z., & Yang, K. (2018). Connected vehicles–based smart horizontal curve road-departure avoidance system via in-vehicle heads-up display. *The 97th Annual Meeting of Transportation Research Board*, Washington D.C.

- **In progress:**
  1. **Wang, S.**, & Li, Z. (2021+). Modeling Driver's Visual Distraction Mechanism under the Connected & Automated Vehicle Environment with Incorporating Eye-tracking Data. *Transportation Research Part C: Emerging Technologies*

  2. **Wang, S.**, & Li, Z. (2021+). Quantifying Driver's Cognitive Distraction under the Connected & Automated Vehicle Environment with Incorporating Eye-tracking Data. *Transportation Research Part C: Emerging Technologies*

  3. **Wang, S.**, & Li, Z. (2021+). Driver Distraction Mitigation-based Automated Braking System under Conditional Automation with Integrating Artificial Neural Network Methods. *Accident Analysis & Prevention*

  4. **Wang, S.**, Li, T & Li, Z. (2021+). Incorporating Human Errors to Predict Safety Enhancement under

Automated Driving: A Driving Simulator Study. *IEEE Intelligent Transportation Systems Magazine*

5. **Wang, S.**, Gu, Y & Li, Z. (2021+). Modeling the Dynamic Nature of Willingness to Purchase of AV via a Kentucky Case Study. *Transportation Research Part A: Policy and Practice*

NATIONAL MEETING PRESENTATIONS:

- **Podium presentation**
  - **2017**, **Wang, S**. "Connected Vehicle-based Smart Road-Departure Avoidance System at Horizontal Curves via In-Vehicle Heads-Up Display", International Highway Engineering Exchange Program, Covington, KY

- **Poster presentation**
  - **2022, Wang, S.**, Li, Z., Wang, Y. Evidence of Automated Vehicle Safety's Influence on People's Acceptance of the Automated Driving Technology. Transportation Research Board 101st Annual Meeting *(Accepted for presentation).*
  - **2022, Wang, S.**, Li, Z., Wang, Y., Wyatt, D. A., Ma, M. How Effective is Automated Vehicle Education? – A Kentucky Case Study Revealing the Dynamic Nature of Education Effectiveness. Transportation Research Board 101st Annual Meeting *(Accepted for presentation).*
  - **2021**, **Wang, S**. and Li, Z. "Investigation on Factors that Influence People's Acceptance of Automated Driving – A Kentucky Case Study", 100th Transportation Research Board Annual Meeting, Washington D.C.
  - **2019**, **Wang, S**. and Li, Z. "Roadside sensing information enabled horizontal curve crash avoidance system based on connected and autonomous vehicle technology", 98th Transportation Research Board Annual Meeting, Washington D.C.
  - **2019**, **Wang, S**. "Quantifying Distraction and Modeling its Interaction with Safety in Connected Vehicle Safety Application and Automated Vehicle

Environment", 98th Transportation Research Board Annual Meeting, Washington D.C.

- **2018**, **Wang, S**., Li, Z., Wang, Y., Yao, Z., & Yang, K. "Connected vehicles–based smart horizontal curve road-departure avoidance system via in-vehicle heads-up display", 97th Annual Meeting of Transportation Research Board, Washington D.C.

REFEREED JOURNALS:

- **Journals:**
  - PloS one
  - IATSS Research
- **Conferences:**
  - Transportation Research Board Annual Meeting (2022)
  - Transportation Research Board Annual Meeting (2019)
  - 20th COTA International Conference of Transportation Professionals, 2020
  - 19th COTA International Conference of Transportation Professionals, 2019
  - 18th COTA International Conference of Transportation Professionals, 2018